DIMENSIONLESS RATIOS FOR SURGE WAVES IN OPEN CANALS

by

HENRY JAW-HERE WU

B.Sc. (Civil Engineering)

Provincial Cheng-Kung University, 1963

A THESIS SUBMITTED IN PARTIAL FULFILMENT OF

THE REQUIREMENTS FOR THE DEGREE OF

MASTER OF APPLIED SCIENCE

in the Department

of

Civil Engineering

We accept this thesis as conforming to the

required standard

THE UNIVERSITY OF BRITISH COLUMBIA

April 1970

In presenting this thesis in partial fulfilment of the requirements for an advanced degree at the University of British Columbia, I agree that the Library shall make it freely available for reference and Study. I further agree that permission for extensive copying of this thesis for scholarly purposes may be granted by the Head of my Department or by his representatives. It is understood that copying or publication of this thesis for financial gain shall not be allowed without my written permission.

Department of Civil Engineering

The University of British Columbia
Vancouver 8, Canada

Date April 29, 1970.

ABSTRACT

This study investigates the propagation of a surge wave in a power canal following load rejection or reduction. Dimensionless relationships are derived to predict (a) the initial wave height, (b) the variation of the wave height along the canal and (c) the maximum stage of water depth at the downstream end for straight prismatic canals of rectangular, triangular and trapezoidal cross-sections. The effects of various parameters, such as velocity and depth of initial flow, frictional coefficients, bed slope, cross-section of the canal, distance of wave propagation and initial wave height of the surge are studied.

A computer program is developed for the calculations required. It is found that, as a positive surge propagates along the canal, the wave height decreases linearly with distance for a short canal, according to an exponential function for a long canal. An approximate logarithmic relationship is also found between the variation of wave height of a positive surge and canal cross-sectional parameters.

The variation of water depth at the downstream end of the canal is not linear with respect to time. An almost linear relationship between the maximum water depth at the downstream end of the canal and the length of the canal is noted.

The dimensionless relationships derived in this study may be used to establish design criteria for crest elevations of the banks and walls of power canals to avoid overtopping.

TABLE OF CONTENTS

LIST OF FIGURES

NOTATION

A	cross-section area	ft^2
b	width of free surface	ft
b_o	bottom width of canal	ft
c	wave celerity	ft /sec.
$F^{\#}$	Froude number = $V/\sqrt{g \cdot y}$	
g	gravity acceleration	ft/sec^2
H	total head at reservoir	ft
k	dimensionless parameter = $b_o/m \cdot y_o$	
L	canal length	ft
L_R	reference length = y_o/S_o	ft
1/m	canal side slope	
n	resistance coefficient in the Manning formula	
R	hydraulic radius	ft
P	wetted perimeter	ft
Q	discharge	$ft^3/sec.$
r	dimensionless parameter = $1+\frac{1}{1+k}$	
S_f	friction slope (energy gradient)	
S_o	slope of bottom	
t	time	sec.
V	water velocity	ft/sec.
V_w	absolute wave velocity = V+ c	ft/sec.
w	unit weight of water	lb/ft^3
x	distance	ft
x^*	distance of wave propagation	ft
y	water depth	ft
$\bar{y}$	centroidal depth of cross-section area	ft

\# note that some Authors use $F = \frac{V^2}{g \cdot y}$ as Froude number

Z	surge wave height	ft
λ	dimensionless parameter = V_{wo}/V_o	
β	dimensionless parameter = Z_o/y_o	
τ	discharge ratio = Q/Q_o	
τ_o	unit shear force on bottom and sides of canal	lb/ft^2
μ	energy coefficient	
ϕ	dimensionless parameter = $\left(\frac{X}{L_R}\right)_{r=1} \Big/ \left(\frac{X}{L_R}\right)_{r=n}$	

Subscript o refers to initial steady state condition

ACKNOWLEDGMENT

The author wishes to express his grateful appreciation to his supervisor Dr. E. Ruus, for his valuable guidance and encouragement during the research, preparation, and development of this thesis. Appreciation is also extended to Mr. P. Donnelly for his advice and suggestions.

CHAPTER 1 INTRODUCTION

The prediction of the height and velocity of a surge wave, the maximum stage and the other flow characteristics in a canal due to large instantaneous changes in discharge has been of interest to engineers for many years. The designer of a hydro-electric headrace canal, for example, must determine the maximum stage of water that could occur as a result of a sudden load rejection in power output, considering both the surge wave crest and the subsequent unsteady rise in stage at any point.

In hydro-electric head or tailrace canals, large changes in discharge are initiated by opening or closing of turbine gates. These discharge changes cause positive or negative surge waves. A wave, which results from an increase in water depth is called a positive wave. A wave, which results from a decrease in water depth is called a negative wave. In a positive surge wave, the higher portions of the wave have a greater velocity of propagation than the lower ones. Hence the front of the wave tends to become steeper and steeper until the slope of the front is enough to create a roller. The front of the wave then resembles a moving hydraulic jump. After a positive surge-wave front in a head race canal passes a given section, the water level at that section does not, in general, remain stationary, but continues to rise. The unsteady water surface rise behind the surge wave persists until interrupted by the negative wave, which results from the reflection of the positive wave at the reservoir at the upstream end of the canal.

The negative waves are not stable in form, because the upper portions of the wave travel faster than the lower portions. This results in a gradual flattening of the wave front as it moves along the canal.

At solid boundaries, such as closed gates, a positive wave is reflected as a positive wave and a negative wave as a negative wave. At the reservoir, a positive wave is reflected as a negative wave and a negative wave as a positive wave. In a short canal, the wave front may travel back and forth several times before a new steady state is reached. However, the first maximum stage is higher than the subsequent peaks on the water surface oscillation cycle and is the most significant for design considerations.

This study includes four parts:

(1) Determination of initial surge wave height and velocity (Chapter 2),

(2) The method of computation of the propagation of surge waves (Chapter 3),

(3) The variation of wave heights for positive and for the reflected negative surges (Chapter 4), and

(4) The variation of water depth at the downstream end of the canal (Chapter 4).

The study deals with:

(a) Initial uniform steady flow with Froude numbers from 0.05 to 0.20 inclusive.

(b) Straight canals of constant longitudinal slope, shape, size of cross-section and frictional coefficient throughout. Rectangular, triangular and trapezoidal cross-sections are considered.

(c) Positive waves caused by an instantaneous load rejection at the downstream end and travelling upstream toward the upper end of the canal.

(d) Downstream travelling negative waves, resulting from reflection of positive waves reaching the reservoir at the upper end of the canal.

Several approximate methods for computation of the propagation of surge waves in canals have been developed by previous investigators. The methods suggested by R. D. Johnson[1]*, and H. Favre[2] are in current use. According to Johnson's method, the total length of channel is divided into several reaches. The slopes in the water surface and the canal bed in each reach are represented by a vertical drop in the water surface and in the canal floor at junctions between the reaches. The water surface and canal floor within each reach are assumed level. When a wave reaches the junction, two component waves emerge, one of which travels upstream and the other downstream. When the downstream travelling component wave reaches the downstream end of the canal, it will be reflected and travels upstream. When the upstream travelling component wave reaches another junction farther upstream, it will be transmitted and reflected again into two component waves which travel in opposite directions. When two waves travelling in opposite directions meet, another pair of waves is generated. The wave heights and water depths at any section of canal can be computed step by step.

Favre introduced a method using two empirical equations for the com-

* Numerals in parentheses refer to corresponding items in References.

putation of a surge wave propagating along a canal. He made the assumption that the longitudinal profile of the water surface behind the wave front is a straight line. In addition, the whole length of canal is considered as one reach. This method may be applied to relatively short canals with a straight and moderate slope, to obtain an approximate solution.

Because these manual computational methods are laborious their usefulness is restricted. In recent years, the advances in computer technology has stimulated the development and application of more rigorous approaches. On such rigorous solution is described in this study.

In this thesis, equations of momentum and continuity for a rapidly varied flow are used to solve the height and velocity of a surge wave.

The partial differential equations of motion and continuity governing the gradually-varied, unsteady flow in the front of, or behind, the wave region are converted into total differential equations by using the method of characteristics and solved by a finite difference technique.

A mathematical model is set up on an x-t plane with characteristic grids. Using this model, a computer program is developed for calculation of the wave height and velocity at any section of the canal as a surge wave is travelling upstream. Similarly flow parameters at any section in front of and behind the wave region, are obtained for the downstream travelling wave from computer calculations.

Although a simple and idealized canal is considered in this study, the method and techniques employed and relationships derived may be modified for the computation of surge wave propagation in a complicated real power canal.

CHAPTER 2

DETERMINATION OF WAVE HEIGHT AND VELOCITY FOR INITIAL SURGE WAVES

2.1 Fundamental Equations Governing the Surge-Wave Height and Velocity

If the velocity of the water flowing in a canal is changed rapidly, a wave is generated with a sudden change in depth. Figure 2-1 illustrates a surge wave resulting from a sudden change in flow, due to a gate motion, that increases the water depth. The depth of flow is always considered to be positive with reference to the channel bottom. Wave velocity, celerity and water velocity are assumed to be positive in the downstream direction. The water between two cross-sections, one just upstream and the other just downstream of the wave front, is considered. The velocity of the mass of water between these sections 1 and 2 is decreased from V_1 to V_2, and the momentum is decreased accordingly. By Newton's second law of motion, the unbalanced force required to change the momentum is the product of the mass per unit time and the change in velocity. This unbalanced force is equal to the difference between the hydrostatic pressure forces acting on the area A_2 and A_1 at section 2 and 1. It follows that:

$$\frac{w}{g} \cdot A_1 \cdot (V_1 - V_w) \cdot (V_1 - V_2) = w \cdot A_2 \cdot \bar{y}_2 - w \cdot A_1 \cdot \bar{y}_1 \quad \ldots (2\text{-}1)$$

Where

w = specific weight of water
g = acceleration of gravity
A = cross-sectional area
V = water velocity

V_w = absolute wave velocity

$\bar{y}$ = centroidal depth of cross-section area.

Subscripts 1 and 2 indicate parameters at sections 1 and 2 respectively.

The equation of continuity between section 1 and 2 is

$$A_2 \cdot (V_2 - V_w) = A_1 \cdot (V_1 - V_w) \qquad \ldots\ldots \quad (2\text{-}2)$$

By substituting Eq. (1-2) into Eq. (1-1) and solving for V_w ,

$$V_w = V_1 + c \qquad \ldots\ldots \quad (2 - 3')$$

where c = celerity (relative to flowing water),

$$c = \pm \sqrt{\frac{g \cdot (A_2 \cdot \bar{y}_2 - A_1 \cdot \bar{y}_1)}{A_1 \cdot (1 - A_1/A_2)}} \qquad \ldots\ldots \quad (2 - 3)$$

Eq. (2-3) is the general expression for the absolute wave velocity in a power canal. The sign in front of the square-root term in Eq. (2-3) depends on the direction of wave propagation. A positive sign is used if the wave moves downstream, and a negative one if the wave moves upstream. If V_w is eliminated from Eqs. (2-1) and (2-2),

$$A_2 \cdot \bar{y}_2 - A_1 \cdot \bar{y}_1 = \frac{A_1 \cdot A_2}{g \cdot (A_2 - A_1)} \cdot (V_1 - V_2)^2 \qquad \ldots\ldots \quad (2\text{-}4)$$

The above equation represents the relationship between velocities and depths of flow at sections 1 and 2. From Eqs. (2-2) and (2-4) y_2 or V_2 may be determined by a process of trial and error, given the other three independent variables. The magnitude of the wave height is equal to $(y_2 - y_1)$. Positive values of $(y_2 - y_1)$ indicate an increase in depth while negative values indicate a reduction in depth.

Although the above equations are derived for the case shown in Fig. 2-1, they can be applied to positive or negative waves travelling either upstream or downstream. For initial surge waves, Eqs. (2-3) and (2-4) may be rewritten as:

$$V_{wo} = V_o + c_o \qquad \cdots\cdots\cdots \quad (2\text{-}5)$$

$$c_o = \pm\sqrt{\frac{g\cdot(A\cdot\bar{y} - A_o\cdot\bar{y}_o)}{A_o\cdot(1 - A_o/A)}}$$

and

$$A\cdot\bar{y} - A_o\cdot\bar{y}_o = \frac{A_o\cdot A}{g\cdot(A - A_o)}\cdot(V_o - V)^2 \qquad \cdots\cdots \quad (2\text{-}6)$$

where subscript o indicates parameters of the undisturbed initial flow.

With these equations, the initial wave parameters, such as celerity, height, etc., may be determined for any cross-section of the canal. If a wave travels in still water, V_o is equal to zero. Thus, in this case, the absolute wave volocity is identical to the celerity.

Solving Eqs. (2-5) and (2-6) by trial and error is laborious. To simplify calculations, therefore, a dimensionless form of the equations is given below for three types of prismatic canals.

2.2 Initial Surge Waves in Canals of Rectangular Cross-Section.

For the rectangular canal (Figure 2-2), Eqs. (2-1) and (2-2) can be simplified to

$$y^2 - y_o^2 = \frac{2}{g} \cdot y_o \cdot (V_o - V_{wo}) \cdot (V_o - V) \quad .... \quad (2\text{-}7)$$

and

$$y_o \cdot (V_o - V_{wo}) = y \cdot (V - V_{wo}) \quad ..... \quad (2\text{-}8)$$

where y is the depth of flow

Eliminating V_{wo} from Eqs. (2-7) and (2-8) gives

$$y^2 - y_o^2 = \frac{2}{g} \cdot \frac{y_o \cdot y \cdot V_o^2 \cdot (1 - V / V_o)^2}{(y - y_o)} \quad ..... \quad (2\text{-}9)$$

Dividing Eq. (2-9) by y_o^3 results in

$$(\frac{y}{y_o} + 1) \cdot (\frac{y}{y_o} - 1)^2 = \frac{2}{g} \cdot \frac{y}{y_o} \cdot \frac{V_o^2}{y_o} \cdot (1 - \frac{V}{V_o})^2 \quad ... \quad (2\text{-}10)$$

Let

$$\beta = \frac{Z_o}{y_o} \quad , \text{ where } Z_o = y - y_o$$

and discharge ratio,

$$\tau = \frac{Q}{Q_o} \quad , \text{ where } Q_o = A_o \cdot V_o \quad \text{and } Q = A \cdot V$$

then

$$\frac{y}{y_o} = 1 + \beta \quad ..... \quad (2\text{-}11)$$

and

$$\frac{V}{V_o} = \frac{\tau}{1 + \beta} \quad ..... \quad (2\text{-}12)$$

Using Eqs. (2-11) and (2-12), Eq. (2-10) gives the dimensionless equation

$$F_o^2 = \frac{\beta^2 \cdot (1+\beta) \cdot (2+\beta)}{2\,(1+\beta-\tau)^2} \qquad \cdots\cdots\cdots \quad (2\text{-}13)$$

where

$$F_o = \frac{V_o}{\sqrt{g \cdot y_o}}$$

Eq.(2-13) shows that the initial wave height in canals of rectangular cross-section is a function of the Froude number of the initial flow and the discharge ratio. For a constant discharge ratio, the initial wave height is only a function of the Froude number of the flow. The family of curves corresponding to Eq. (2-13) is shown on log-log paper in Figure 2-3. Given the Froude number of the initial flow, and the change in discharge after the gate opening or the gate closure, the initial wave height can be obtained directly from this graph.

Solving Eq. (2-2) for the absolute wave velocity, gives

$$V_{wo} = \frac{y_o \cdot V_o - y \cdot V}{y_o - y}$$

or

$$\frac{V_{wo}}{V_o} = \frac{y_o \cdot V_o \cdot \left(1 - \frac{y}{y_o} \cdot \frac{V}{V_o}\right)}{y_o \cdot V_o \cdot \left(1 - \frac{y}{y_o}\right)} \qquad \cdots\cdots \quad (2\text{-}14)$$

Substitution of Eqs. (2-11) and (2-12), Eq. (2-14) can be simplified to

$$\lambda = \frac{\tau - 1}{\beta} \qquad \cdots\cdots\cdots \quad (2\text{-}15)$$

where λ is the ratio of absolute wave velocity to the initial flow velocity, $\lambda = V_{wo}/V_o$. Substituting Eq. (2-15) into Eq. (2-13) and simplifying gives

$$F_o^2 = \frac{(\lambda - 1 + \tau) \cdot (2\lambda - 1 + \tau)}{2\lambda^2 \cdot (1 - \lambda)^2} \qquad \cdots\cdots \quad (2\text{-}16)$$

Eq. (2-16) gives the relationship between the wave velocity V_{wo}, the Froude number F_o of the initial flow and the discharge ratio τ. For a given value of τ, the initial wave velocity is a function of the Froude number. Eq. (2-16) is shown graphically in Figure 2-3.

2.3 Initial Surge Waves in Canals of Triangular Cross-Section.

For a triangular canal (Figure 2-4), Eq. (2-6) may be simplified to:

$$\frac{1}{3}(y^3 - y_o^3) = \frac{y_o^2 \cdot y^2}{g \cdot (y^2 - y_o^2)} \cdot V_o^2 \cdot \left(1 - \frac{V}{V_o}\right)^2 \qquad \cdots (2\text{-}17)$$

In a triangular canal

$$\frac{V}{V_o} = \frac{Q/A}{Q_o/A_o} = \frac{\tau}{(1+\beta)^2}$$

By using the relation above and Eq. (2-11), Eq. (2-17) can be rewritten as:

$$\frac{1}{3}\left[(1+\beta)^3 - 1\right] = F_o^2 \cdot \frac{(1+\beta)^2}{(1+\beta)^2 - 1} \cdot \left[1 - \frac{\tau}{(1+\beta)^2}\right]^2$$

or

$$F_o^2 = \frac{(1+\beta)^2 \cdot \left[(1+\beta)^2 - 1\right] \cdot \left[(1+\beta)^3 - 1\right]}{3\left[(1+\beta)^2 - \tau\right]^2} \qquad \cdots (2\text{-}18)$$

If Eq. (2-2) is solved for absolute wave velocity, and a similar substitution of the dimensionless parameters, τ and β is used, then

$$\frac{V_{wo}}{V_o} = \frac{(1+\beta)^2 \cdot \frac{\tau}{(1+\beta)^2} - 1}{(1+\beta)^2 - 1}$$

or

$$\lambda = \frac{\tau - 1}{(1+\beta)^2 - 1} \qquad \cdots\cdots\cdots \qquad (2\text{-}19)$$

Eq. (2-18) shows that the initial wave height in a symmetrical canal of triangular cross-section is a function of the Froude number of the initial flow and the discharge ratio.

Eq. (2-19) shows that the absolute wave velocity is a function of the wave height. In other words, the ratio of wave velocity to that of the initial flow is also a function of the Froude number and the discharge ratio. The graphical form of Eqs. (2-18) and (2-19) is shown on Figure 2-5.

2.4 Initial Surge Waves in Canals of Trapezoidal Cross-Section.

In a trapezoidal canal (Figure 2-6), the cross-sectional parameters, b, A, y, at sections upstream and downstream of the wave front are

$$b_1 = b_o + 2\,m \cdot y_o$$

$$A_o = y_o \cdot (b_o + m \cdot y_o)$$

$$\bar{y}_o = \frac{y_o}{6} \cdot \frac{3\,b_o + 2\,m \cdot y_o}{b_o + m \cdot y_o}$$

and

$$b_2 = b_o + 2\,m \cdot y$$

$$A = y \cdot (b_o + m \cdot y)$$

$$\bar{y} = \frac{y}{6} \cdot \frac{3\, b_o + 2\, m \cdot y}{b_o + m \cdot y}$$

Substitution of these relations into Eq. (2-4) gives

$$\frac{y^2}{6} \cdot (3\, b_o + 2\, m \cdot y) - \frac{y_o^2}{6} \cdot (3\, b_o + 2\, m \cdot y_o)$$

$$= \frac{V_o^2 \cdot y_o \cdot y \cdot (b_o + m.y) \cdot (b_o + m.y_o) \cdot (1 - V/V_o)^2}{g \cdot \left[(b_o + m.y) \cdot y - (b_o + m.y_o) \cdot y_o \right]}$$

Dividing by $m \cdot y_o^3$ results in

$$\frac{1}{6} \cdot (\frac{y}{y_o})^2 \cdot (\frac{3\, b_o}{m.y_o} + \frac{2\, y}{y_o}) - \frac{1}{6} \cdot (\frac{3 b_o}{m.y_o} + 2)$$

$$= \frac{V_o^2}{g \cdot y_o} \cdot \frac{y}{y_o} \cdot \frac{(\frac{b_o}{m.y_o} + 1) \cdot (\frac{b_o}{m.y_o} + \frac{y}{y_o}) \cdot (1 - \frac{V}{V_o})^2}{(\frac{b_o}{m.y_o} + \frac{y}{y_o}) \cdot \frac{y}{y_o} - (\frac{b_o}{m.y_o} + 1)} \quad \cdots (2\text{-}20)$$

Let

$$k = \frac{b_o}{m.y_o} \qquad \cdots\cdots\cdots \quad (2\text{-}21)$$

then

$$\frac{V}{V_o} = \frac{\tau \cdot (k + 1)}{(k + 1 + \beta) \cdot (1 + \beta)} \qquad \cdots\cdots\cdots \quad (2\text{-}22)$$

Substituting Eqs. (2-21) and (2-22) into Eq. (2-20) gives

$$\frac{1}{6} (1 + \beta)^2 \cdot \left[3\, k + 2 (1 + \beta) \right] - \frac{1}{6} (3\, k + 2)$$

$$= F_o^2 \cdot \frac{(k + 1) \cdot \left[(k + 1 + \beta) \cdot (1 + \beta) - \tau \cdot (k + 1) \right]^2}{\left[(k + 1 + \beta) \cdot (1 + \beta) - (k + 1) \right] \cdot (k + 1 + \beta) \cdot (1 + \beta)}$$

or

$$F_o^2 = \frac{\left\{ (1+\beta)^2 \cdot \left[3\, k + 2(1+\beta) \right] - (3k+2) \right\} \cdot \left[(k+1+\beta) \cdot (1+\beta) - (k+1) \right] \cdot (1+\beta) \cdot (k+1+\beta)}{6(k+1) \cdot \left[(k+1+\beta) \cdot (1+\beta) - \tau \cdot (k+1) \right]^2}$$

$$\cdots\cdots\cdots \quad (2\text{-}23)$$

In a trapezoidal cross-section, one additional variable, k, which is a function of the bottom width, side slope of the cross-section and the depth of the initial flow, appears together with discharge ratio and Froude number, to determine the initial wave height.

Physically, (1 + k) is a ratio of the area of a trapezoidal cross-section to that of a triangular cross-section with the same depth and side slope. For a constant value of k, β is independent of the individual value of bottom width, side slope or the depth of initial flow. If the same relation in Eqs. (2-11) and (2-22) are used, then from the continuity equation, it follows that

$$\frac{V_{wo}}{V_o} = \frac{\frac{(1+\beta).(k+1+\beta)}{(k+1)} \cdot \frac{\tau.(k+1)}{(k+1+\beta).(1+\beta)} - 1}{\frac{(1+\beta).(k+1+\beta)}{(k+1)} - 1}$$

or

$$\lambda = \frac{-(1-\tau).(k+1)}{(1+\beta).(k+1+\beta) - (k+1)} \qquad \text{.....} \qquad (2\text{-}24)$$

It may be noted that the shape factor, k, also appears in the wave velocity equation. Eqs. (2-23) and (2-24) are shown graphically on Figures 2-7 (a) - (j). It should be noted that the rectangular and the triangular canals are the particular or limiting cases of the trapezoidal canal. A

trapezoidal canal, when its side slopes become vertical ($k = \infty$), is a rectangular canal. When $k = \infty$, Eq. (2-23) is identical to Eq. (2-13), and Eq. (2-24) to Eq. (2-15). When the bottom width of a trapezoidal canal is reduced to zero ($k = 0$), it becomes a triangular canal. For $k = 0$, Eq. (2-23) is identical to Eq. (2-18), and Eq. (2-24) to Eq. (2-19). Therefore, the rectangular and the triangular cross-sections are the two limits of the trapezoidal cross-section. This can also be seen from Figure 2-7 (a) - (j). Thus Eqs. (2-23) and (2-24) are also valid for both rectangular and triangular canals.

CHAPTER 3

NUMERICAL CALCULATIONS FOR SURGE-WAVE PROPAGATION

3.1 General

When an initial surge wave is generated at the upstream or downstream end of a channel, it travels immediately away from the source of generation with its velocity of propagation. This velocity of propagation is usually considerably in excess of the mean steady-flow velocity. A positive wave caused by a rapid change of discharge has a profile with a steep front similar to a moving hydraulic jump. If the initial profile of the negative surge wave is formed with a steep front, it will soon flatten out as the surge wave moves along the channel.

A rigorous solution for the calculation of the propagation of surge waves does not exist. A rapid approach by the aid of computer is introduced in this chapter. In this approach, the surge wave is determined by using the equations of continuity and momentum (see Chapter 2), and the flow velocities and depths at the upstream and the downstream of wave front boundaries are calculated using the unsteady-flow equations. These unsteady-flow equations are solved by using the method of characteristics by which the partial differential equations are transformed into particular total differential equations. The numerical solution is obtained by a first order finite-difference technique.

3.2 Basic Assumptions

The application of the method of characteristics to unsteady-flow in an open channel is based on the following simplifying assumptions.

(a) Homogeneous water, neither density currents nor sediment movement are considered.

(b) Lateral flow is neglected, i.e., one dimensional flow is considered.

(c) Friction due to the motion over a rough channel bed obeys Manning's formula.

(d) Channel slope is small enough so that $\cos\theta \simeq 1$.

(e) Vertical component of the acceleration has a negligible effect on the pressure.

(f) The pressure distribution along a vertical line is hydrostatic.

3.3 The Equations of Characteristics

Various ways have been used for deriving the equations of characteristics. The expressions developed by V. L. Streeter[3] are used in this study. According to Streeter, two pairs of the equations of characteristics, written for a gradually varied unsteady-flow in an open channel, are

$$C^{+}\begin{cases} \dfrac{dV}{dt} + \sqrt{\dfrac{g\cdot B}{A}}\cdot\dfrac{dy}{dt} + \dfrac{g\cdot\tau_o}{w\cdot R} - g\cdot S_o = 0 & \cdots\cdots (3\text{-}1) \\ \dfrac{dx}{dt} = V + \sqrt{\dfrac{g\cdot A}{B}} & \cdots\cdots (3\text{-}2) \end{cases}$$

$$C^- \begin{cases} \dfrac{dV}{dt} - \sqrt{\dfrac{g \cdot B}{A}} \cdot \dfrac{dy}{dt} + \dfrac{g \cdot \tau_o}{w \cdot R} - g \cdot S_o = 0 & \cdots\cdots (3\text{-}3) \\ \dfrac{dx}{dt} = V - \sqrt{\dfrac{g \cdot A}{B}} & \cdots\cdots (3\text{-}4) \end{cases}$$

where

w = the specific weight of water,

A = the cross-sectional area,

B = the surface width of cross-section,

R = the hydraulic radius,

S_o = slope of bottom

τ_o = the unit shear force on the bottom and sides of a channel,

$\sqrt{\dfrac{g \cdot A}{B}}$ = the celerity of an infinitesimal wave.

The first group of equations are called positive characteristics or C^+ equations, while the second ones are called negative characteristics or C^- equations. The first equation of each group is valid only when the second equation of the group is satisfied.

3.4 Solution of Equations of Characteristics for a Gradually Varied Unsteady Flow

The equations can be represented graphically on an x-t plane, as shown in Figure 3-1. The point P represents the position of the canal section under consideration at time t_p and the points R and S represent, respectively, the position of certain upstream and downstream sections at time t_R and t_S. The velocity of wave propagation can be represented by the slope of the lines constructed on the x-t plane using Eqs. (3-2) and (3-4). Point

R represents the position of the upstream section from which an infinitesimal wave, once developed, will arrive at section P after the time interval $\Delta t = t_p - t_R$.

Similarly, point S represents the position of the downstream section from which a wave once developed will arrive at section P after $\Delta t = t_p - t_S$. Values of V and y at the intersection point P are obtained by solving Eqs. (3-1) and (3-3) simultaneously. In order to accomplish this, the first order finite difference technique is used. The equations of characteristics are transformed as follows:

$$C^+ \begin{cases} V_P - V_R + GR \cdot (y_P - y_R) + GNR \cdot (t_P - t_R) = 0 & \ldots (3\text{-}5) \\ x_P - x_R = (V_R + RG) \cdot (t_P - t_R) & \ldots (3\text{-}6) \end{cases}$$

$$C^- \begin{cases} V_P - V_S - GS \cdot (y_P - y_S) + GNS \cdot (t_P - t_S) = 0 & \ldots (3\text{-}7) \\ x_P - x_S = (V_S - SG) \cdot (t_P - t_S) & \ldots (3\text{-}8) \end{cases}$$

where the subscripts indicate the variables at the corresponding points, and

$$GR = \sqrt{\frac{g \cdot B_R}{A_R}}, \quad RG = \sqrt{\frac{g \cdot A_R}{B_R}}, \quad GS = \sqrt{\frac{g \cdot B_S}{A_S}}, \quad SG = \sqrt{\frac{g \cdot A_S}{B_S}},$$

$$GNR = g \cdot (S_R - S_o)$$

and

$$GNS = g \cdot (S_S - S_o)$$

S_R and S_S are the frictional slopes at points R and S respectively. According to the Manning formula, the frictional slope can be

expressed as

$$S = \frac{n^2 . V . |V|}{2.21\ R^{4/3}}$$

where n is the coefficient of roughness on the canal bottom and sides (or Manning's n), and V is the mean velocity of flow. $V.|V|$ indicates that the frictional resistance is always in the opposite direction of the flow. Knowing the variables, x, t, V and y, at points R and S, the four unknown variables x, t, V and y, at point P, can be found using equations, Eqs. (3-5) through (3-8).

A grid of characteristics is established to facilitate a computer solution. A particular section of the canal may be arbitrarily chosen. For simplicity, the canal of length L is divided into a number of equal lengths. The procedure for calculation follows.

3.4.1. Preliminary computation

Compute the initial velocity and depth of the flow by using Manning's formula, $V = \frac{1.486}{n} \cdot R^{2/3} \cdot S^{1/2}$, and store the known values of x, t, V, and y at points P (m, 1), m = 1, 3, 5, ..., etc., (Figure 3-2).

3.4.2 Computation for the flow in the channel

Based on the values of x, t, V and y at point R, the characteristic line RP for a short distance can be laid

out at a slope of $1/(V_R+RG)$ from Eq. (3-6). Similarly, based on the values of x, t, V and y at point S, the characteristic line SP can be drawn to represent Eq. (3-8). These two characteristic lines from R and S intersect at point P. The values of x, t, V and y at P are then obtained by solving Eqs. (3-5) through (3-8) simultaneously, i.e.,

$$t_P = \frac{x_S - x_R + t_R \cdot (V_R + RG) - t_S \cdot (V_S - SG)}{V_R + RG - V_S + SG} \quad \ldots\ldots(3-9)$$

$$x_P = x_R + (V_R + RG) \cdot (t_P - t_R) \quad \ldots\ldots\ldots\ldots(3-10)$$

$$y_P = \frac{V_R - V_S + GR \cdot y_R + GS \cdot y_S - GNR \cdot (t_P - t_R) + GNS \cdot (t_P - t_S)}{GR + GS} \quad \ldots(3-11)$$

and

$$V_P = V_R - GR \cdot (y_P - y_R) - GNR \cdot (t_P - t_R) \quad \ldots\ldots\ldots(3-12)$$

3.4.3. Computation for the flow at boundaries

At either end of the channel, only one group of the characteristic equations is available. For an upstream boundary (Figure 3-3-a), Eqs. (3-7) and (3-8) hold, and for a downstream boundary (Figure 3-3-b), Eqs. (3-5) and (3-6) are valid. Therefore two auxiliary equations derived from the given boundary conditions at either boundary are needed so that four unknowns can be solved.

Some examples are solved and illustrated as follows:

Example 3-1. A rectangular channel 1000 ft. long and 12 ft. wide carries 720 cfs water at normal depth. S_o = 0.001 and Manning's n = 0.014. At the upstream end, the flow is given by Q = 720 + 180. sin (0.03 t) and at the downstream end the depth is maintained constant at $y = y_o$. Calculate the flow conditions in the channel.

Solution: The computer program in IBM 7044 computer system for this problem is given in Appendix A(1). A portion of the solution is shown in Figure 3-4.

Example 3-2. A rectangular channel 20 ft. wide and 10,000 ft. long is discharging under steady-uniform flow condition at y_o = 6.0 ft. Channel slope S_o is 0.0016. At time t = 0, the flow is increased at the upstream end linearly until it has doubled in 20 minutes. The flow is then decreased linearly until it is one-half the original flow in 10 additional minutes. For Manning's n = 0.0185, find the velocity and depth in the channel for the first 40 min. of unsteady flow. The gage-height-discharge curve at the downstream end is $Q = 132\ (y - 2.32)^{3/2}$.

Solution: The computer program for this problem is listed in Appendix A(2), and a portion of the solution is given in Fig. 3-5.

The solutions of examples 1 and 2 have been checked with the Example 15.5 and Example 15.6 in reference (3). A good agreement was obtained.

3.5 Numerical Calculations for Positive Waves Propagating in Power Canals.

A continuous unsteady flow in an open channel can be solved by the method of characteristics only by making the assumption that the vertical acceleration of flow is small and therefore can be neglected. For surge problems, the steep step in the wave region constitutes a discontinuity, and the vertical acceleration of the flow cannot be neglected. A rigorous theory for the computation of surge waves has not come to the author's knowledge. However, a surge wave resembles a moving hydraulic jump in an open channel. In the regions upstream or downstream of the wave front, the flow is steady, or gradually varied unsteady flow and can be solved by the method of characteristics introduced in the previous sections. The wave front region itself represents rapidly varied unsteady flow and its solution must be based on the equations of continuity and momentum, i.e., Eq. (2-1) and (2-2). The calculation procedures for a surge wave caused by a load rejection at the downstream end from an initial steady flow follows.

3.5.1 Initial flow condition

The origin of abscissa x on the x-t plane is chosen at the upstream end (Figure 3-6). Assume that the initial flow conditions are known throughout the canal at t = 0. A canal is divided into reaches of equal lengths, and the known values of x, t, V and y at points P(1,1), P(3,1), ... are stored as x(1,1), x(3,1), x(5.1), ...,

t(1,1), t(3,1), t(5,1), ... , V(1,1), V(3,1), V(5,1), ... , y(1,1), y(3,1), y(5,1), ... The values of x, t, V and y at points P(2,2), P(4,2), ... are obtained from the points P(1,1), P(3,1), ... etc., by the method of characteristics. For example, the values of x, t, V and y at point P(6,2) are obtained from the equations of characteristics which pass through P(5,1) and P(7,1).

3.5.2 Initial positive surge wave at downstream end of canal

The equations of continuity and momentum, together with the given change in discharge due to a load rejection, are used to determine the initial wave height and wave velocity. x_A = L (Figure 3-6), and t_A is obtained by the manner mentioned in section 3.4.3. Thus, the variables x, t, V and y at point A are determined. The variables at other points upstream of the wave region, P(1,3), P(3,3), ..., are determined by the method of characteristics.

3.5.3 Wave propagation along the channel

3.5.3.1 Wave travels from A to B (Figure 3-6)

(a) Determine the point B:

Assume that the surge wave travels from A to B with the velocity equal to its initial velocity at A as the first approximation.

t_B and x_B are then obtained by solving equations

$$x_B - x_E = \left(V_E + \sqrt{\frac{g.A_E}{B_E}} \right) \cdot (t_B - t_E) \qquad \text{.....(3 - 13)}$$

$$x_B - x_A = (-V_w) \cdot (t_B - t_A) \qquad \text{.....(3 - 14)}$$

where the subscripts A, B, E indicate the values of V, A,

B, x and t at the corresponding points.

(b) Determine point C

By using the equations of continuity and momentum, determine the water velocity and depth behind the wave front at B. For the first approximation these are not different from ones found at A. t_C, V_C and y_C are obtained from Eqs. (3-5) and (3-6) and boundary conditions in which $x_C = L$.

(c) Determine point D

First, the velocity and depth at point D are estimated, then the variables at B can be obtained from those at D by the equations of characteristics by considering an infinitesimal wave travelling along the characteristic line DB and reaching point B at the same time as a surge wave travelling from A to B along AB. t_D is obtained for the first approximation by the equation

$$x_B - x_D = \left(V_B - \sqrt{\frac{g \cdot A_B}{B_B}} \right) \cdot (t_B - t_D) \quad \ldots\ldots (3 - 15)$$

where the approximate values of parameters x, t, V and y at B are determined in above procedures, and $x_D = L$. Then, y_D is obtained by linear interpolation from those at A and C, assuming that the rate of change of water surface at the downstream end during t_A to t_B is linear with respect to time. With this new value of y_D, determine the new value of t_D along characteristic line BD. Continue this iteration until the two successive relative values of t_D meet the requirement, say, the difference less

than 0.001.

(d) Determine V_B and y_B by using characteristic equation, Eq. (3-7), along DB and the equations of momentum and continuity at B.

(e) Compute the new value of wave velocity at B (Eq. (2-3)), and average the wave velocities at A and B. This is the new wave velocity with which the wave travels from A to B.

(f) With the new wave velocity obtained from (e) repeat the procedures of calculation from (a) to (e) until the differences of two successive calculated relative values of V and y at B, C, and D are less than 0.001.

(g) Determine the variables at all necessary points upstream of the wave front (at point B) by the method of characteristics.

3.5.3.2. Wave travels from B to G, L etc. —

Using the calculation process similar to that in section 3.5.3.1. the variables at G and F are obtained. The values of V and y at C are given from the previous set of computation. The new variables at H are obtained from those at G and C by equations of characteristics. It is necessary in this step to carry on the calculation for the other points at the downstream end, such as I (Figure 3-6) in this step,

along the characteristic line GH to provide the information for carrying on the next step of calculation for wave propagation. By this procedure, a trace of the propagation of the surge wave along the prismatic canal is obtained and terminates when the wave front reaches the upstream reservoir. It should be noted that, for a positive surge wave, the velocity of wave propagation is always greater than that of an infinitesimal wave in the region before the front of the surge wave, and less than that of an infinitesimal wave in the region behind the front of the surge wave, i.e., the inverse slope of the line KE is less than the inverse slope of the line AB, which is again less than the inverse slope of line CH. Eventually, as a surge wave travels continuously along the canal, these lines would converge and intersect each other. Because positive surge waves have an abrupt front, the characteristic lines cannot project from one side of the surge to the other. When the characteristic lines before and behind the wave region and the trace of wave propagation meet, (see figure 3-6), flow parameters at M are determined from P, and those at P are obtained from points O and Q.

The flow chart of the computer program for this computation is shown on Figure 3-8. For a positive wave occurring at the upstream end and travelling to the downstream end, the characteristic lines will be similar to these in Figure 3-7.

The process of computation for a positive surge wave starting

at the downstream end and propagating upstream in the canal has been programmed in FORTRAN IV for the IBM 7044 computer. Examples have been selected to examine the computer program. Parallel hand calculations by the Favre method are shown for comparison.

Example 3.3. A rectangular channel 38,800 ft. long, 45 ft. wide and 41.175 ft. deep carries a flow with a velocity at 7.101 ft/sec. S_o = 0.0002376. Suddenly, the flow is completely stopped at the downstream end by closing a gate. Compute the initial wave height, and wave height when it reaches the upstream end.

Solution: The results of computer computation using method of characteristics give Z_o = 8.39 ft. and Z = 4.23 ft., where Z_o and Z are the downstream and upstream wave heights respectively, (Figures 3-9 and 3-10). Details of the computations are shown graphically on Figure 3-11.

The alternative calculation for this example carried out by the Favre method gave Z = 4.15 ft. for the wave reaching the upstream end of canal. Details are shown on Fig.3-12 .

Comparing the results from the two different methods, a fairly good agreement is observed. It should be noted that, in the Favre method, the water surface in the downstream area is assumed straight line when the wave front reaches the upstream end.

When the wave reaches the reservoir, the actual water surface for the case of complete closure is fairly close to a horizontal line in the lower end of canal, while it is somewhat sloped in the upper end. From Figure 3-11, it can be seen that the variation of wave height when it travels along the channel is nearly linear and therefore Favre's assumption is justified.

Example 3.4 A rectangular channel 1000 ft. long and 12 ft. wide carries 720 cfs water at normal depth. S_o = 0.001 and Manning's n = 0.014. The flow at the downstream end is suddenly shut off. Carry out the calculation of flow conditions and propagation of surge wave along the channel.

Solution: The results of calculation are shown on Figure 3-13, and have been compared with the example on page 258, reference (3).

3.6 Numerical Calculations for Negative Waves Propagating in Power Canals

When a positive wave reaches the upper end of the canal, it is reflected as a negative wave and proceeds towards the downstream end. If the wave height is small or moderate compared to the depth, it can be assumed that the steep wave front is retained during the travel and the equations derived for a positive wave can be applied without introducing significant errors. The height of

the negative wave reflected from the reservoir is usually relatively small. On the assumption that the profile of a negative wave will not change significantly, a scheme for computer computations is used as follows.

3.6.1 Determination of the initial reflected negative wave

Assuming that there is no entrance loss and no velocity head recovery (see section 4-7), the water level immediately behind the wave front of the reflected negative wave at the extreme upper end of channel is the same as that in the reservoir. It follows that

$$H = y_o + \frac{V_o^2}{2g} \qquad \ldots\ldots\ldots\ldots\ldots\ldots \quad (3\text{-}16)$$

where y_o and V_o are the water depth and velocity of the initial steady flow (Fig. 3-14 (a)). At the reservoir, which is the upstream boundary of the canal, $x_R = 0$ and $y_R = H$. The velocity of the negative wave is according to Eq. (2-3).

$$V_w = V_1 + \sqrt{\frac{g.(A_2.\bar{y}_2 - A_1.\bar{y}_1)}{A_1.(1 - A_1/A_2)}} \qquad \ldots\ldots \quad (3\text{-}17)$$

where y_2 and V_2 (Figure 3-15) are given in the last step of the calculation in the propagation of the positive wave. By using the equation of continuity, V_1 is obtained, i.e.:

$$V_1 = \frac{A_2.(V_2 - V_w)}{A_1} + V_w \qquad \ldots\ldots \quad (3\text{-}18)$$

and the height of the negative wave is

$$Z = y_2 - y_1 \quad \text{.....(3-19)}$$

where $y_1 = H$

Here Z has negative value which indicates the negative wave.

3.6.2 Reflected Negative Wave Propagates Along the Channel

3.6.2.1 Determination of the negative wave travelling from R to P (Figure 3-16)

(a) Assume for the first approximation, that the wave travels from point R to point P (Figure 3-16) with a velocity equal to its initial velocity at R. Determine t_p and x_p by solving equations

$$x_P - x_R = V_w \cdot (t_P - t_R) \quad \text{. . . . . (3-20)}$$

$$x_P - x_E = (V_E - \sqrt{\frac{g \cdot A_E}{B_E}}) \cdot (t_P - t_E) \quad \text{. . . (3-21)}$$

Then, calculate the variables downstream of the wave front, y_2 and V_2, by linear extrapolation from those at E and S.

(b) Determine the water depth and velocity behind the wave front, y_1 and V_1 by using the equations of continuity and momentum and values extrapolated above.

(c) Determine the new value of wave velocity at P by Eq. (3-17). Further determine the new value of wave velocity propagating from R to P by averaging the velocities at R and P.

(d) Repeat the procedures (a) through (c) until the desired accuracy is reached.

(e) Determine the variables at D by equations of characteristics from points R and P.

(f) Determine the variables at Q by equations of characteristics through D Q and the boundary conditions.

3.6.2.2. Determination of the negative wave travelling from R to P, etc. (Figure 3-17)

(a) Determine the variables y_E and V_E , at E, by equations of characteristics.

(b) Determine the wave height and velocity at P by using the procedures mentioned above in 3.6.2.1.a through 3.6.2.1.f.

(c) Determine the variables at points F, Q, ..., K by equations of characteristics.

(d) Continue these computing processes until the negative wave reaches the downstream end.

It should be noted that, for a negative surge wave, the velocity of wave propagation is always less than that for an infinitesimal wave in the region before the front of the surge wave and greater than that for an infinitesimal wave in the region behind the surge wave, i.e., the inverse slope of the line RE (Figure 3-17) is greater than RP which is greater than that of line RF. Therefore, as a negative surge travels downstream continuously along the canal, these lines would diverge. The investigation shows that the unsteady rise behind the positive surge or in the front of a negative surge varies nearly linearly. Therefore, it is logical to assume that the variation of velocity and depth of the flow in the front of the negative wave at P is

linear with respect to time, in a short time period from t_E to t_P, without introducing appreciable errors.

CHAPTER 4 RESULTS OF ANALYSIS

4.1 General

In previous chapters equations and techniques have been developed to calculate the magnitude of the initial wave height and the wave height at any point as the surge wave propagates along the canal. The purpose of this chapter is to find appropriate dimensionless relationships between the variables governing the variation of wave height, the distance of propagation and other flow parameters.

4.2 Dimensionless Ratios

When solving hydraulic transient problems, it is convenient to make use of dimensionless ratios. The introduction of such ratios usually reduces the number of variables involved in the problem and simplifies the solution. In the problem of the variation of wave height, Z, of a surge wave propagating along a power canal, the independent variables involved are the depth y_o, velocity V_o of the initial flow, side slope 1/m and bottom width b_o, canal longitudinal bed slope S_o, the distance x^* of wave propagation, gravitational acceleration g, and the initial wave height Z_o, i.e.,

$$Z = f_1 (g, y_o, V_o, S_o, m, b_o, x^*, Z_o) \quad \ldots\ldots\ldots\ldots \quad (4\text{-}1)$$

It should be noted that the frictional effect is included in Eq. (4-1) because, given the parameters in this equation, the friction factor can be calculated from Manning's formula.

The effect of gravity is represented by a ratio of inertial forces to those of gravity. This ratio is given by the Froude number, defined as

$$F_o = \frac{V_o}{\sqrt{g \cdot y_o}}$$

where V_o and y_o are the mean velocity and depth of the initial flow, g is the gravitational acceleration. This is normally the most important dimensionless ratio in open channel problems and is well-known as Froude's Law.

The ratio x^*/L_R is adopted for the dimensionless abscissa of the distance of wave propagation, where x^* is the distance of propagation of a surge wave from the downstream end, and L_R is the reference length of channel, i.e.,

$$L_R = \frac{y_o}{S_o}$$

Physically, L_R is the length of a horizontal line passing through the water surface at the downstream end and the canal bottom at some point upstream (see Fig. 4-1).

The ratio Z/Z_o is used to represent the relative value of the wave height at any section of canal to its initial value at the downstream end. The shape factor k represents the cross-section characteristics, where $k = b_o/m \cdot y_o$. It should be noted, that the initial wave height Z_o is a function of the Froude number F_o and water depth y_o of the

initial flow, section factor k of the canal and discharge ratio τ. Thus, the Eq. (4-1) may be reduced to

$$\frac{Z}{Z_o} = f_2 (F_o, x^*/L_R, k) \quad \ldots\ldots\ldots\ldots \quad (4\text{-}2)$$

It is thus assumed that the variation of Z/Z_o is a function of F_o and x^*/L_R for a constant value of k. The analysis for the variation of surge waves for different values of k will be discussed for canals of rectangular, triangular and trapezoidal cross-sections, separately.

4.3 Variation of Positive Surge Wave Height in Rectangular Canals

In a rectangular canal, the cross-sectional area is governed by the width and depth of the flow. In this case, m is equal to zero (vertical wall) and the factor k is equal to infinity. Eq. (4-2) is the reduced to

$$\frac{Z}{Z_o} = f_3 (F_o, x^*/L_R) \quad \ldots\ldots\ldots\ldots \quad (4\text{-}3)$$

In order to determine the relationships in Eq. (4-3), F_o, y_o, b_o and S_o were kept as independent variables and V_o, n and Z_o as dependent variables. V_o is determined by Froude's law and the frictional coefficient, n, is determined from Manning's formula. The analyses were carried out by varying the values of F_o, y_o, b_o and S_o systematically in addition to giving values of the initial change in discharge and canal length as the input data for the computer program. When y_o varies from 5 ft. to 40 ft. at 5 ft. intervals, the results of computer runs for given values of F_o,

b_o and S_o, which resulted in a positive wave, that occurred at the downstream end and travelled upstream, are plotted on a dimensionless plane with x^*/L_R as abscissa and Z/Z_o as ordinate. The plot shows that the relationship x^*/L_R versus Z/Z_o does not vary, although the value of y_o varies. Similarly, for given values of F_o, y_o and S_o, the value of b_o is varied from 1 ft. to 60 ft. at 5 ft. intervals, and for given values of S_o is varied from 0.0001 to 0.01 at 0.0005 intervals. Again, the relationship, x^*/L_R versus Z/Z_o does not vary. However, when F_o is varied, while keeping y_o, S_o and b_o constant, the relationship curve does vary. It is therefore concluded that the relation curve Z/Z_o against x^*/L_R varies only with F_o and is independent of the individual values of y_o, b_o and S_o, as indicated in Eq. (4-3). Similar computer runs were carried out for the values of F_o from 0.050 to 0.200 at 0.025 intervals. Results are plotted on Fig. 4-2. It can be seen from this figure that, for a given F_o, the curve is nearly a straight line at higher values of Z/Z_o. The figure shows that the rate of variation of Z/Z_o is initially rapid and nearly constant and then decreases gradually. Theoretically, a wave would need to propagate to infinity before it completely disappears. In this study, the lower limit of Z/Z_o is set to 0.025. Thus, in summary:

(a) The relation curve, Z/Z_o against x^*/L_R, varies with F_o only. It is not effected by the change of individual values of other parameters such as the cross-section, longitudinal slope of the channel, and the roughness of the channel.

(b) For a constant value of Z/Z_o, the higher the value of F_o, the higher will be the value of x^*/L_R. This does not imply, that the wave travels a longer distance to reach a given reduction in wave height, because a flow with a higher value of F_o is always associated either with a larger longitudinal slope S_o and a smaller value of L_R, or with a smaller roughness of channel and a smaller depth of flow y_o, and thus with a smaller L_R.

4.4 Variation of Positive Surge-Wave Height in Triangular Canals

A canal with a triangular cross-section is not often used in practice. It is a limiting case of the trapezoidal cross-section where the bottom width is zero. Two variables, depth and side slope, are involved in controlling the cross-section area. In this case, the shape factor k is equal to zero. Eq. (4-2) is then again reduced to Eq. (4-3). A systematic analysis similar to that for rectangular canals in section 4-3 was used. Similar relation curves were obtained. Eq. (4-3) is valid for a triangular canal. The characteristics of the variation of relative wave height Z/Z_o against x^*/L_R in section 4-3(a) and (b) also hold. The curve does not depend on side slope of the canal. The results of the variation of a positive wave propagating along a triangular canal with F_o from 0.05 to 0.20 at 0.025 intervals are plotted in Fig. 4-3.

4.5 Variation of Positive Surge Wave Height in Trapezoidal Canals

The trapezoidal cross-section is one of the most common shapes used for canals. For this case, the cross-sectional area is governed by depth y_o, bottom width b_o and side slope 1/m. The shape factor k can vary between 0 and ∞. For given values of F_o and k, a systematic analysis similar to that for rectangular and triangular canals is used, i.e., the value of one variable is changed and the others held constant. The results show that the curve Z/Z_o against x^*/L_R does not change for fixed values of F_o and k. Therefore, Eq. (4-2) is valid for a surge variation in a trapezoidal canal.

For given values of F_o, and for values of k = 0, 0.333, 0.500, 1.000, 1.667, 2.500, 5,000 and ∞ surge calculations were made. Results for F_o = 0.200, are plotted on Fig. 4-4. From this family of curves, it can be seen that the higher the value of k, the higher is the value of x^*/L_R for a given Z/Z_o. The curves with $k = \infty$ and k = 0 are two limiting curves. These coincide with those drawn for a rectangular and a triangular canal respectively.

For a given k, the relation curve Z/Z_o versus x^*/L_R, varies with F_o. For each given value of k, there is a family of curves corresponding to various values of F_o. For r = 1+1/(1+k) having

values of 1.50 and 1.75, the results for F_o varying from 0.05 to 0.20 at 0.025 intervals are shown on Figs. 4-5 and 4-6 respectively, where r is given in Eq. (4-6).

The remarks in section 4.3(b) also apply for a trapezoidal canal.

4.6 Approximate Equations

As it has been mentioned earlier, the relation curve Z/Z_o against x^*/L_R is nearly a straight line at higher values of Z/Z_o. Therefore for Z/Z_o values greater than 0.6, the curve may be approximated by a straight line without introducing significant errors. When Z/Z_o is less than 0.6, the curve may be expressed by an exponential function. The approximated formulas representing the best fit by the "least square" method are given in the following sections:

4.6.1 Approximate equations for the variation of a positive surge wave propagating along a rectangular canal

(a) For $\frac{Z}{Z_o}$ greater than 0.60 the equation suggested is

$$\frac{Z}{Z_o} = 1.0 + 0.1876 \left[1.0 - \frac{1.0}{0.3899\ F_o - 0.00037} \right] \cdot \left(\frac{x^*}{L_R} \right) \quad \ldots\ldots\ldots (4\text{-}4a)$$

(b) For $\frac{Z}{Z_o}$ less than 0.60 the equation suggested is

$$\frac{Z}{Z_o} = A + B \cdot \exp\left(C \cdot x^*/L_R\right) \quad \ldots\ldots\ldots (4\text{-}4b)$$

where $A = \dfrac{F_o}{26.54\ F_o - 6.7334} - 0.01589$

$B = 1.167 + 0.6728\ F_o$

$C = 3.045 - 1.702\ F_o^{-0.7985}$

Eqs. (4-4a) and (4-4b) are plotted on Fig. 4-2 for comparison. It can be seen that the values estimated from the equations are good approximations. When a surge wave travels along the channel with a given initial flow for which the Froude number is different than those shown on Fig. (4-2), the variation of the wave height may be obtained from the above equations.

4.6.2 Approximate equations for the variation of a positive surge wave propagating along a triangular canal.

(a) For $\frac{Z}{Z_o}$ greater than 0.60 use equation

$$\frac{Z}{Z_o} = 1.0 + 3.041 \left[1.0 - \frac{1.0}{0.4358\ F_o + 0.000092} \right] \cdot \left(\frac{x^*}{L_R}\right) \qquad \ldots\ldots\ldots (4\text{-}5a)$$

(b) For $\frac{Z}{Z_o}$ less than 0.60 use equation

$$\frac{Z}{Z_o} = A + B \cdot \exp\left(C \cdot x^*/L_R\right) \qquad \ldots\ldots\ldots (4\text{-}5b)$$

where $A = -(0.0352 + 1.479 \cdot F_o^2)$

$B = 0.642 \cdot F_o + 1.205$

$C = -(0.7485 \cdot F_o^{-1.135} + 0.6106)$

Eqs. (4-5a) and (4-5b) are also plotted on Fig. 4-3. For a surge propagating along a triangular canal, the variation of wave height may be predicted from these equations.

4.6.3 Approximate equations for the variation of a positive surge wave propagating along a trapezoidal canal.

From Fig. 4-4, it is seen that the value of k varies from zero to infinity for various sizes of trapezoidal cross-section canals. To simplify mathematical treatment, the parameter r was used to substitute for k, where,

$$r = 1 + \frac{1}{1 + k} \quad \ldots\ldots\ldots\ldots\ldots\ldots \quad (4\text{-}6)$$

Thus $r = 1$ when $k = \infty$, and $r = 2$ when $k = 0$. The value of r varies between 1 and 2 for trapezoidal cross-sections. For a given F_o and Z/Z_o, the variation of x^*/L_R versus k is nonlinear. A parameter ϕ may be defined, such that

$$\phi = \frac{\left(\frac{x^*}{L_R}\right)_{r = n}}{\left(\frac{x^*}{L_R}\right)_{r = 1}} \quad \ldots\ldots\ldots\ldots\ldots\ldots \quad (4\text{-}7)$$

in which $\left(\frac{x^*}{L_R}\right)_{r = 1}$ is the value of $\left(\frac{x^*}{L_R}\right)$ appropriate to the curve of r = 1, i.e., for a rectangular canal; and $\left(\frac{x^*}{L_R}\right)_{r = n}$ is that for the curve of r = n of a given trapezoidal canal for a given Z/Z_o. Values of ϕ were plotted against r on log-log paper, Fig. 4-7, and it was found that the points located approximately on a straight line. Therefore, it

may be concluded that the relationship between ϕ and r is a logarithmic function. It may be assumed to be

$$\phi = c\, r^{-d} \quad \ldots\ldots\ldots\ldots\ldots\ldots \quad (4\text{-}8)$$

where c and d are the coefficients to be determined. This relationship holds for various values of Z/Z_o and F_o. Because all curves have to pass the point of $x^*/L_R = 0$ and $Z/Z_o = 1.0$, i.e., when $r = 1.0$ and $\phi = 1.0$, c is equal to 1.0. Thus Eq. (4-8) is simplified to

$$\phi = r^{-d} \quad \ldots\ldots\ldots\ldots\ldots\ldots \quad (4\text{-}9)$$

where the value of d is equal to the negative slope of the curve on Fig. (4-7). The exponent d, determined by the least square method is equal to 0.565. Eq. (4-8) then becomes

$$\phi = r^{-0.565} \quad \ldots\ldots\ldots\ldots\ldots\ldots \quad (4\text{-}10)$$

Using this equation, the value of ϕ may be obtained provided the shape factor k is given. From Eq. (4-7), the distance of propagation of a surge for a certain amount of reduction of wave height in a trapezoidal canal can be predicted by

$$\left(\frac{x^*}{L_R}\right)_{r=n} = \phi \cdot \left(\frac{x^*}{L_R}\right)_{r=1} \quad \ldots\ldots\ldots \quad (4\text{-}11)$$

where $\left(\frac{x^*}{L_R}\right)_{r=1}$ may be obtained from Eqs. (4-4a) or (4-4b) provided F_o is given. Comparison of the estimate from Eqs. (4-4a), (4-4b) and (4-11) with the computer results are shown

on Figs. 4-5 and 4-6. Two examples are shown to illustrate the application of these formulas.

Example 4 - 1

Given $F_o = 0.1$, $S_o = 0.001$, $m = 1.0$, $b_o = 10$ ft, $y_o = 10$ ft. For the case of total closure and for $Z/Z_o = 0.3$, find the distance of propagation of a surge moving along a trapezoidal canal.

Solution

$$L_R = \frac{y_o}{S_o} = 10{,}000 \text{ ft.}$$

$$k = \frac{b_o}{m.y_o} = 1.0$$

$$r = 1 + \frac{1}{1 + k} = 1.5$$

when $F_o = 0.1$, and $Z/Z_o = 0.3$, it is found from Fig. 4-4

$$\left(\frac{x^*}{L_R}\right)_{r = 1} = 0.1715$$

$$\phi = r^{-0.565} = 0.7958$$

$$\left(\frac{x^*}{L_R}\right)_{r = 1.5} = 0.1715 \cdot (0.7958) = 0.1365$$

$$x^* = 1365 \text{ ft.}$$

From Fig. 4-5, $\left(\frac{x^*}{L_R}\right)_{r = 1.5} = 0.1370$

$$x^* = 1370 \text{ ft.}$$

It may be seen that the distance estimated from proposed formula is fairly accurate.

The above equations may also be used to estimate the wave height or the distance of propagation of a surge travelling in a triangular canal in which r = 2.0 and ϕ = 0.6761.

Example 4-2

Given $F_o = 0.125$, $Z/Z_o = 0.30$, $S_o = 0.001$, $y_o = 10$ ft., find the distance of propagation of a surge wave travelling along a triangular canal.

Solution:

$$L_R = \frac{10}{0.001} = 10{,}000 \text{ ft.}$$

(a) From Fig. 4-2, $\left(\frac{x^*}{L_R}\right)_{r=1} = 0.2160$

By using Eq. (4-11)

$$\left(\frac{x^*}{L_R}\right)_{r=2} = 0.6761 \cdot (0.2160) = 0.1465$$

$$x^* = 1465 \text{ ft.}$$

(b) From Fig. 4-3, it is found $\left(\frac{x^*}{L_R}\right)_{r=2} = 0.1480$

$$x^* = 1480 \text{ ft.}$$

(c) Using Eq. (4-5b), A = 0.583, B = 1.2850 and C = 8.5296

$$\frac{x^*}{L_R} = 0.1498$$

$$x^* = 1498 \text{ ft.}$$

Percentage error of (a) $= \frac{1480 - 1465}{1480} = 1.6\%$

Percentage error of (c) $= \frac{1480 - 1498}{1480} = -1.2\%$

4.7 Reduction of Wave Height After Reflection at a Reservoir located at the Upper End of the Canal

When water enters a mild slope channel, the depth y_1 (Fig. 4-8) is related to the static reservoir level by the energy equation. The relation between the depths y_1 and y_R can be expressed by

$$y_R = y_1 + y_e + \mu \cdot \frac{V_1^2}{2g} \quad \ldots\ldots\ldots \quad (4\text{-}12)$$

where y_e is the head loss due to friction at entrance and may be expressed in terms of the velocity head at the entrance of the canal, that is

$$y_e = C_e \cdot \frac{V_1^2}{2g} \quad \ldots\ldots\ldots\ldots\ldots \quad (4\text{-}13)$$

in which C_e is a coefficient which depends on the conditions at entrance.

Assuming the entrance loss y_e is negligible, Eq. (4-12) can be rewritten

$$y_R = y_1 + \mu \cdot \frac{V_1^2}{2g} \quad \ldots\ldots\ldots\ldots \quad (4\text{-}14)$$

When the water empties into a reservoir, an amount of kinetic energy equal to $\mu \cdot \frac{V_1^2}{2g}$, carried with the flowing water, is expected to be restored as a potential energy. Thus, the reservoir level should be higher by this amount than the water level at the upstream end of the canal. This energy, however is usually dissipated in eddies and whirls. In practical calculations it may be ignored, and y_1 may be regarded as equal to y_R (no velocity head recovery).

A positive surge wave reaching the reservoir at the upstream end of the canal will be reflected as a negative wave which then proceeds downstream. The flow direction at the entrance after the wave is reflected, will depend on the length and slope of the channel. In general, in a short channel, of mild slope water velocity will be reversed i.e., water flows into the reservoir. In a long canal however, the velocity of flow is reduced but usually there is no change in direction (water still flows into the canal). The amount of reduction of wave height will therefore, depend on the direction of the flow at the section of entrance immediately after the negative wave passes. If the flow direction changes (reverse to the initial direction), the reduction of wave height ΔZ is:

$$\Delta Z = y_2 - y_1 \simeq y_R - y_1$$

or
$$\Delta Z = \mu \cdot \frac{V_1^2}{2g} \qquad \ldots\ldots\ldots \quad (4\text{-}15)$$

If the flow does not change direction, the reduction of wave height is:

$$\Delta Z = y_R - y_1 - \mu' \cdot \frac{V_2^2}{2g} \ldots\ldots\ldots \quad (4\text{-}16)$$

Assuming the value of V_2 is small and $\mu' \cdot \frac{V_2^2}{2g}$ is negligible, Eq. (4-16) is identical to Eq. (4-15), and ΔZ is a function of initial velocity. Therefore, the reduction of wave height after reflection at the entrance of the canal can be obtained approximately by Eq. (5-15) regardless the direction of the flow after reflection at that section.

It has been shown in Chapter 2 that the initial wave height at the downstream end depends on the Froude number of the flow. Thus the ratio $\Delta Z/Z_o$ is a function of the Froude number (see Fig. 4-10). The approximate equations for calculating $\Delta Z/Z_o$ in rectangular, triangular and trapezoidal canals are found in the following.

4.7.1 Equation for rectangular canals

For rectangular canals, $\Delta Z/Z_o$ varies with Froude number, and the distribution is linear on log-log paper with F_o as abscissa and $\Delta Z/Z_o$ as ordinate. Using the least square method for best fit, the equation obtained is

$$\frac{\Delta Z}{Z_o} = 0.4533\ F_o^{0.968} \quad \ldots\ldots\ldots\ldots \quad (4\text{-}17)$$

4.7.2 Equation for triangular canals

For triangular canals, the corresponding equation is

$$\frac{\Delta Z}{Z_o} = 0.6631\ F_o^{0.979} \quad \ldots\ldots\ldots\ldots \quad (4\text{-}18)$$

4.7.3 Equation for trapezoidal canals

For trapezoidal canals, it is found that $\Delta Z/Z_o$ varies not only with Froude number but also with the parameter r. For a given value of r, the relationship between $\Delta Z/Z_o$ and F_o is similar to that for the rectangular and triangular canals. The equation is of the form

$$\frac{\Delta Z}{Z_o} = P_1 \cdot F^{P_2} \quad \ldots\ldots\ldots\ldots\ldots\ldots \quad (4\text{-}19)$$

where p_1 and p_2 are the coefficients to be determined. P_1 and

p_2 are the functions of r. They are determined as

$$p_1 = 0.4533\ r^{0.5490} \quad \ldots\ldots\ldots\ldots \quad (4\text{-}20)$$

$$P_2 = 0.9680\ r^{0.01628} \quad \ldots\ldots\ldots\ldots \quad (4\text{-}21)$$

Therefore Eq. (4-19) becomes

$$\frac{\Delta Z}{Z_o} = 0.4522\ r^{0.5490} \cdot F_o^{\,0.9680\ r^{0.01628}} \quad \ldots \quad (4\text{-}22)$$

Eq. (4-22) is valid for the values of r from 1.0 to 2.0 which means that Eq. (4-22) is also valid for rectangular and triangular canals because when the values of r are equal to 1.0 and 2.0, the Eq. (4-22) is identifical to Eq. (4-20) and (4-21) respectively.

4.7.4 Alternative procedure

$\Delta Z/Z$ also can be found by an alternative procedure based on derivations in Chapter 2. Dividing both sides of the equation

$$\Delta Z = \frac{V_1^2}{2g}$$

by Z_o, it becomes

$$\frac{\Delta Z}{Z_o} = \frac{V_1^2}{2g \cdot Z_o} = \frac{F_o^{\,2}}{\frac{2Z_o}{y_o}} = \frac{F_o^{\,2}}{2\beta} \quad \ldots \quad (4\text{-}23)$$

where $\beta = Z_o/y_o$

The values of $\Delta Z/Z_o$ for various flows in rectangular, triangular and trapezoidal canals can be found from Eq. (4-23) with Eqs. (2-13), (2-18) and (2-23) respectively.

4.8 Propagation of Negative Waves Reflected from a Reservoir at the Upper End of a Prismatic Power Canal

Negative waves are not stable in form because points on the upper part of the wave travel faster than those on the lower part. If the height of the wave is relatively large, compared with the depth of the flow, the wave velocity varies from point to point along the wave front. The initial profile of negative surge waves having a steep front will flatten out as the waves travel along the canal. If the height of the wave is moderate or small, the equations in Chapter 2, derived for a positive wave, can be applied to determine approximately the height and velocity of negative waves. The negative waves reflected from the reservoir may be small, compared with the depth. For a wave with a height of less than 20% of the depth the error introduced by assuming that the negative wave proceeds downstream with an unchanging profile will be insignificant. In this study the calculations for negative waves are based on the above assumption. The equations for positive waves (Chapter 2) are then assumed to be valid for negative waves.

The basic expressions for calculating the propagation of negative waves, which result from reflection at the upper end of the canal are presented in Chapter 3.

Similarly to the calculations for a positive surge wave, systematic variation of the variables for different shapes of canals was used as the input to the computer program. Results obtained for the negative waves are plotted on the same dimensionless plane

together with those for positive waves. The variation of the relative height, Z/Z_o, of the negative wave in term of x^*/L_R is shown in Figure 4-10a through 4-12g.

From these figures the following points are observed:

1. When a wave is reflected at a given value of x^*/L_R (or a given value of Z/Z_o) the shape of the curve is independent of the initial parameters y_o, V_o and S_o for a given F_o and r.
2. For a given F_o and r the shape of curve for a reflected wave depends on the location (x^*/L_R) of the point of reflection.
3. The rate of reduction in height of a negative wave diminishes gradually as the wave travels downstream.

4.9 Maximum Water Depth at Downstream End of Canal

When a surge wave occurs at the downstream end of the canal due to the load rejection, the water depth at the downstream end increases suddenly by the amount equal to the initial wave height. As the wave front travels upstream, the water surface does not remain stationary. This is because the discharge of the flow is reduced, the velocity is also reduced, and the kinetic energy of the flow is converted to potential energy in the form of an increased height of the water surface at the downstream end. Figs. 4-13 and 4-14 illustrate the elementary fashion of this variation of water depth in the positive and negative wave propagating cycle.

The depth of water at the downstream end increases with time. The rate of increase is initially approximately linear with time.

If the depth is expressed by the ratio y/y_o, then the rate of variation of y/y_o with respect to time increases with larger values of the Froude number. For a flow with a given Froude number, the rate of increase in y/y_o also varies with canal characteristics, such as longitudinal bed slope, frictional roughness and shape. If the cross-section of the canal is given, the rate of increase in y/y_o increases with the increasing of S_o.

As an example, for a rectangular canal, with b_o = 30 ft., y_o = 30 ft. and n = 0.03095, the curves with various given Froude numbers are plotted in Fig. 4-15. Similar curves for the triangular canal of y_o = 22.36 ft., m = 2.0 and n = 0.03095 and the trapezoidal canal of b_o = 25.5 ft., m = 1.5, n = 0.03095 and r = 1.5 are plotted in Fig. 4 - 16 and Fig. 4 - 17 respectively. It is interesting to note that the slopes of curves increase as the values of cross-sectional shape factor r decrease.

After gate closure the depth at the downstream end increases continuously until this is interrupted by the arriving negative wave, reflected from the upper end of the canal and then decreases rapidly by an amount of about twice the negative wave height. The maximum water depth therefore occurs at the time immediately before the arrival of the negative wave front. As has been mentioned before, this maximum water depth is one of the most important items of information in the design of the canal.

In this study, systematic variation of individual variables was

used as input to the computer program. Results are plotted on a dimensionless plane with y_{max}/y_o as ordinate and $2L/L_R$ as abscissa, where L is the canal length. For rectangular canals, it is found that the curve of y_{max}/y_o against $2L/L_R$ does not change with the various values of b_o, y_o and S_o if the Froude number of initial flow, F_o is fixed. This relation also holds for triangular canals. For the trapezoidal canal, one more variable, r, is introduced. The curve y_{max}/y_o against $2L/L_R$ varies not only with F_o but also with r. For a given Froude number, the value of y_{max}/y_o increases with increasing value of r. For a given r, the value of y_{max}/y_o varies with F_o. The results of computer calculations for a maximum stage developed at the downstream end due to a sudden reduction in discharge in rectangular, triangular and trapezoidal (for r = 1.5) canals are plotted in Figs. 4 - 18, 4 - 19 and 4 - 20.

CHAPTER 5 CONCLUSIONS

The primary objective of this study was to derive dimensionless ratios to describe the initiation and propagation of a surge wave in a power canal following a load reduction or rejection.

The initial surge-wave height, resulting from an instantaneous reduction of discharge, varies with the shape and dimensions of a canal and with the amount of the initial flow. This study shows that, in dimensionless terms, the relative initial wave height is a function of the shape factor k, discharge ratio τ and the Froude number of the initial flow F_o. For a sudden total closure, i.e., $\tau = 0$, β is only a function of F_o in a rectangular and triangular canal, and is a function of F_o and k in a trapezoidal canal. A dimensionless equation, Eq. (2-23), derived in this study can be applied to predict an initial surge wave height due to a sudden total or partial change in discharge in canals of rectangular, triangular and trapezoidal cross-sections.

The results of calculations from the mathematical model developed in this study are in close agreement with those from the methods proposed by previous investigators, in particular, with the results from the Favre method applied to short canals.

When a positive surge wave is initiated at the downstream end of a canal and propagates upstream, the wave height decreases gradually. The rate of decrease of wave height depends on canal parameters such as the frictional coefficients, the bed slope, the shape and dimensions of the cross-section and the initial flow.

This decrease of wave height is approximately linear for a distance, for which Z/Z_o is still greater than 0.6. When Z/Z_o becomes less than 0.6, the variation of wave height is more an expotential function of x^*/L_R. The deviation from Favre's assumption for a straight line water surface profile increases with increasing distance from the point of the initiation of the wave. The writer has derived dimensionless equations from which the wave height of a positive surge at any section of a rectangular and a triangular canal may be predicted. Eq. (4-4) is for rectangular canals, and Eq. (4-5) is for triangular canals. The influence of shape and size of the cross-section of a canal on the variation of wave height of a positive surge, may be expressed by a logarithmatic function. Eqs. (4-10) and (4-11) give the relationship of surge wave heights in a trapezoidal and rectangular cross-section. Using these two equations, the variation of wave height in a trapezoidal canal can be predicted from Eq. (4-4).

In a long canal where a negative surge wave, reflected from the reservoir at the upper end of the canal, travels downstream, the reduction of its height is initially rapid. This becomes gradually smaller as the wave travels toward the greater water depth. In a very long canal, a negative wave may propagate downstream for a long distance with little attenuation after this initial reduction.

The rise of the water surface behind the wave front at the downstream end of the canal is not linear with respect to the time. The rate of this rise in the water surface increases with larger values of the Froude number F_o of initial flow. The maximum water depth at the down-

stream end of the canal, caused by a reduction in discharge, occurs immediately before the arrival of a negative surge wave that resulted from reflection at the upper end of the canal. This maximum depth depends on the slope, length and cross-section of the canal and the initial flow.

The dimensionless relationships derived in this study may be used to establish design criteria for crest elevations of the banks and walls of power canals to avoid overtopping. In this criteria some allowance must be made for secondary surges not analysed in this thesis and for a minimum desired freeboard.

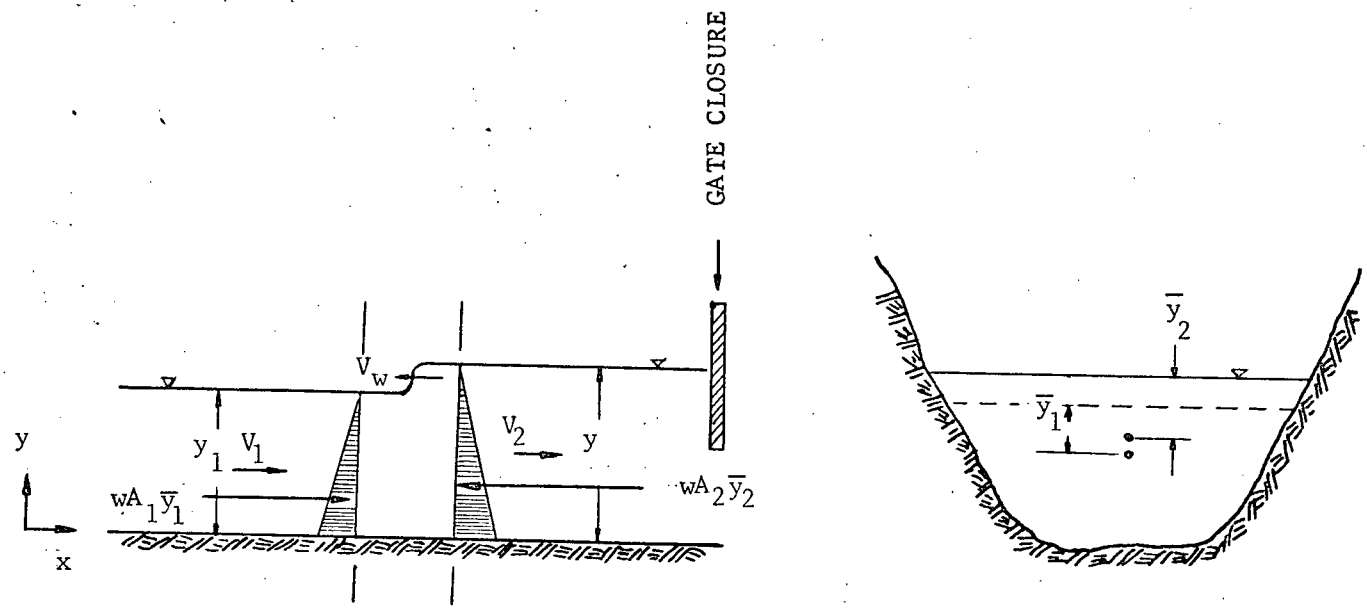

FIG. 2-1 DEFINITION SKETCH : SURGE WAVE IN AN OPEN CHANNEL

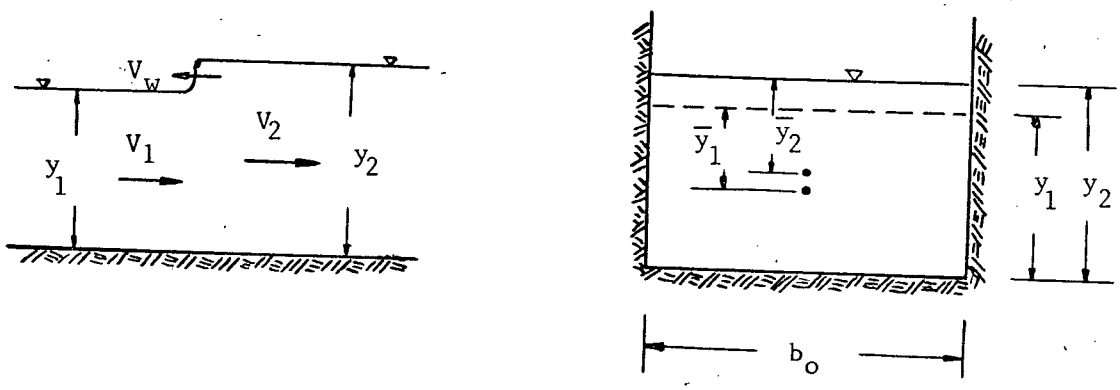

$$A_1 = b_o \cdot y_1 \qquad A_2 = b_o \cdot y_2$$

$$\bar{y}_1 = y_1/2 \qquad \bar{y}_2 = y_2/2$$

FIG. 2-2 DEFINITION SKETCH : SURGE WAVE IN A RECTANGULAR CANAL

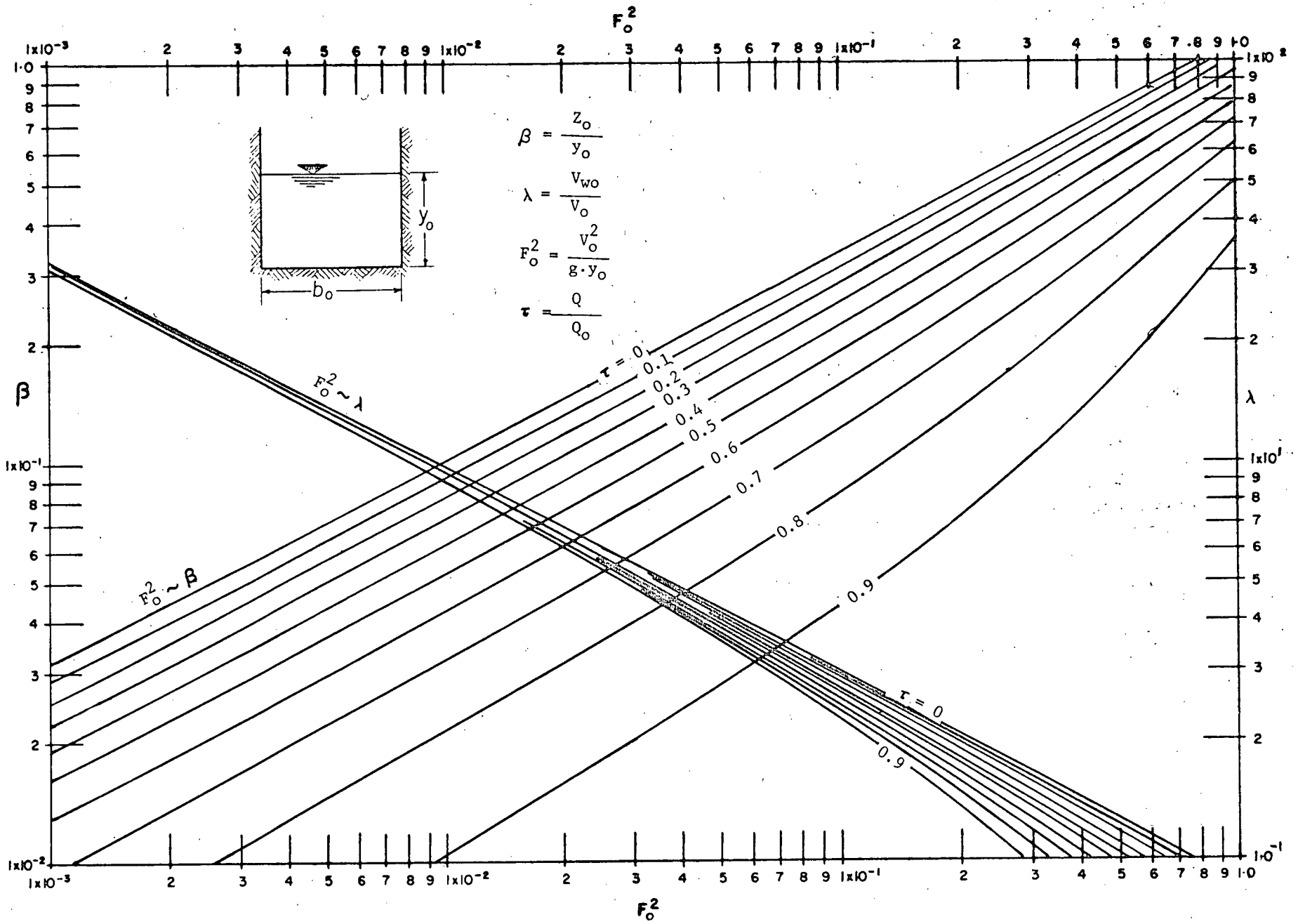

FIG. 2-3 INITIAL SURGE WAVES IN A RECTANGULAR CANAL

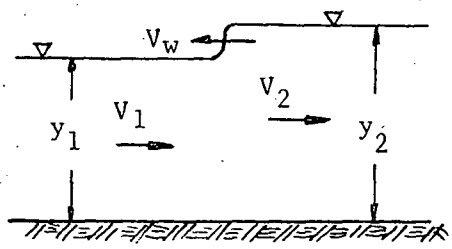

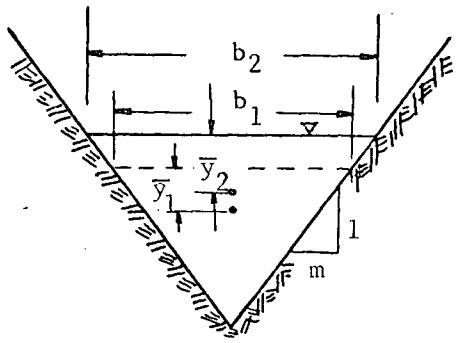

$$A_1 = m \cdot y_1^2 \qquad A_2 = m \cdot y_2^2$$

$$b_1 = 2m \cdot y_1 \qquad b_2 = 2m \cdot y_2$$

$$\bar{y}_1 = y_1/3 \qquad \bar{y}_2 = y_2/3$$

FIG. 2-4 DEFINITION SKETCH : SURGE WAVE IN A TRIANGULAR CANAL

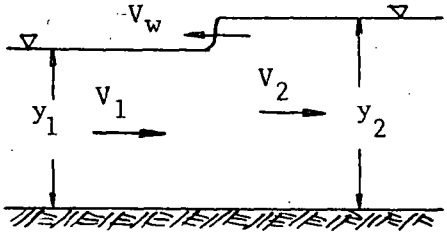

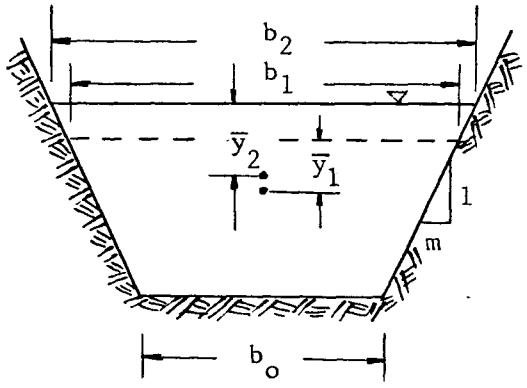

$$b_1 = b_o + 2m \cdot y_1 \qquad b_2 = b_o + 2m \cdot y_2$$

$$A_1 = y_1 \cdot (b_o + m \cdot y_1) \qquad A_2 = y_2 \cdot (b_o + m \cdot y_2)$$

$$\bar{y}_1 = \frac{y_1}{6} \cdot \frac{3b_o + 2m \cdot y_1}{b_o + m \cdot y_1} \qquad \bar{y}_2 = \frac{y_2}{6} \cdot \frac{3b_o + 2m \cdot y_2}{b_o + m \cdot y_2}$$

FIG. 2-6 DEFINITION SKETCH : SURGE WAVE IN A TRAPEZOIDAL CANAL

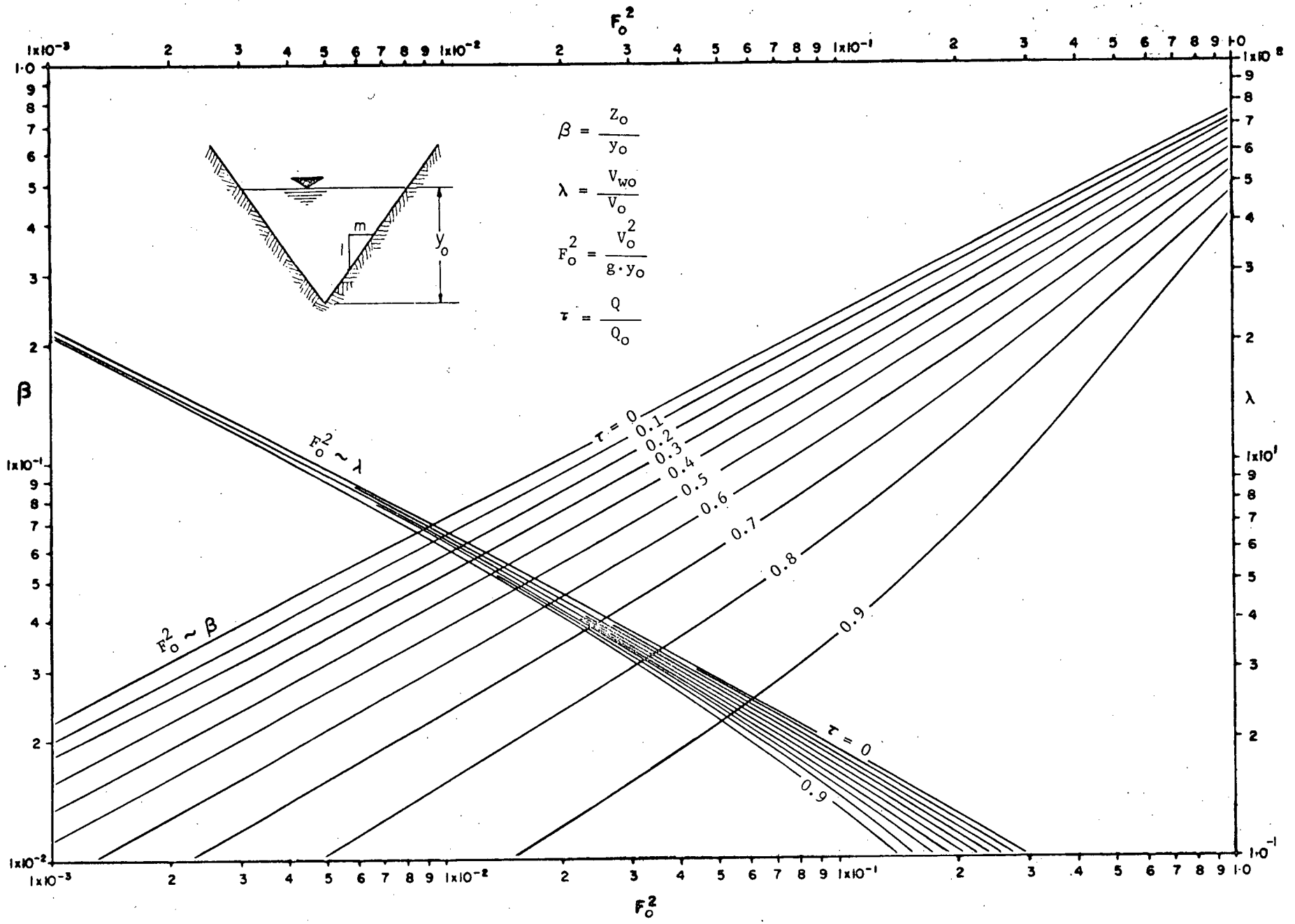

FIG. 2-5 INITIAL SURGE WAVES IN A TRIANGULAR CANAL

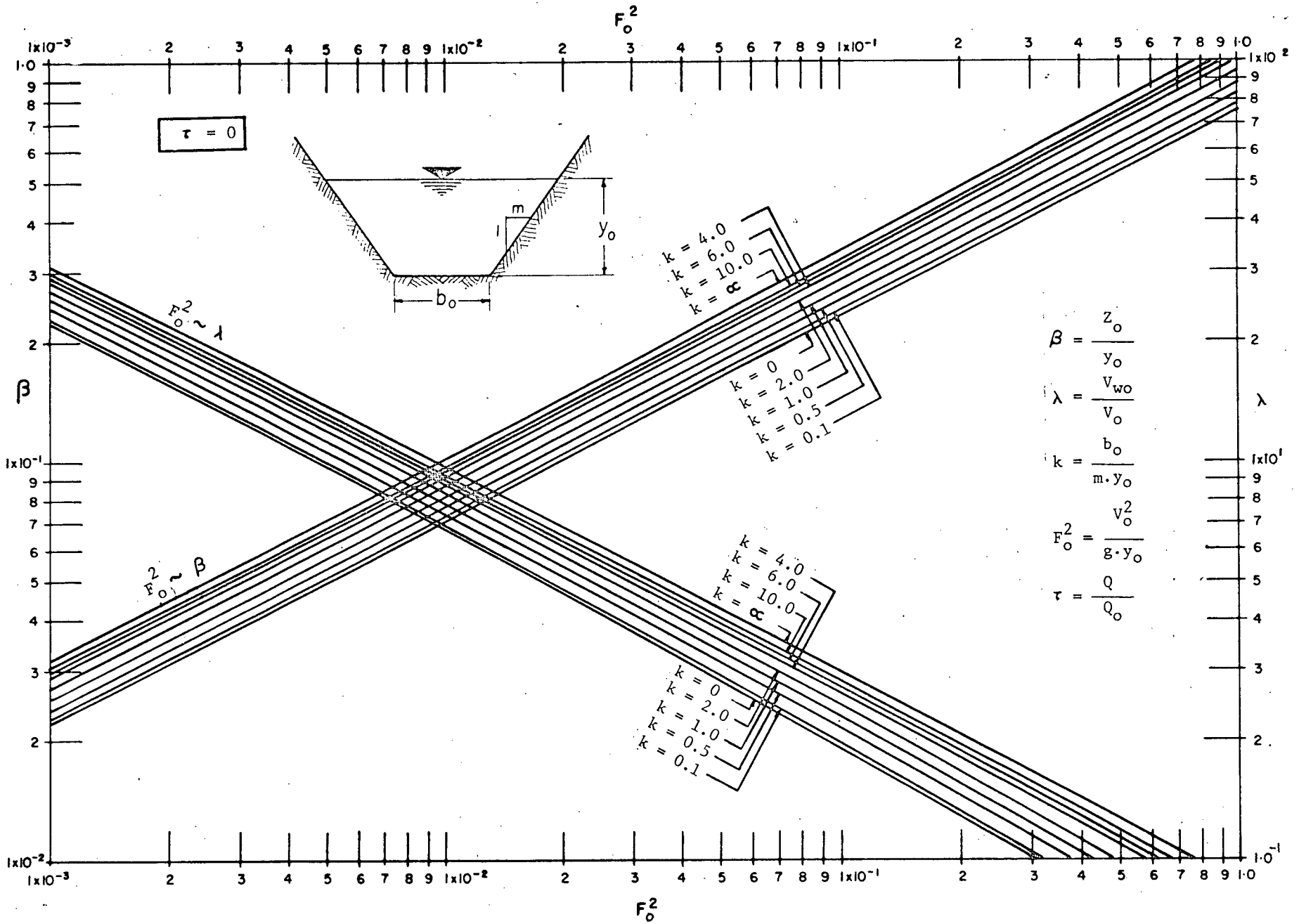

FIG. 2-7 (a) INITIAL SURGE WAVES IN A TRAPEZOIDAL CANAL FOR $\tau = 0$

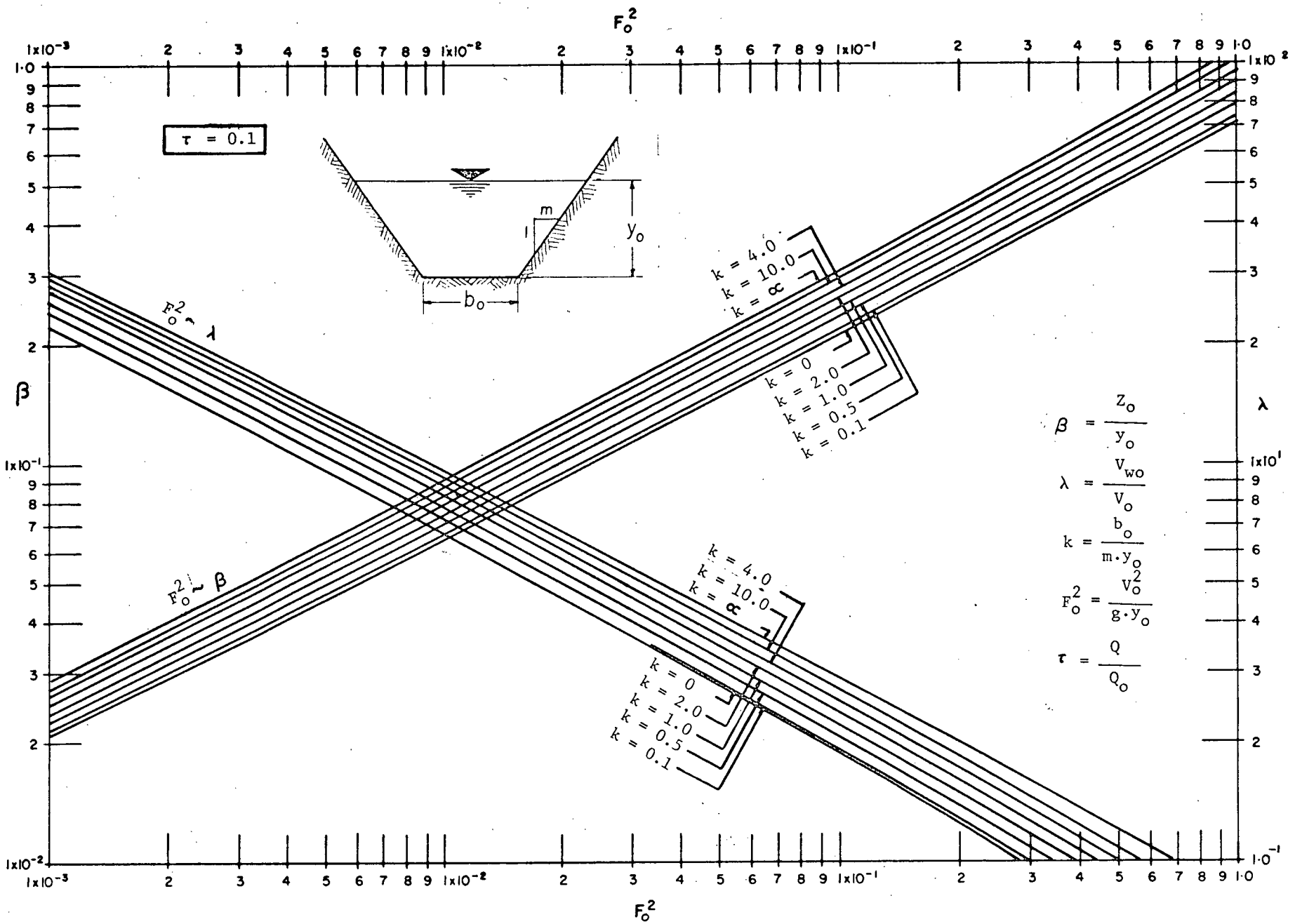

FIG. 2-7 (b) INITIAL SURGE WAVES IN A TRAPEZOIDAL CANAL FOR $\tau = 0.10$

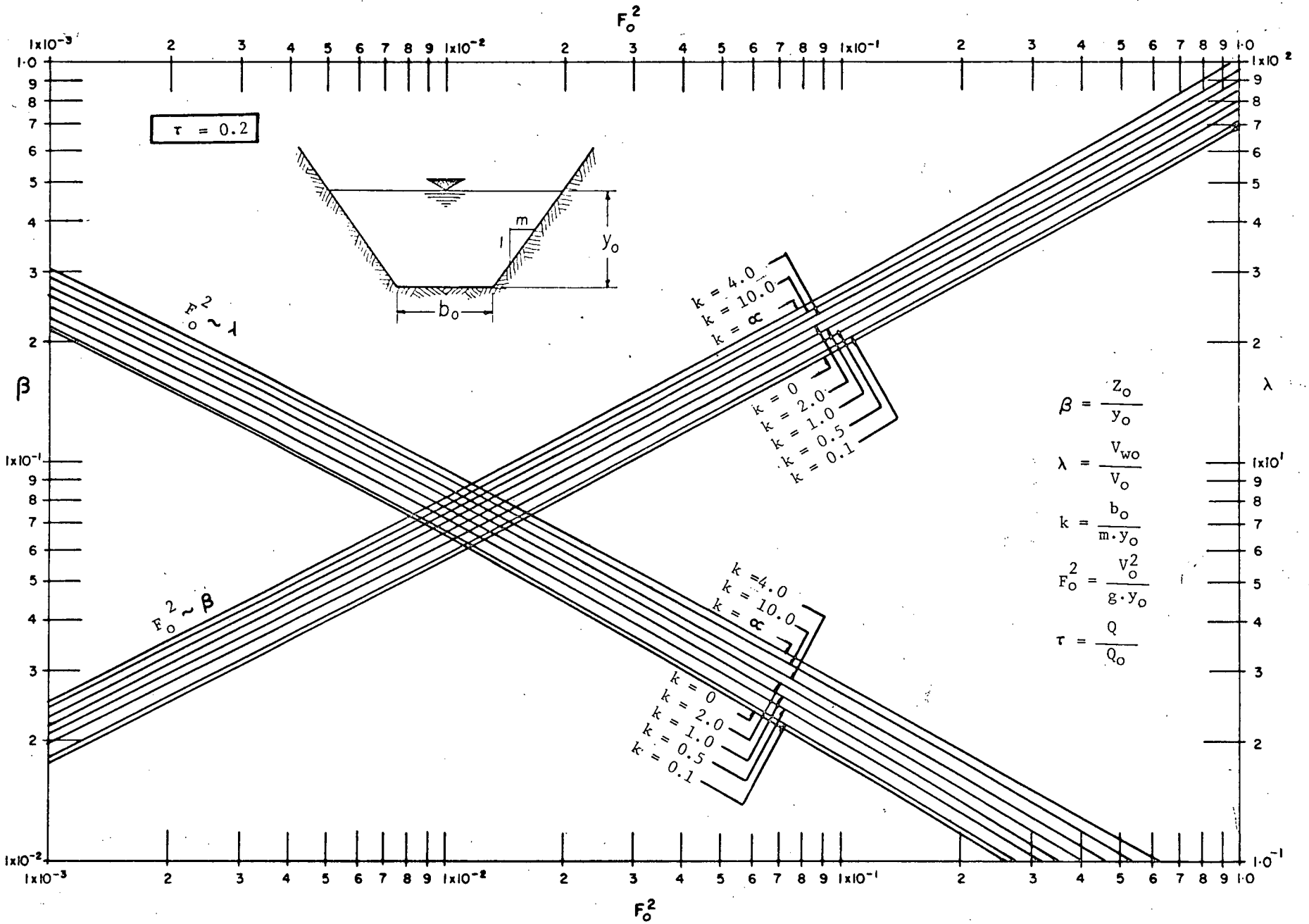

FIG. 2-7 (c) INITIAL SURGE WAVES IN A TRAPEZOIDAL CANAL FOR τ = 0.20

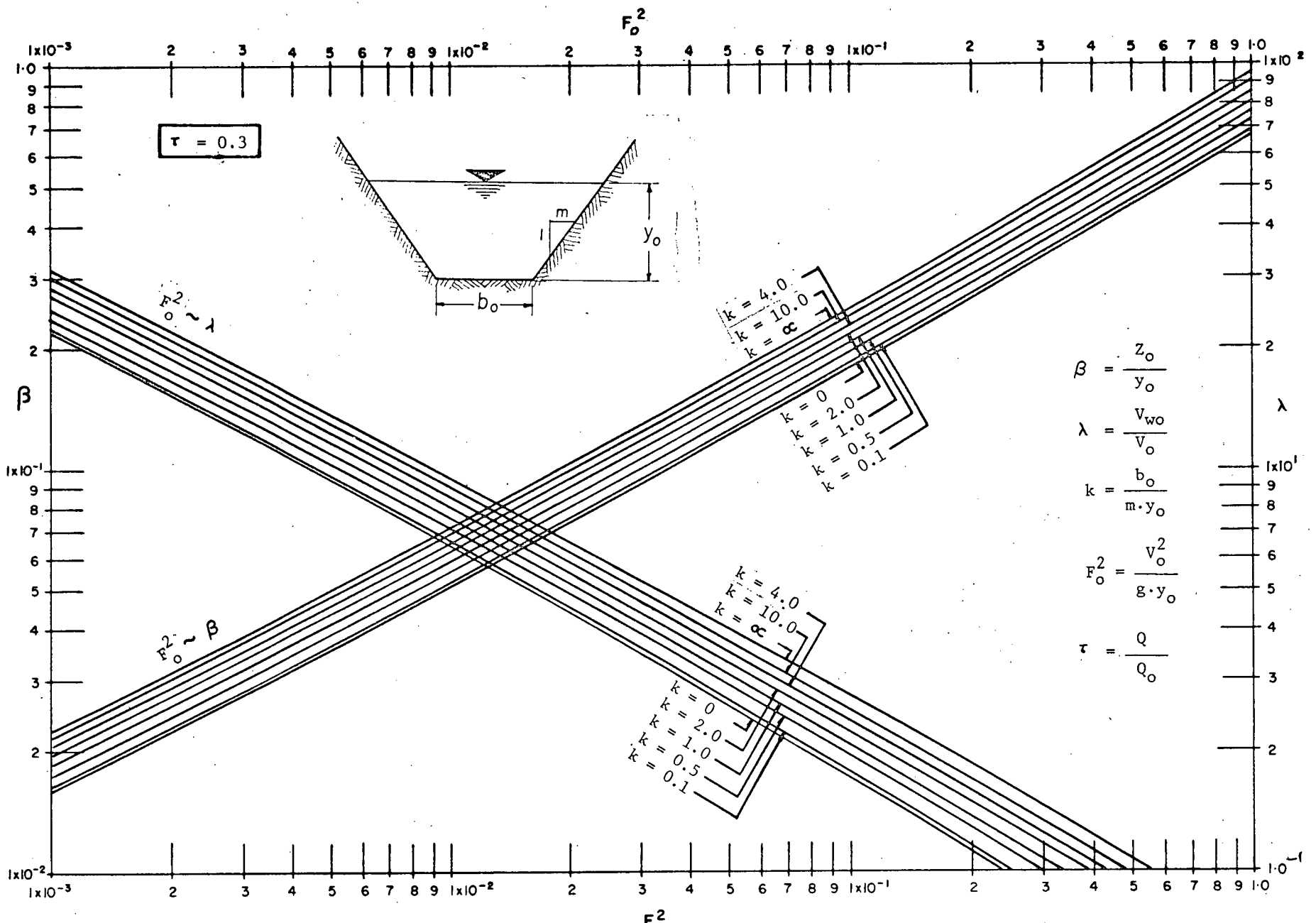

FIG. 2-7 (d) INITIAL SURGE WAVES IN A TRAPEZOIDAL CANAL FOR τ = 0.30

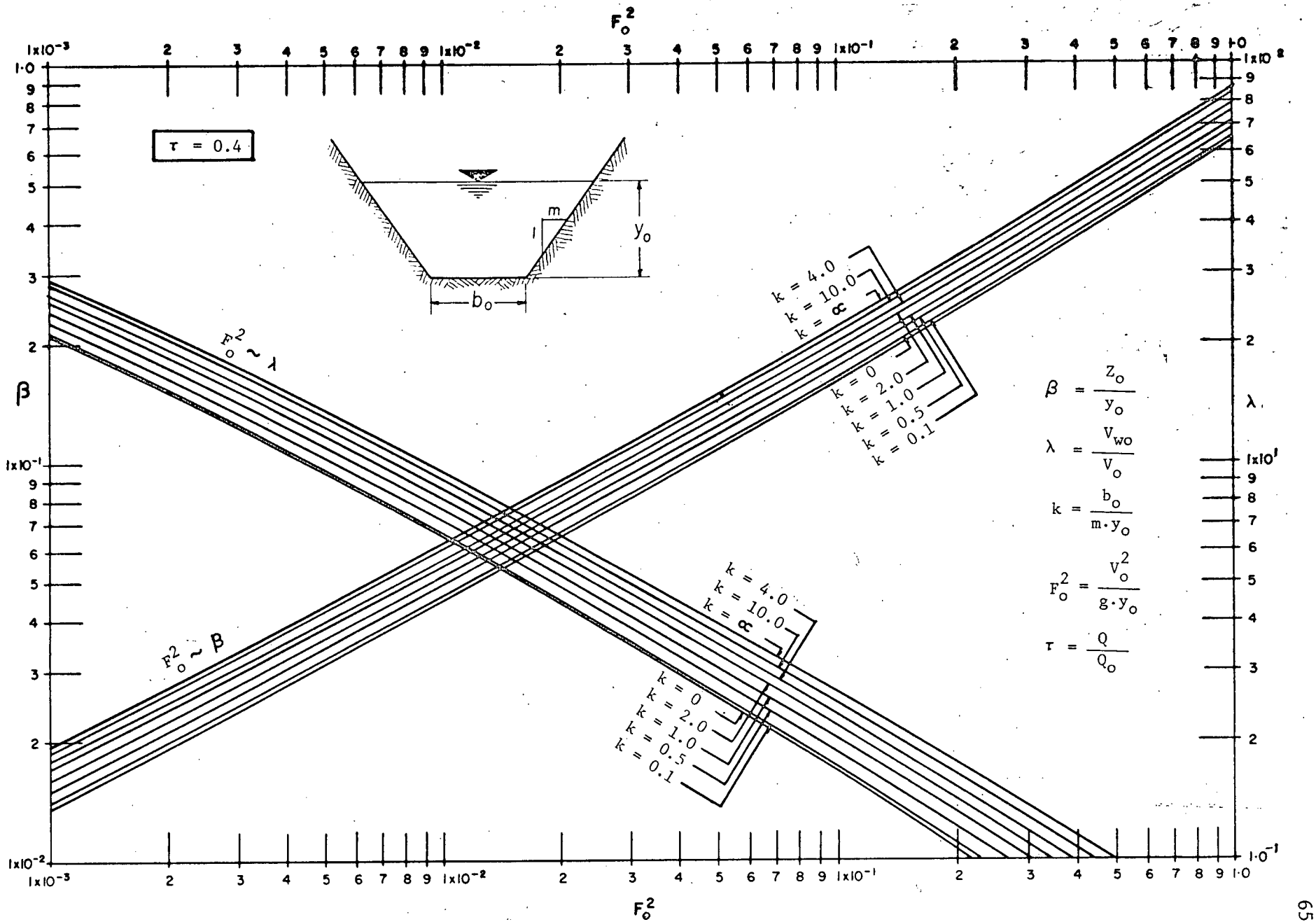

FIG. 2-7 (e) INITIAL SURGE WAVES IN A TRAPEZOIDAL CANAL FOR $\tau = 0.40$

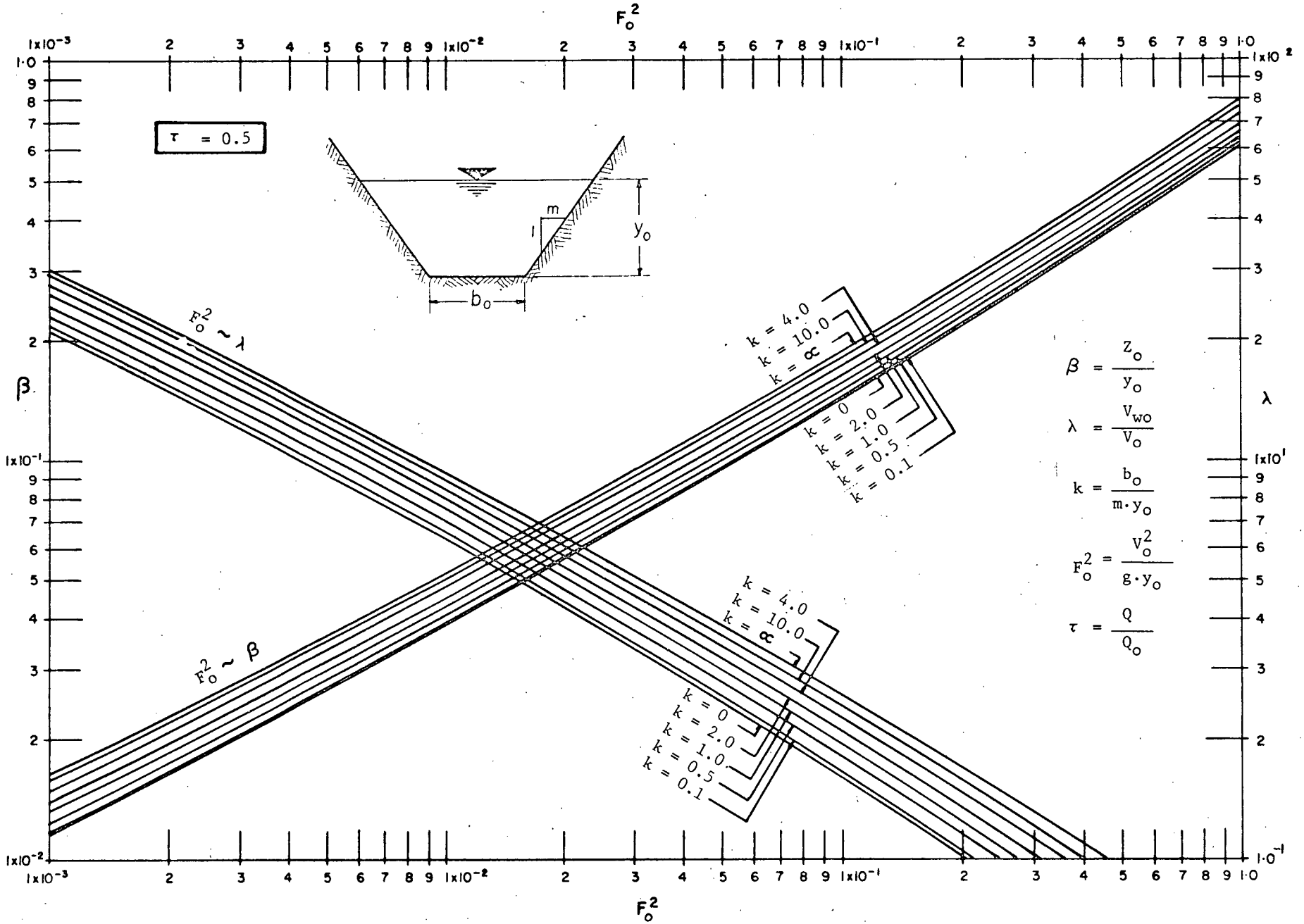

FIG. 2-7 (f) INITIAL SURGE WAVES IN A TRAPEZOIDAL CANAL FOR $\tau = 0.50$

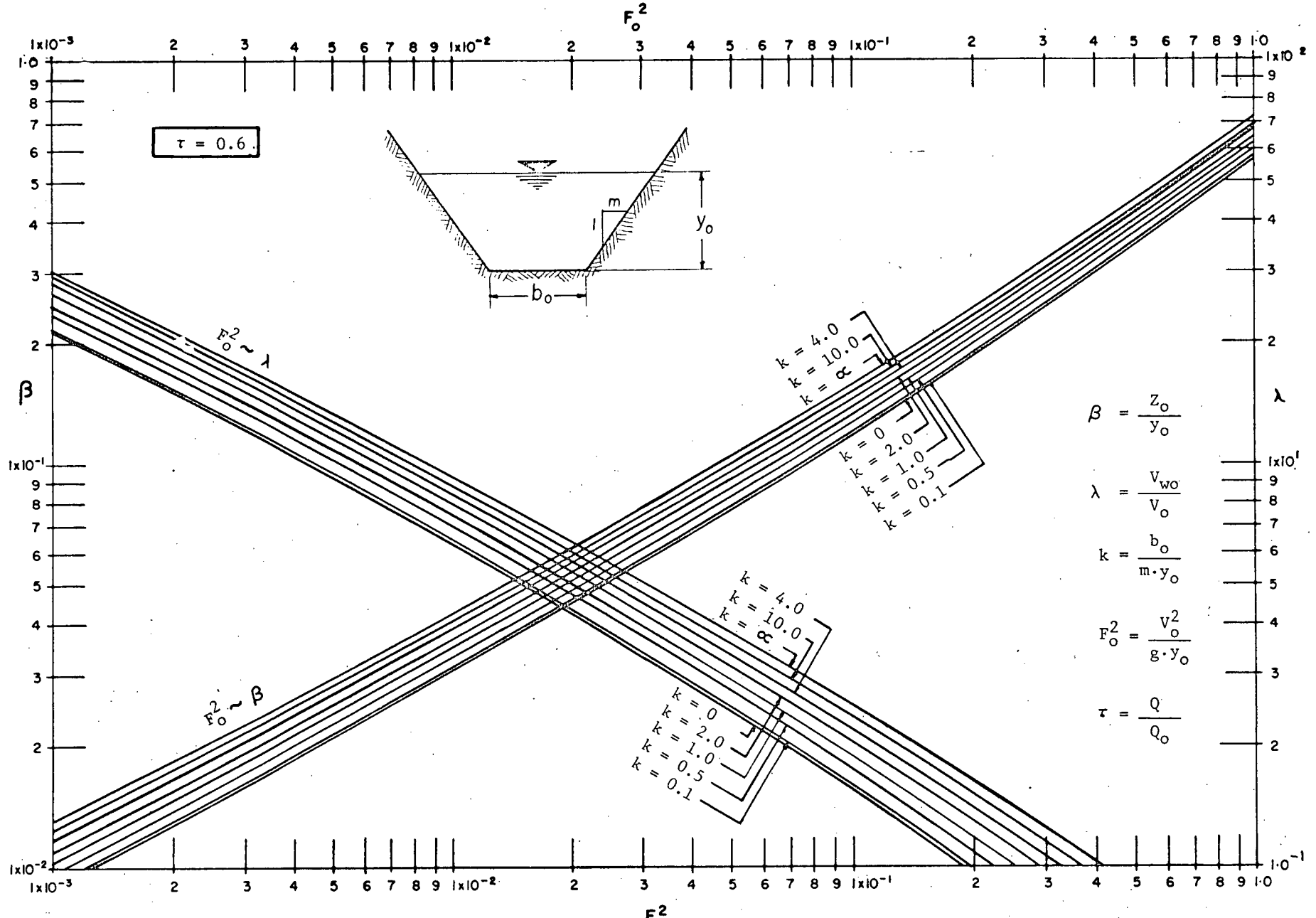

FIG. 2-7 (g) INITIAL SURGE WAVES IN A TRAPEZOIDAL CANAL FOR $\tau = 0.60$

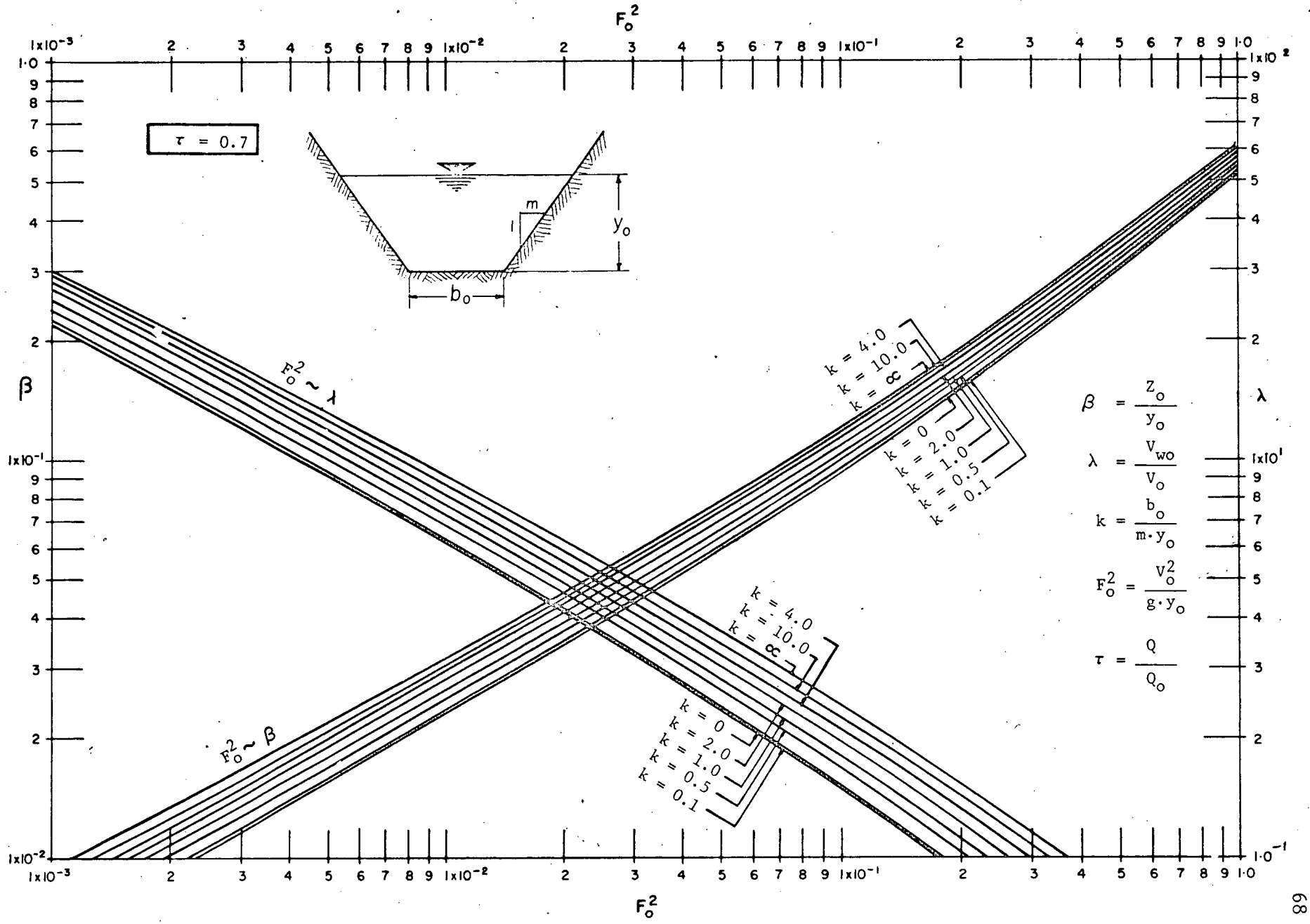

FIG. 2-7 (h) INITIAL SURGE WAVES IN A TRAPEZOIDAL CANAL FOR $\tau = 0.70$

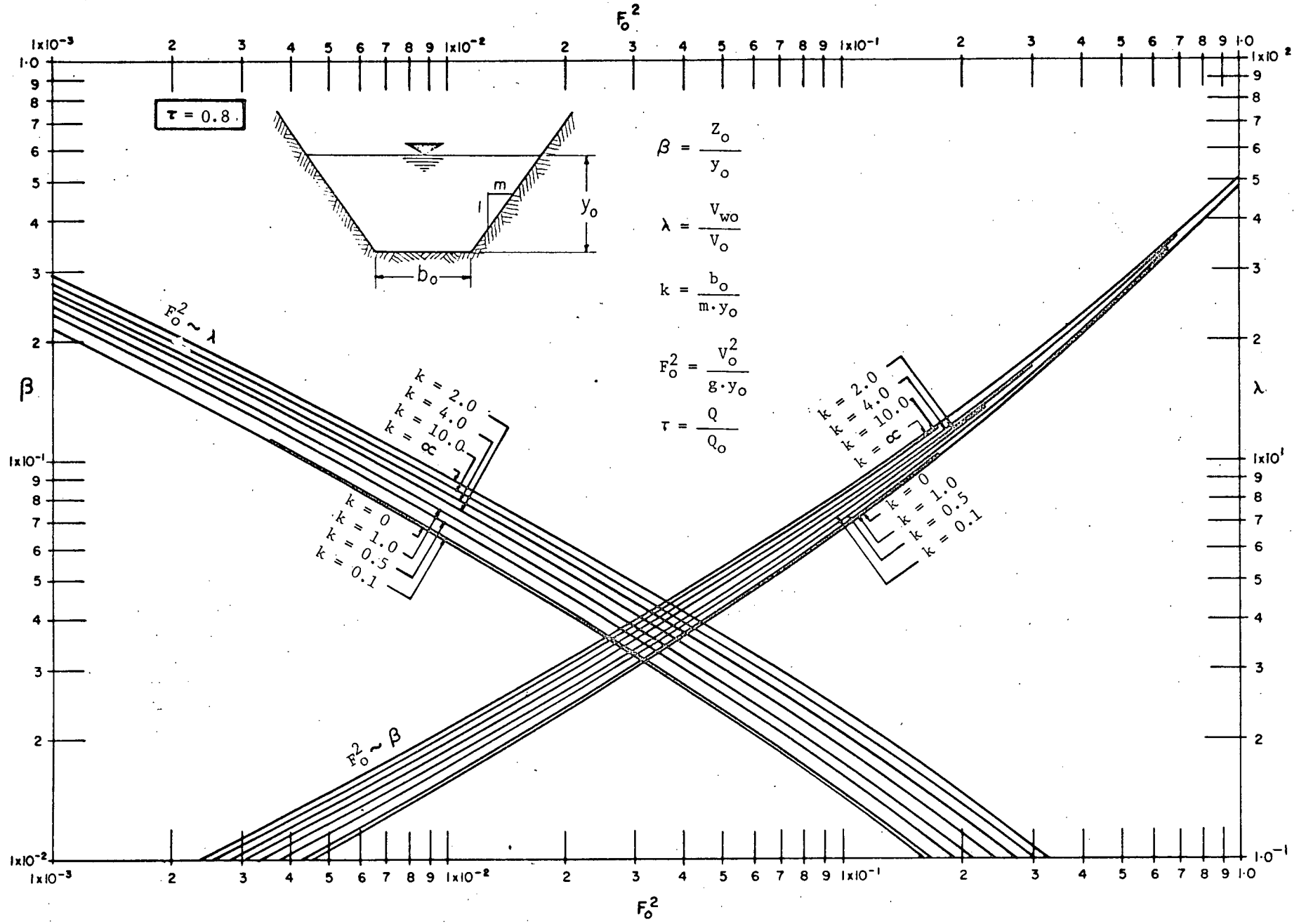

FIG. 2-7 (i) INITIAL SURGE WAVES IN A TRAPEZOIDAL CANAL FOR $\tau = 0.80$

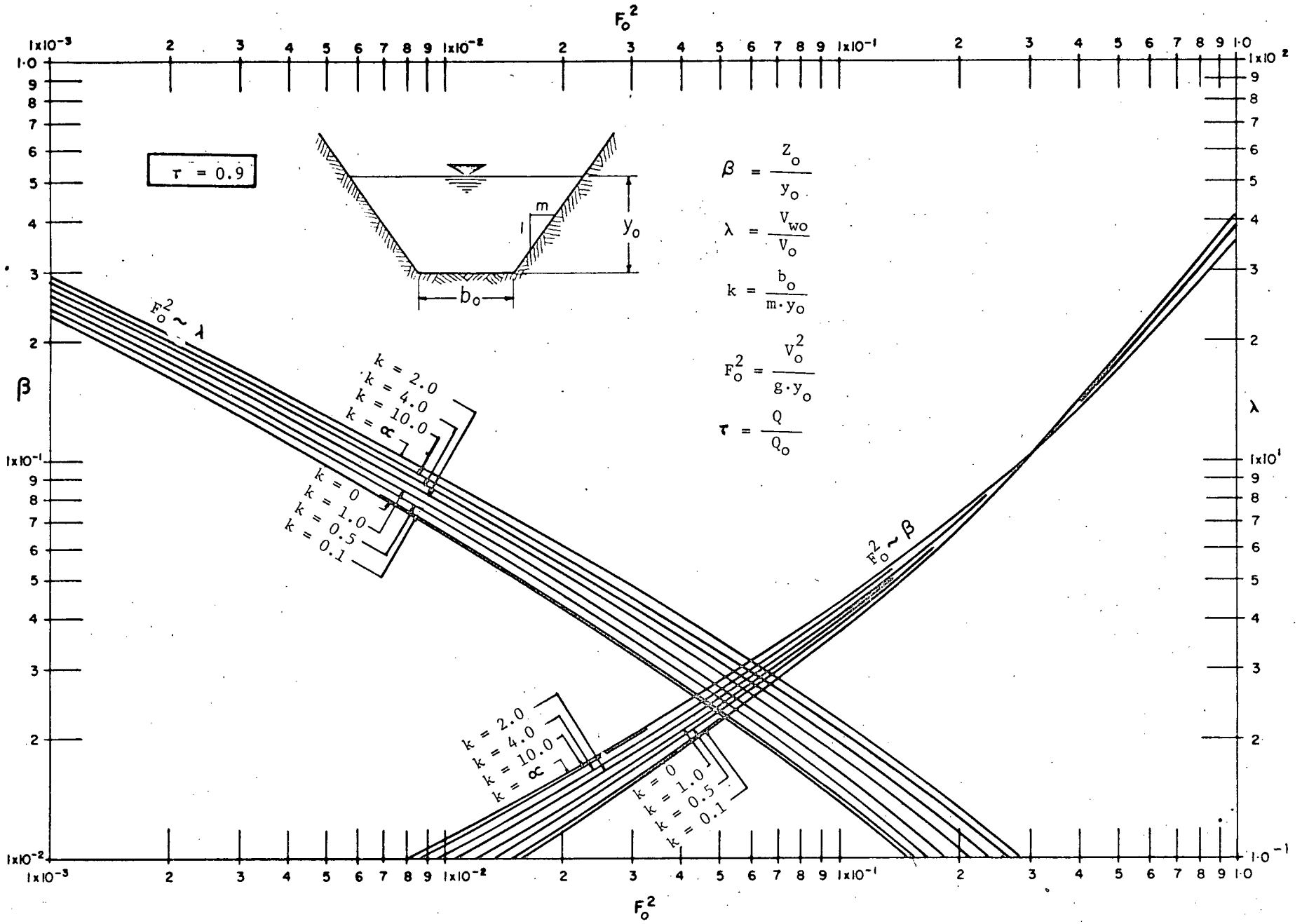

FIG. 2-7(j) INITIAL SURGE WAVES IN A TRAPEZOIDAL CANAL FOR $\tau = 0.90$

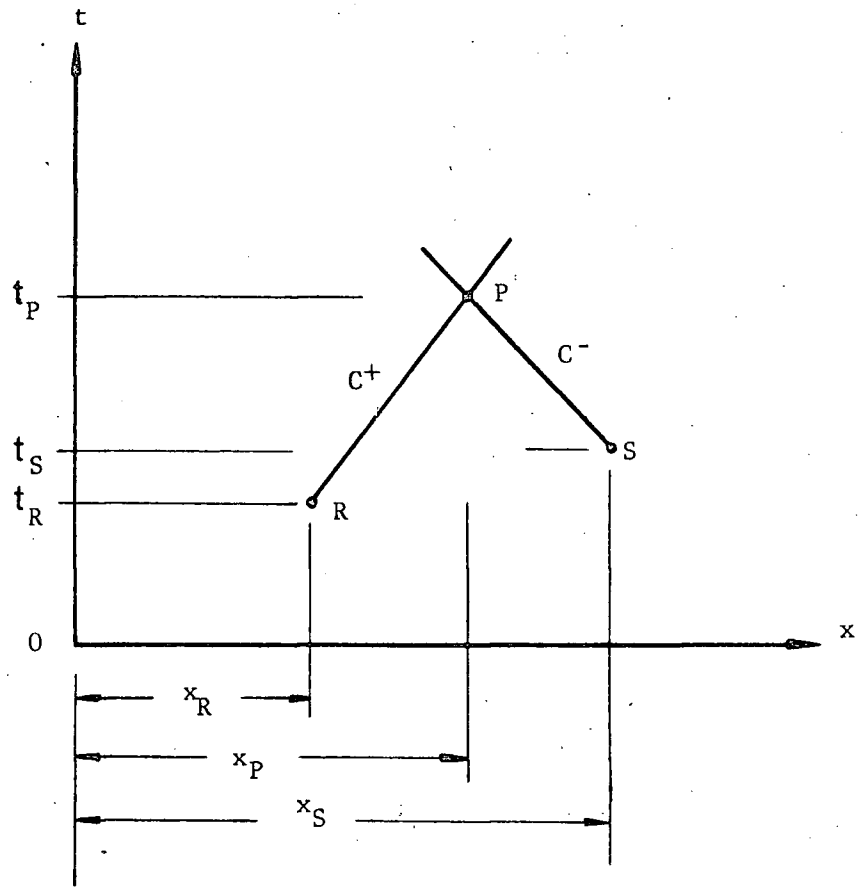

FIG. 3-1 DEFINITION SKETCH : C^+ AND C^- CHARACTERISTIC GRIDS ON THE x-t PLANE

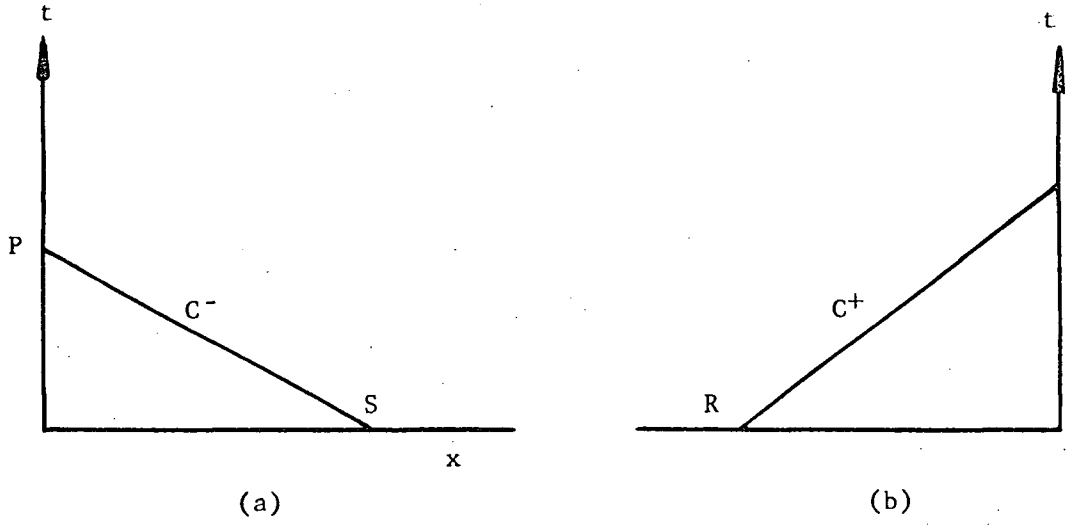

FIG. 3-3 DEFINITION SKETCH :
(a) UPPER END BOUNDARY, (b) DOWNSTREAM END BOUNDARY

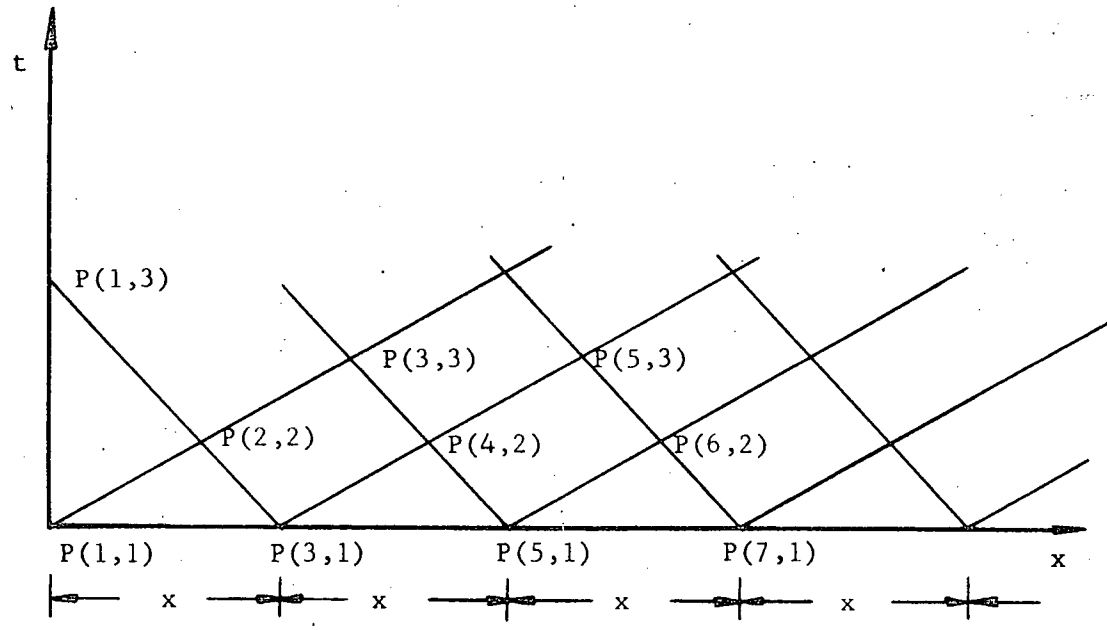

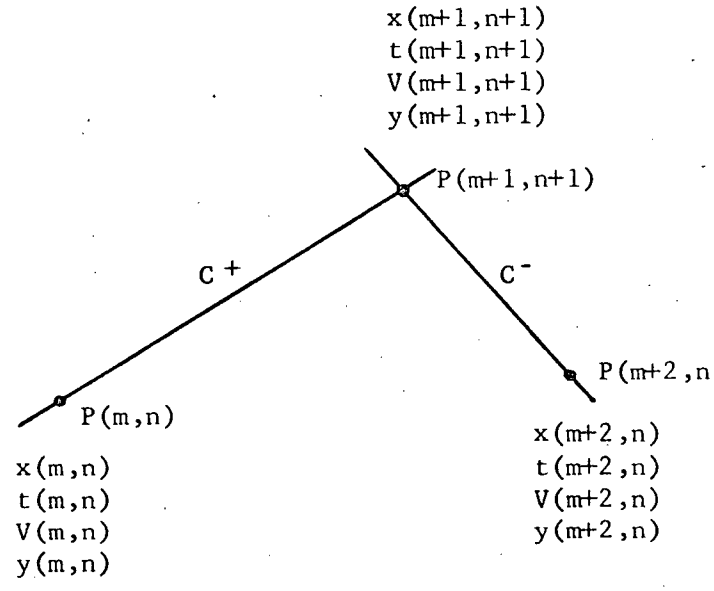

FIG. 3-2 DEFINITION SKETCH : CHARACTERISTIC GRIDS ON THE x-t PLANE

J	I	EXECUTION 1	2	3	4	5	6	7	8	9	10	11
1	V	7.635	7.635	7.635	7.635	7.635	7.635	7.635	7.635	7.635	7.635	7.635
	Y	7.859	7.859	7.859	7.859	7.859	7.859	7.859	7.859	7.859	7.859	7.859
	X	0.000	100.000	200.000	300.000	400.000	500.000	600.000	700.000	800.000	900.000	1000.000
	T	0.000	0.000	0.000	0.000	0.000	0.000	0.000	0.000	0.000	0.000	0.000
2	V		7.634	7.634	7.634	7.634	7.634	7.634	7.634	7.634	7.634	7.634
	Y		7.859	7.859	7.859	7.859	7.859	7.859	7.859	7.859	7.859	7.859
	X		73.998	173.998	273.998	373.998	473.998	573.998	673.998	773.998	873.998	973.998
	T		3.143	3.143	3.143	3.143	3.143	3.143	3.143	3.143	3.143	3.143
3	V	8.083	7.633	7.633	7.633	7.633	7.633	7.633	7.633	7.633	7.633	7.634
	Y	8.081	7.859	7.859	7.859	7.859	7.859	7.859	7.859	7.859	7.859	7.859
	X	0.000	147.994	247.994	347.994	447.994	547.993	647.993	747.993	847.993	947.993	1000.000
	T	12.087	6.286	6.286	6.286	6.286	6.286	6.286	6.286	6.286	6.286	4.246
4	V		8.076	7.632	7.632	7.632	7.632	7.632	7.632	7.632	7.632	7.633
	Y		8.079	7.859	7.859	7.859	7.859	7.859	7.859	7.859	7.859	7.859
	X		74.527	221.985	321.985	421.985	521.985	621.985	721.985	821.985	921.985	973.994
	T		15.165	9.430	9.430	9.430	9.430	9.430	9.430	9.430	9.430	7.391
5	V	8.453	8.070	7.631	7.631	7.631	7.631	7.631	7.631	7.631	7.632	7.632
	Y	8.284	8.076	7.859	7.859	7.859	7.859	7.859	7.859	7.859	7.859	7.859
	X	0.000	149.044	295.974	395.974	495.974	595.974	695.974	795.974	895.974	947.984	1000.000
	T	24.420	18.244	12.573	12.573	12.573	12.573	12.573	12.573	12.573	10.534	8.496
6	V		8.443	8.064	7.630	7.630	7.630	7.630	7.630	7.630	7.631	7.631
	Y		8.280	8.074	7.859	7.859	7.859	7.859	7.859	7.859	7.859	7.859
	X		74.931	223.553	369.959	469.959	569.959	669.959	769.959	869.959	921.972	973.989
	T		27.443	21.323	15.716	15.716	15.716	15.716	15.716	15.716	13.677	11.639
7	V	8.699	8.433	8.058	7.629	7.629	7.629	7.629	7.629	7.630	7.630	7.631
	Y	8.440	8.275	8.071	7.859	7.859	7.859	7.859	7.859	7.859	7.859	7.859
	X	0.000	149.850	298.053	443.941	543.941	643.941	743.941	843.941	895.956	947.976	1000.000
	T	36.946	30.468	24.403	18.859	18.859	18.859	18.859	18.859	16.821	14.782	12.744
8	V		8.687	8.423	8.052	7.628	7.628	7.628	7.628	7.629	7.629	7.630
	Y		8.434	8.270	8.069	7.859	7.859	7.859	7.859	7.859	7.859	7.859
	X		75.180	224.756	372.544	517.921	617.921	717.921	817.921	869.937	921.959	973.985
	T		39.931	33.493	27.484	22.002	22.002	22.002	22.002	19.964	17.925	15.887
9	V	8.789	8.675	8.414	8.047	7.627	7.627	7.627	7.628	7.628	7.629	7.630
	Y	8.528	8.427	8.265	8.067	7.859	7.859	7.859	7.859	7.859	7.859	7.859
	X	0.000	150.345	299.650	447.026	591.897	691.897	791.897	843.916	895.934	947.967	1000.000
	T	49.579	42.918	36.520	30.565	25.146	25.146	25.146	23.107	21.068	19.030	16.992

FIG. 3-4 A PART OF RESULTS OF COMPUTER CALCULATIONS IN EXAMPLE 3-1

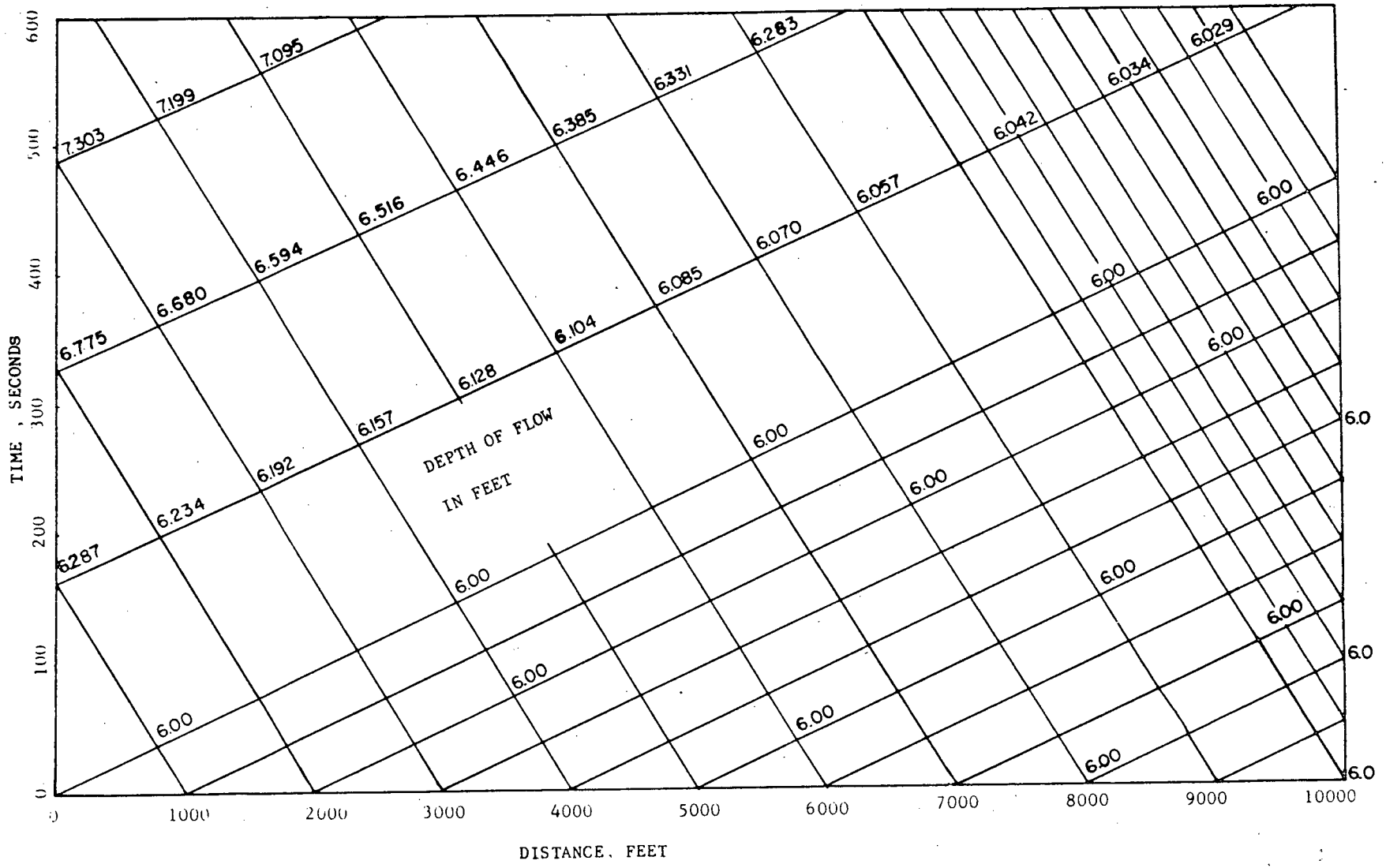

FIG. 3-5 A PART OF RESULTS OF COMPUTER CALCULATIONS IN EXAMPLE 3-2

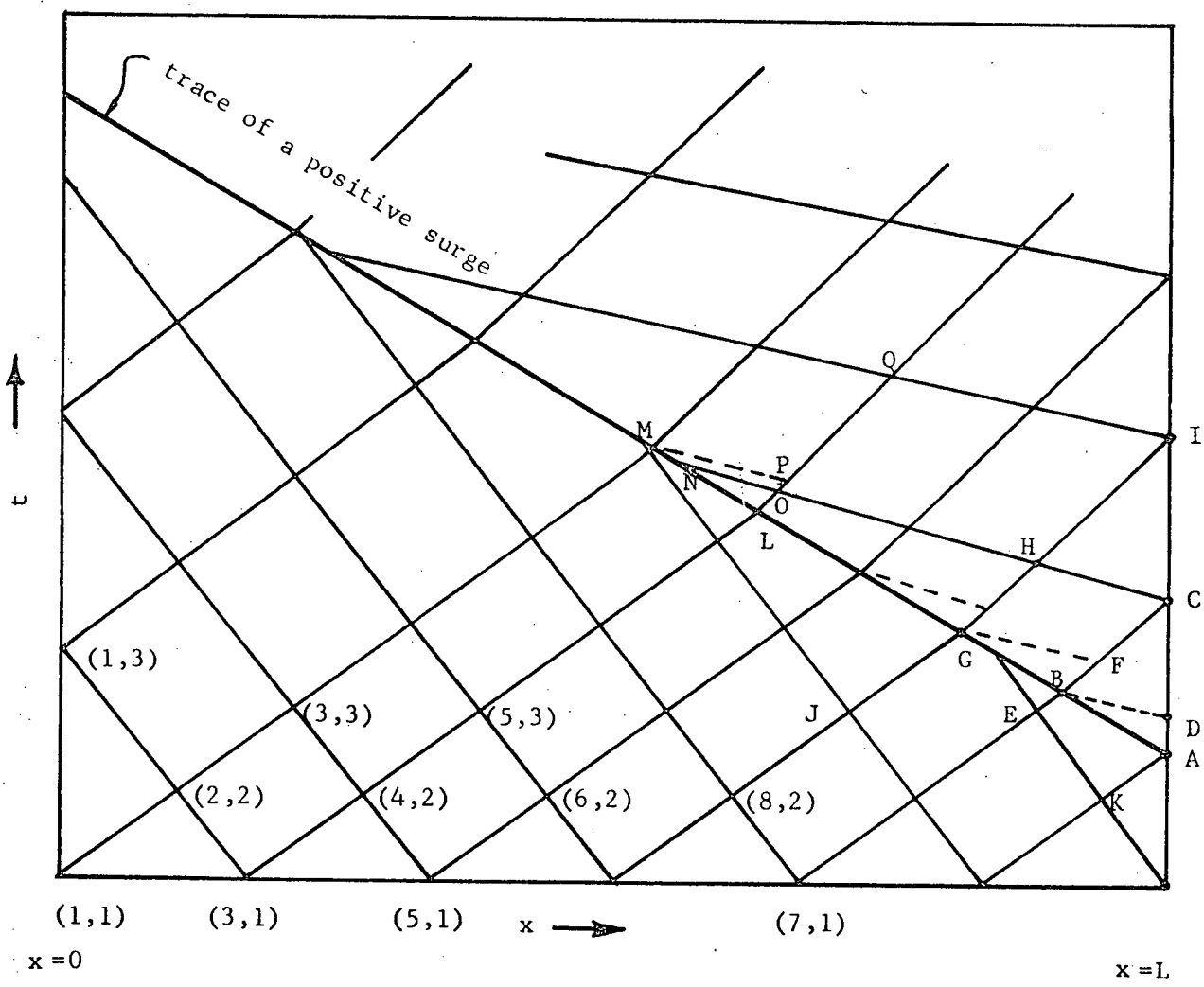

FIG. 3-6 SCHEMATIC PRESENTATION OF CHARACTERISTIC GRIDS FOR A POSITIVE SURGE WAVE PROPAGATING UPSTREAM

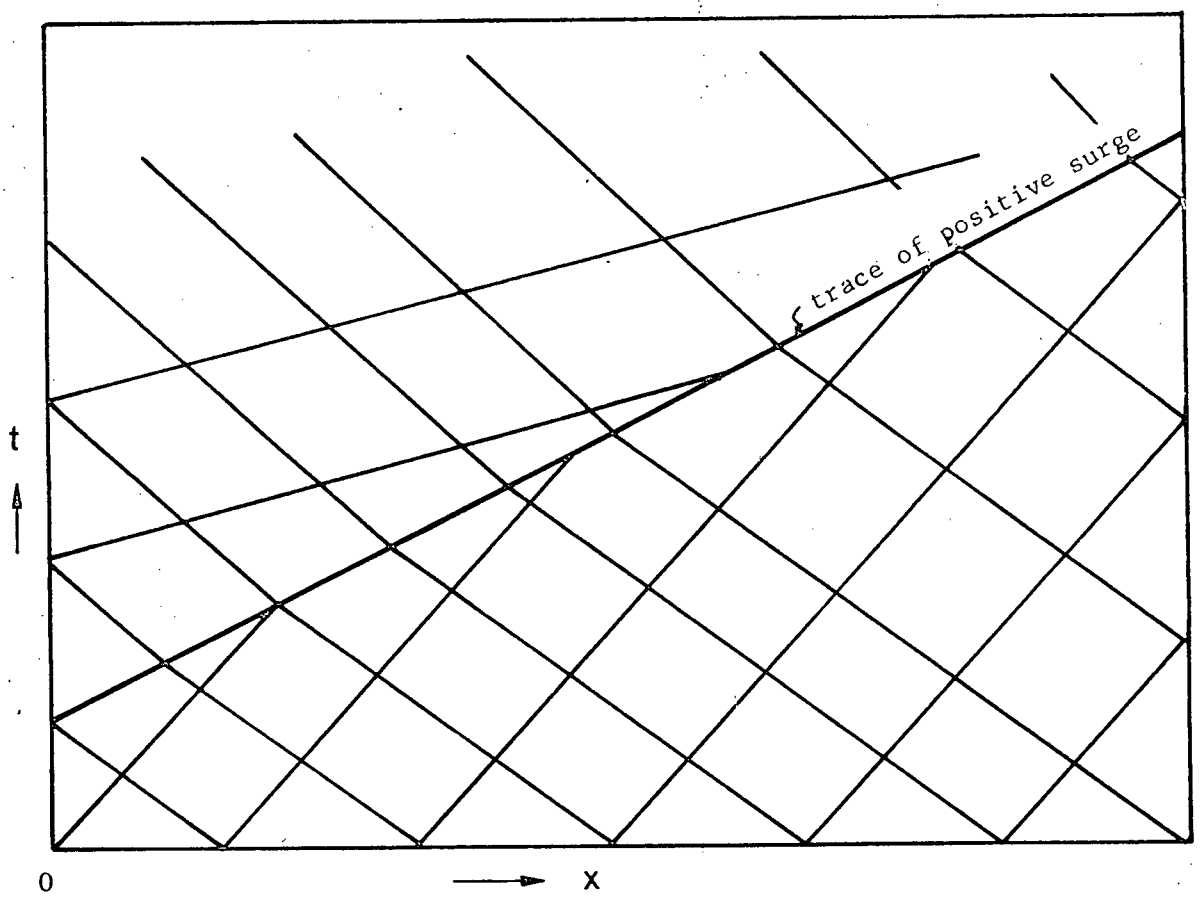

FIG. 3-7 SCHEMATIC PRESENTATION OF CHARACTERISTIC GRIDS FOR A POSITIVE SURGE WAVE PROPAGATING DOWNSTREAM

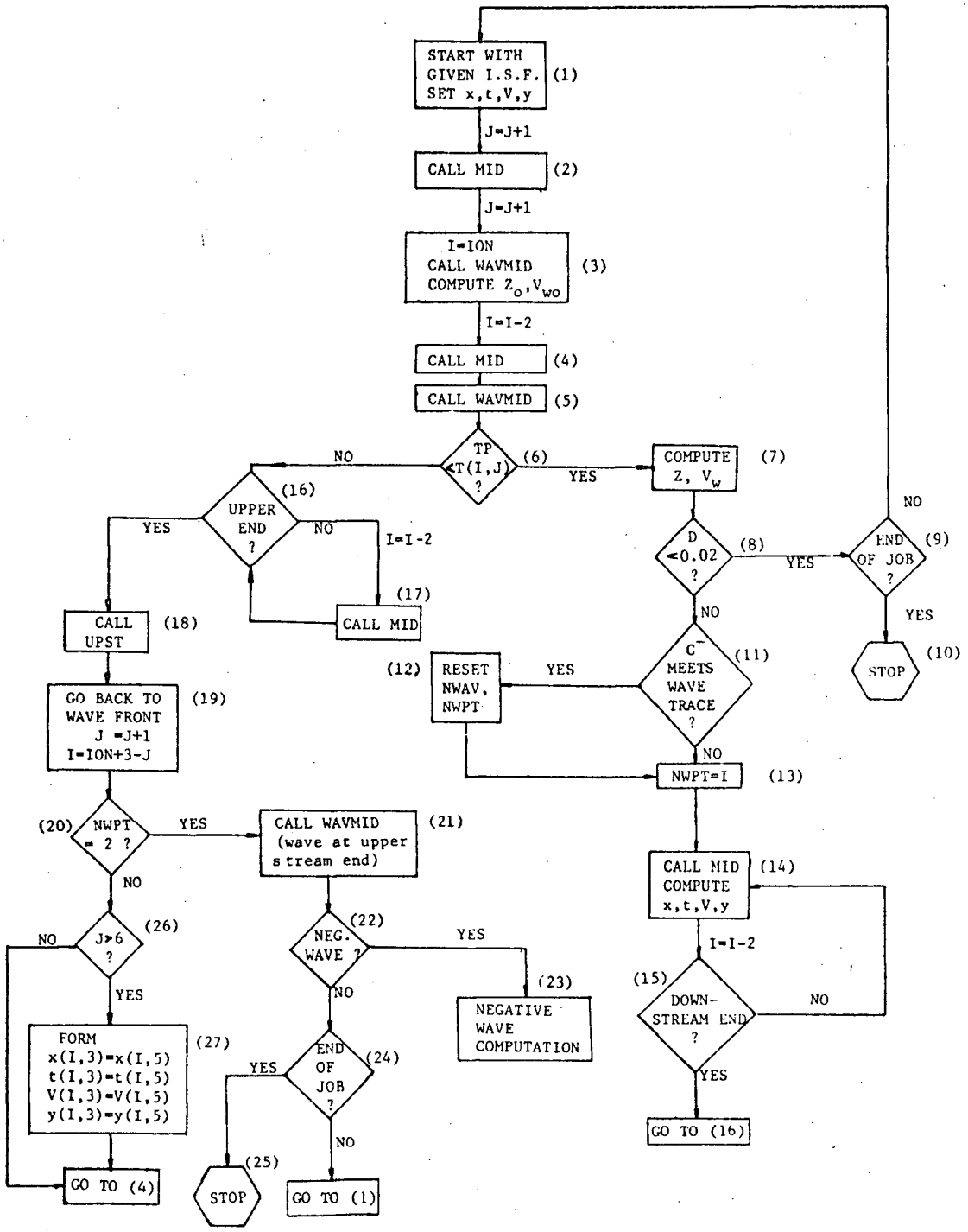

FIG. 3-8 FLOW CHART OF THE COMPUTER PROGRAM FOR A POSITIVE WAVE PROPAGATING UPSTREAM ALONG THE POWER CANAL

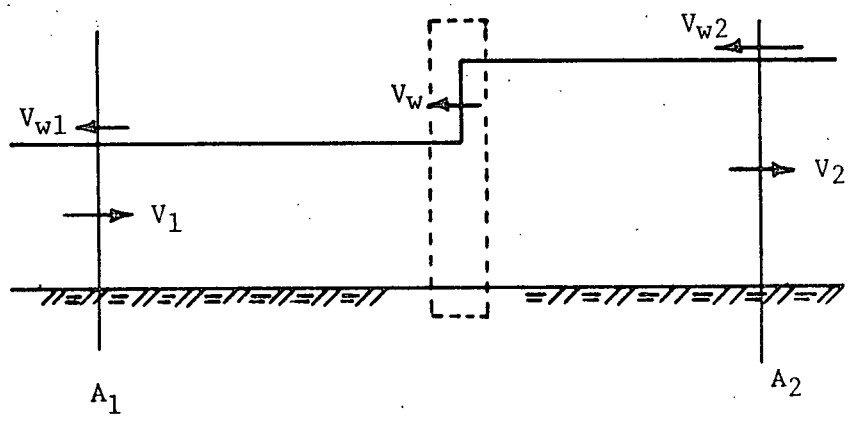

FIG. 3-9 DEFINITION SKETCH FOR EXAMPLE 3-3

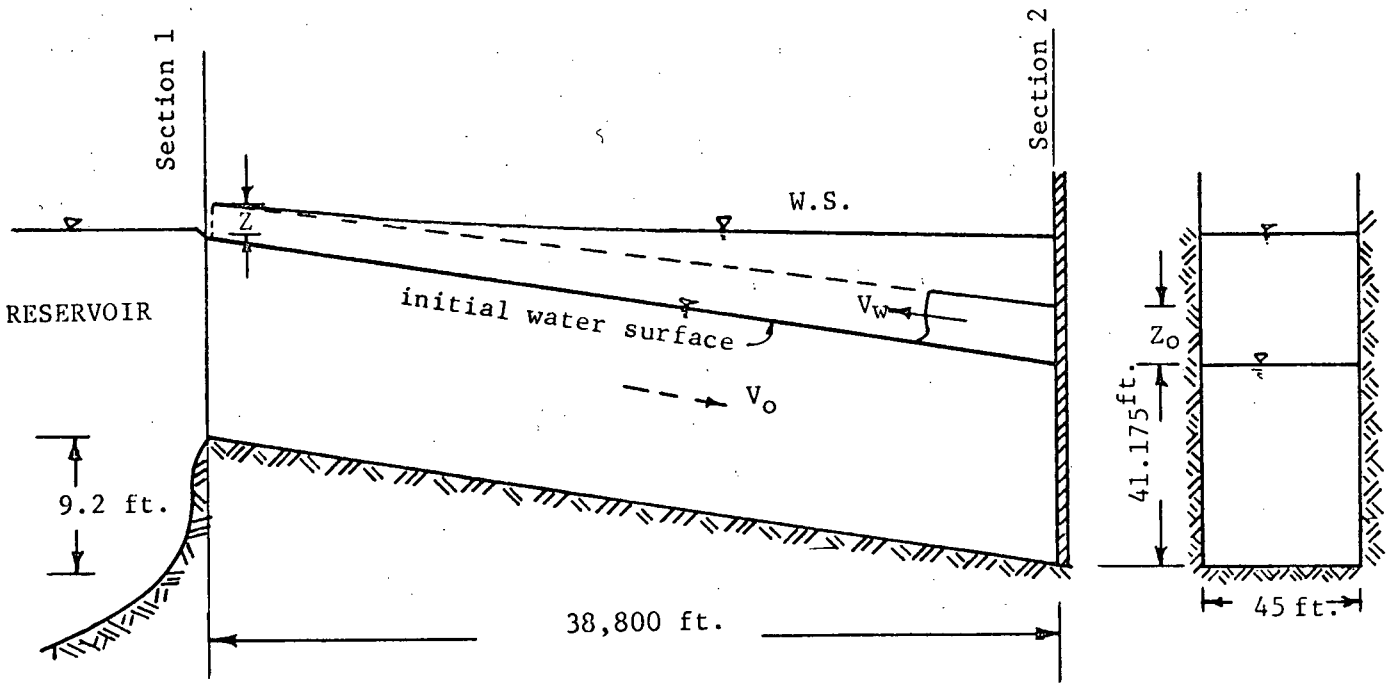

FIG. 3-10 DEFINITION SKETCH FOR EXAMPLE 3-3

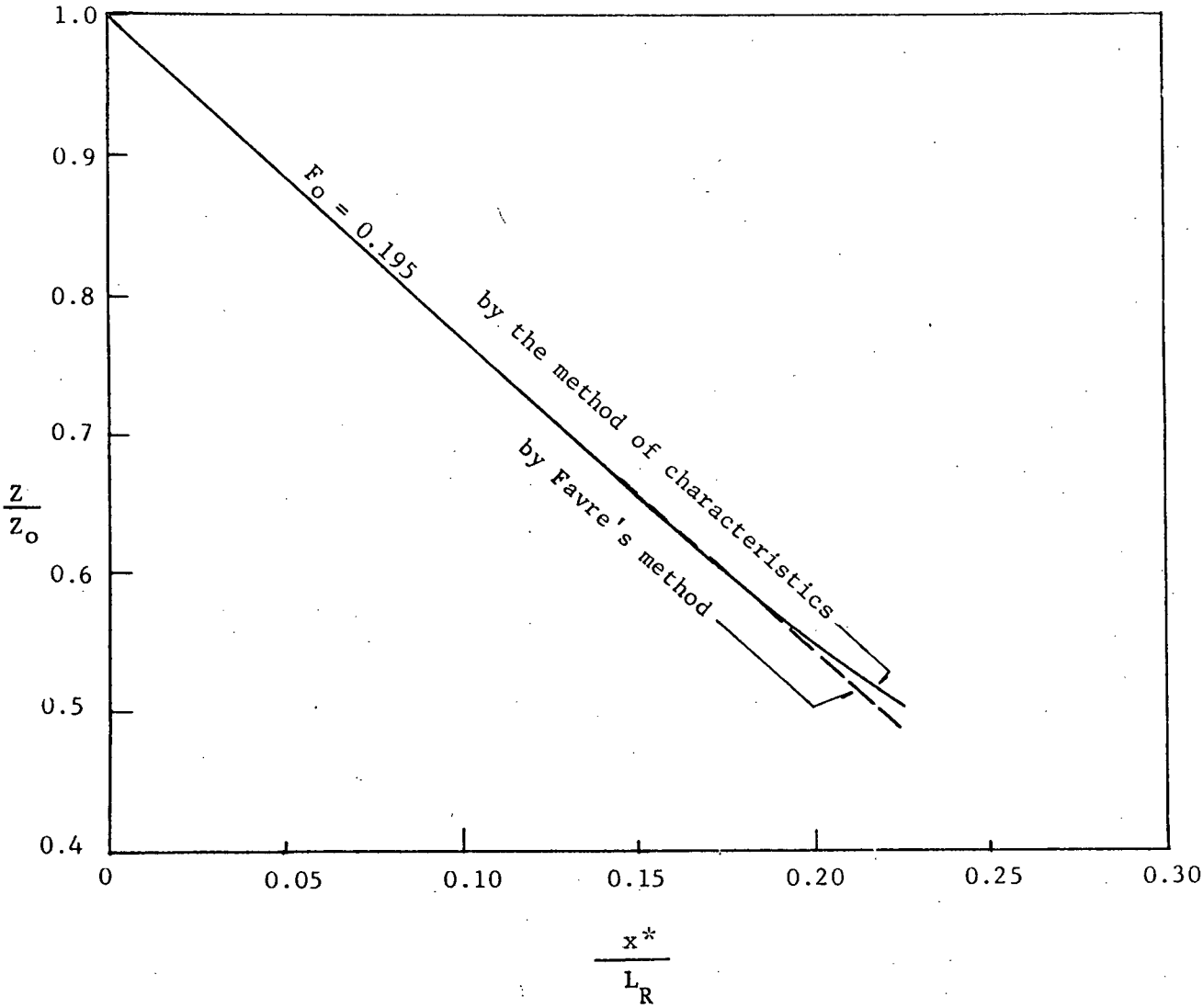

FIG. 3-11 THE COMPARISON OF THE METHOD OF CHARACTERISTICS WITH FAVRE'S METHOD FOR EXAMPLE 3-3

SECTION 0			SECTION 1		
At time t=0 before wave is formed	At time t=0 immediately after wave is formed	At time $t=t_1$	At time t=0 when wave occurs in Section 0	At time $t=t_1$ before wave reaches Section 1	At time $t=t_1$ immediately after wave reaches Sec.1
h_0=41.175	h_0'=49.567	h_0''=54.644	h_1=41.175	h_1^+=41.175	h_1'=41.175+4.27
F_0=41.175x45	F_0'=49.567x45	F_0''=54.644x45	F_1=41.175x45	F_1^+=41.175x45	=45.445
Q_0=292x45	Q_0'=0	Q_0''=0	Q_1=292x45	Q_1^+=292x45	F_1'=45.445x45
V_0=7.101	V_0'=0	V_0''=0	V_1=7.105	V_1^+=7.105	Q_1'=154.7x45
B_0=45	B_0'=45	B_0''=45	B_1=45	B_1^+=45	$\Delta Q_1'$=-137.3x45
	P_0'=144.134	P_0''=154.288			V_1'=3.41
	$R_0'=\frac{49.567x45}{144.134}$	R_0''=15.89			B_1'=45
	=15.45		Δh_1 = 0		P_1'=135.89
	Z_0=8.393		ΔF_1 = 0		R_1'=15.05
	y_0=45		ΔQ_1 = 0		Z_1=4.27
	a_0=-34.84				a_1=-32.14
	C_0=-41.94				y_1=45
	ΔQ_0=-292				C_1=-39.25
	$\Delta F_0'$=8.393x45				$\Delta F_1'$=4.27x45

Assume Z_0''= 5.077 (Horizontal)

y_0''=45

$\Delta F_0''=Z_0''.Y_0''$

=5.077x45

$\Delta Q_0''$=0

$$I_r = \frac{n^2}{1.486^2} \cdot \frac{(V^2)_m}{(R_m)^{4/3}}$$

= +0.00002525

L = - 38800

B_m = 45

ΔB = 0

ΔQ = 0

Δa = 2.699

a_m = 33.49

R_m = 15.47

I_m = 0.000237

V_m =1.705

$(V^2)_m$ = 5.81

Summary of trials:

No. of trial	Guess Z_1	Water Volume $\forall_1$	Water Volume $\forall_2$	
1	4.27	339000 x 45	344000 x 45	$\forall_1 < V_2$
2	4.00	342000 x 45	334000 x 45	$\forall_1 > V_2$
3	4.10	339500 x 45	337500 x 45	$\forall_1 > V_2$
4	4.15	339000 x 45	339200 x 45	$\forall_1 \doteq V_2$

FIG. 3-12 SUMMARY OF CALCULATIONS IN EXAMPLE 3-3 FOLLOWING FAVRE METHOD

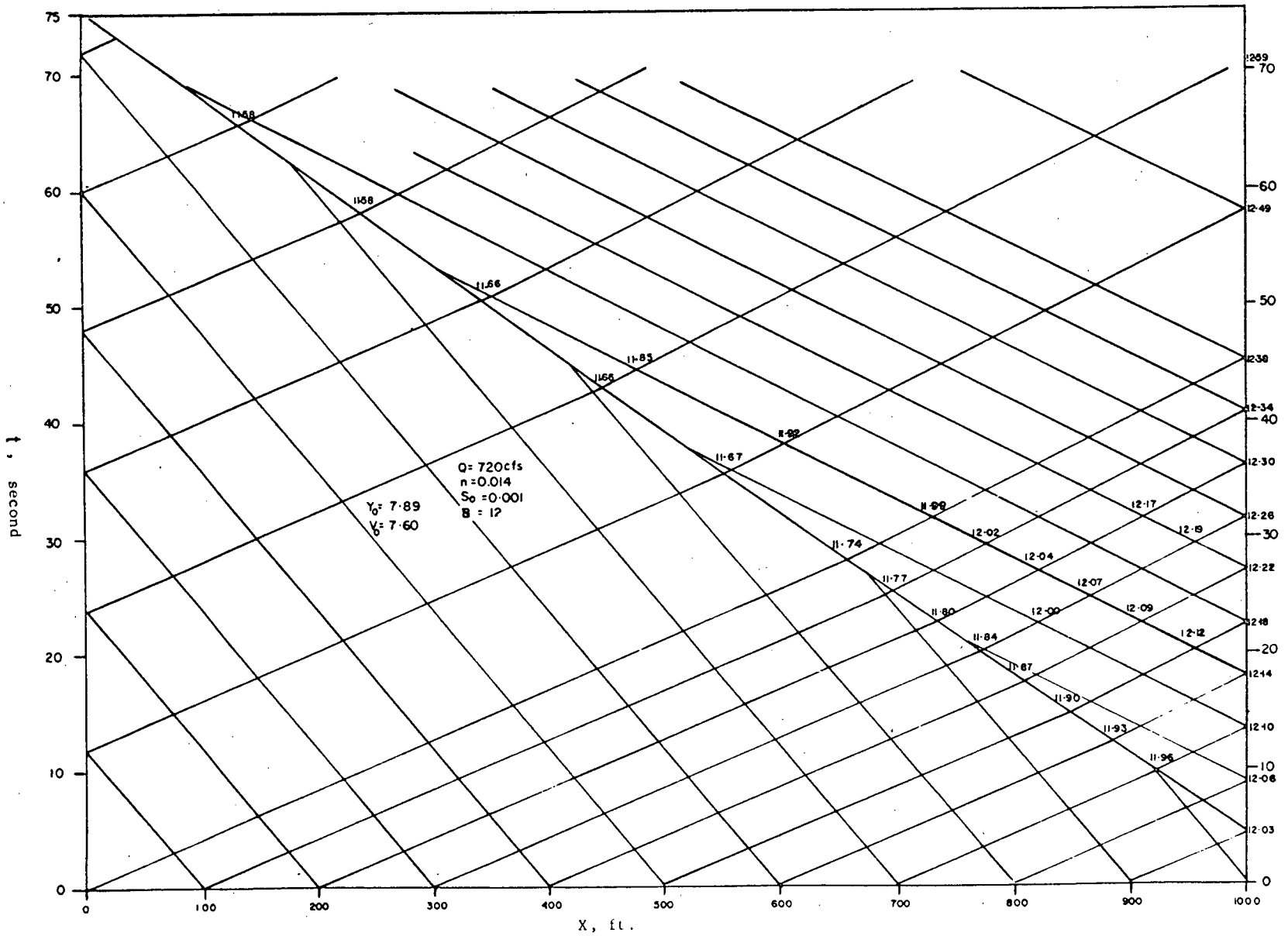

FIG. 3-13 RESULTS OF CALCULATIONS IN EXAMPLE 3-4

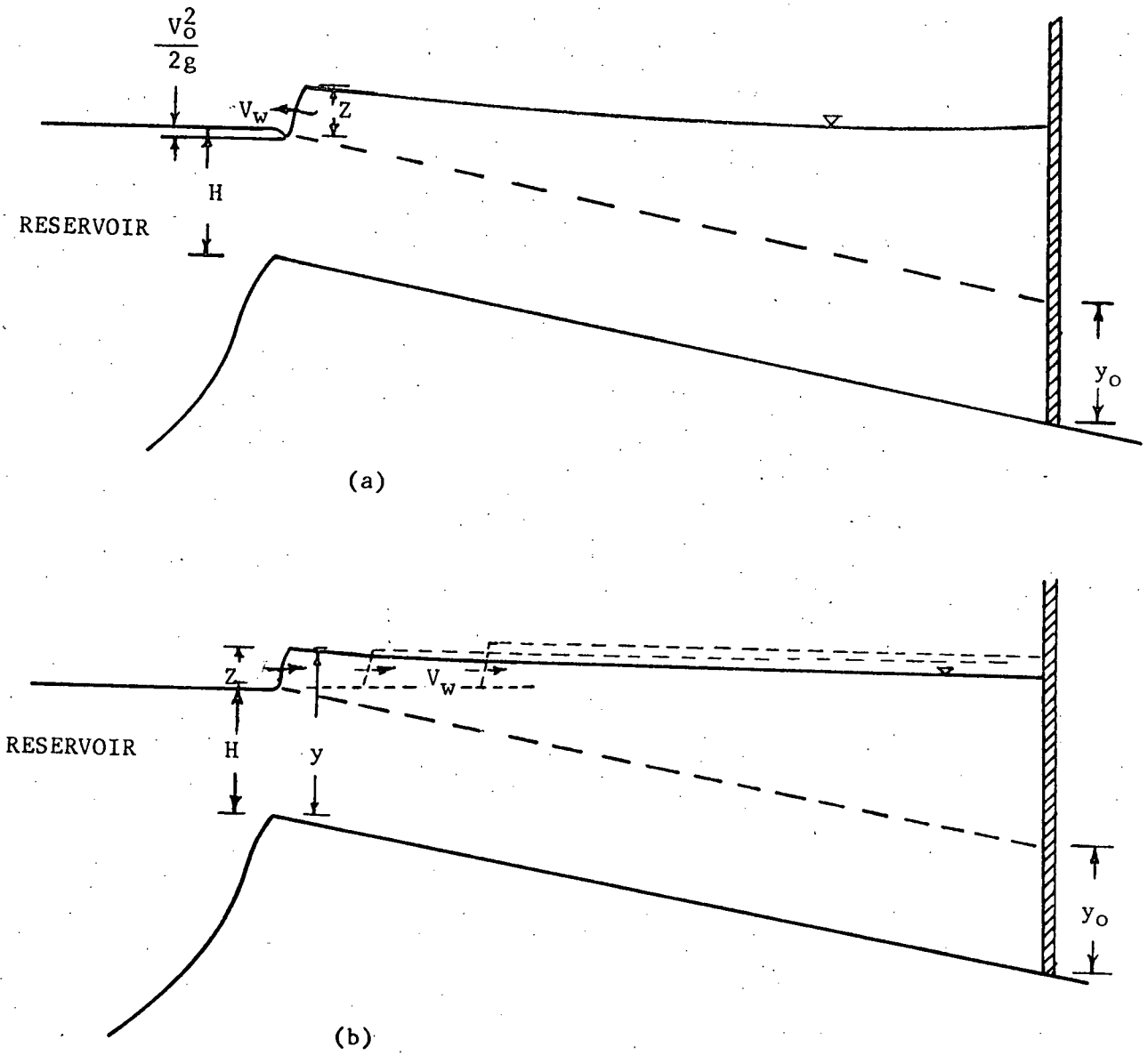

FIG. 3-14 (a) POSITIVE SURGE REACHES THE RESERVOIR AT THE UPPER END OF THE CANAL.
(b) NEGATIVE SURGE REFLECTED FROM THE RESERVOIR.

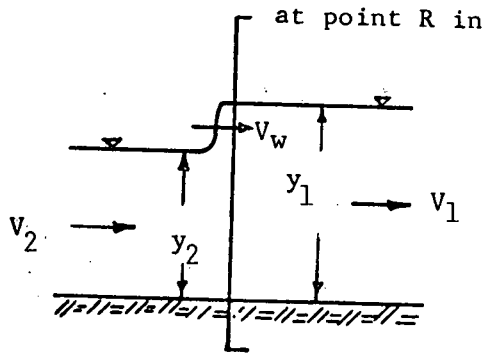

FIG. 3-15 DEFINITION SKETCH FOR POINT R IN FIG. 3-16

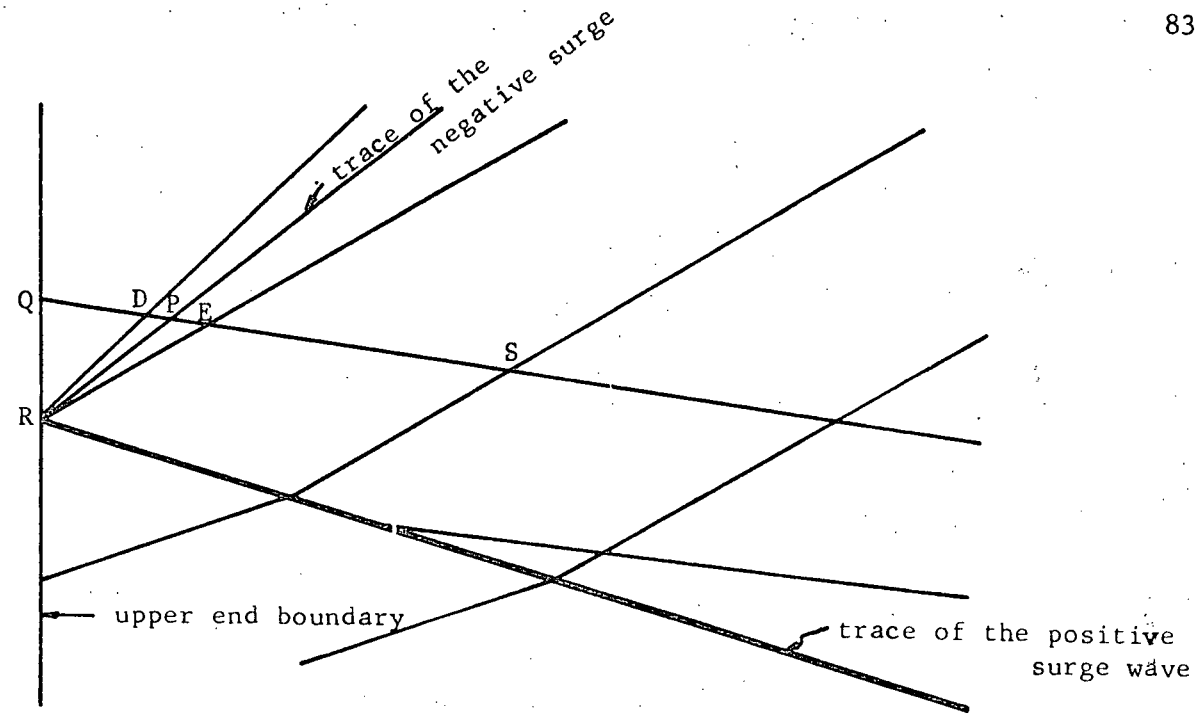

FIG. 3-16 SCHEMATIC DIAGRAM OF CHARACTERISTIC GRIDS FOR THE NEGATIVE WAVE AT POINT R

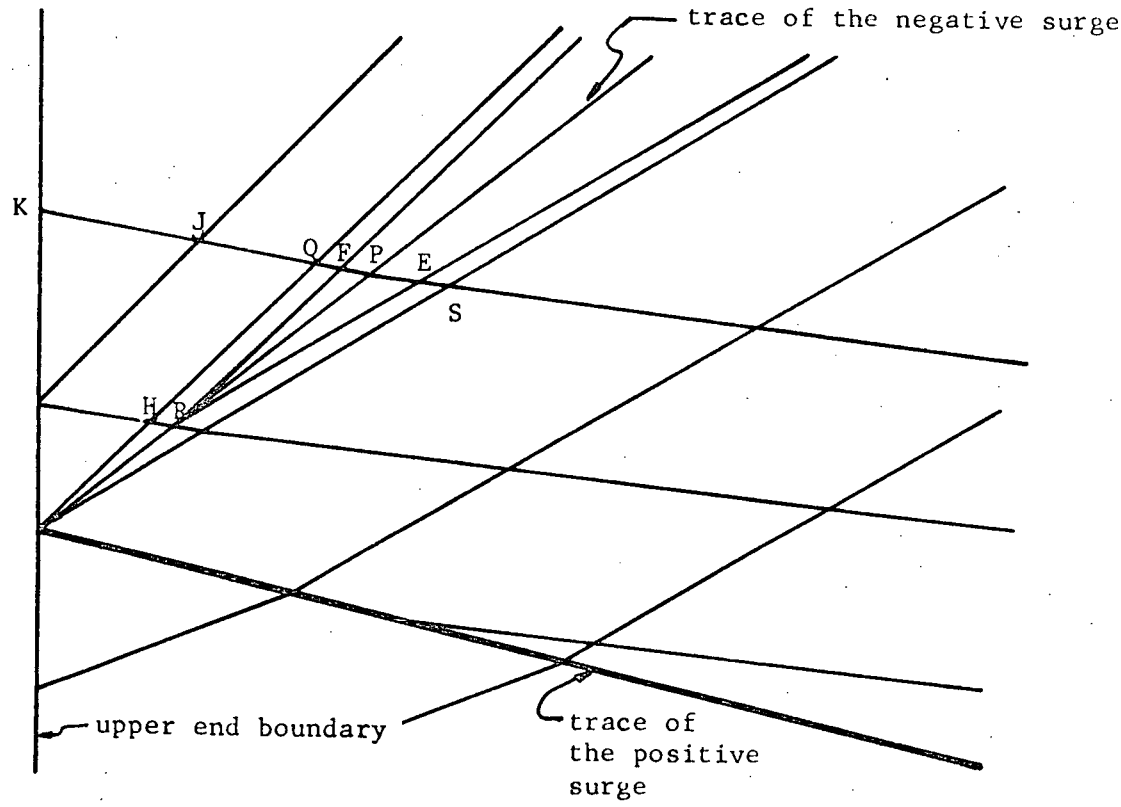

FIG. 3-17 SCHEMATIC DIAGRAM OF CHARACTERISTIC GRIDS FOR THE NEGATIVE WAVE AT POINT R

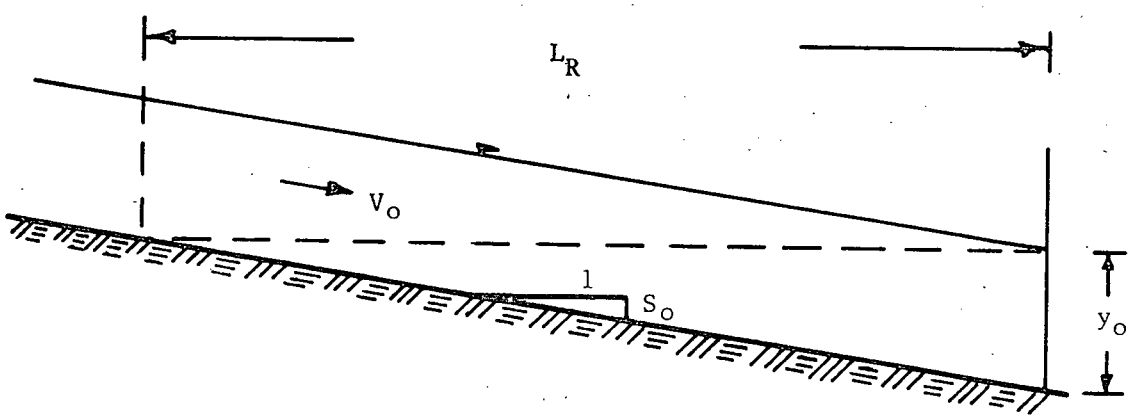

FIG. 4-1 DEFINITION SKETCH

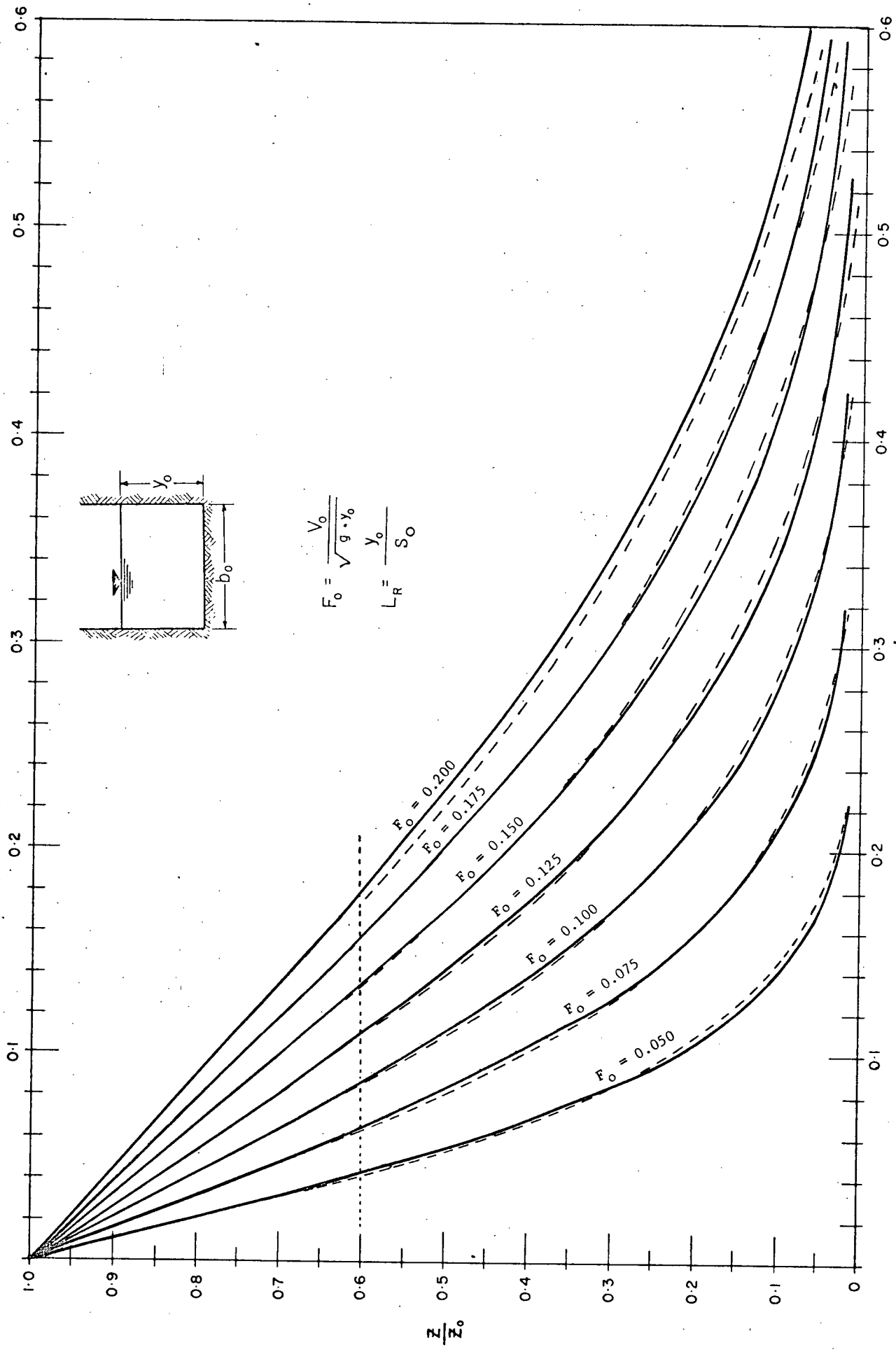

FIG. 4-2 VARIATION OF WAVE HEIGHT OF A POSITIVE SURGE PROPAGATING ALONG A RECTANGULAR POWER CANAL

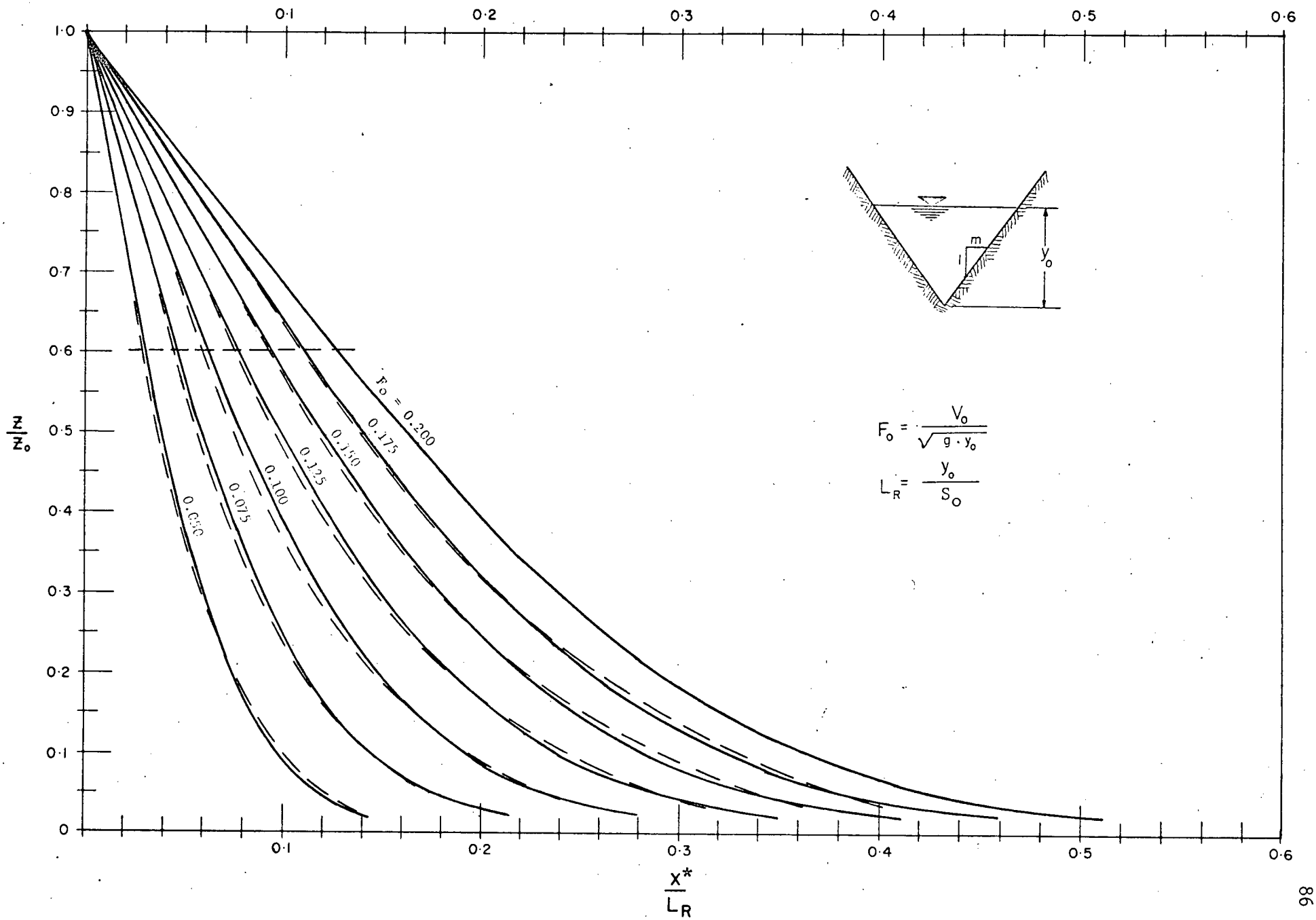

FIG. 4-3 VARIATION OF WAVE HEIGHT OF A POSITIVE SURGE PROPAGATING ALONG A TRIANGULAR POWER CANAL

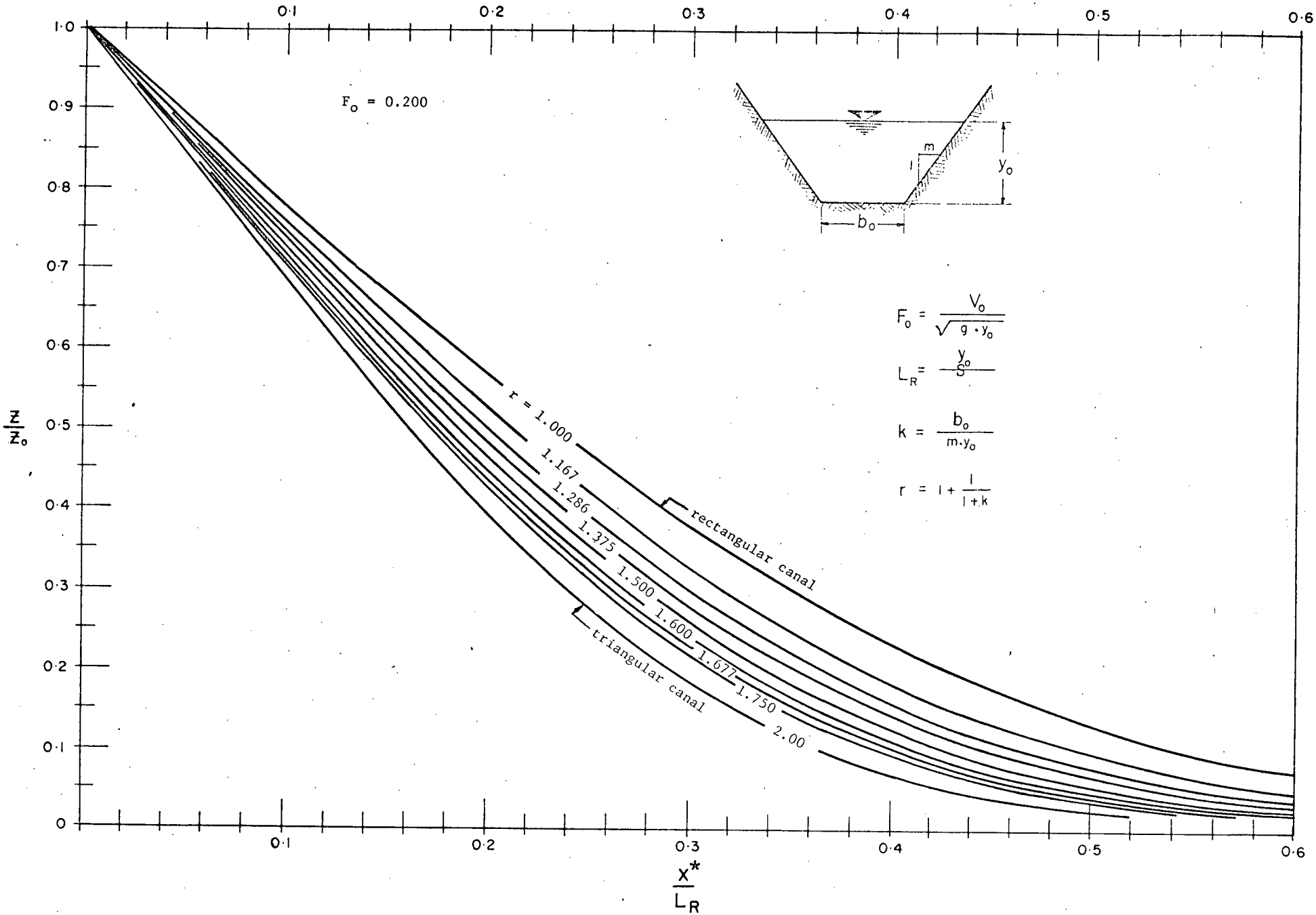

FIG. 4-4 VARIATION OF WAVE HEIGHT OF A POSITIVE SURGE PROPAGATING ALONG A TRAPEZOIDAL POWER CANAL IN AN INITIAL FLOW F_o = 0.20

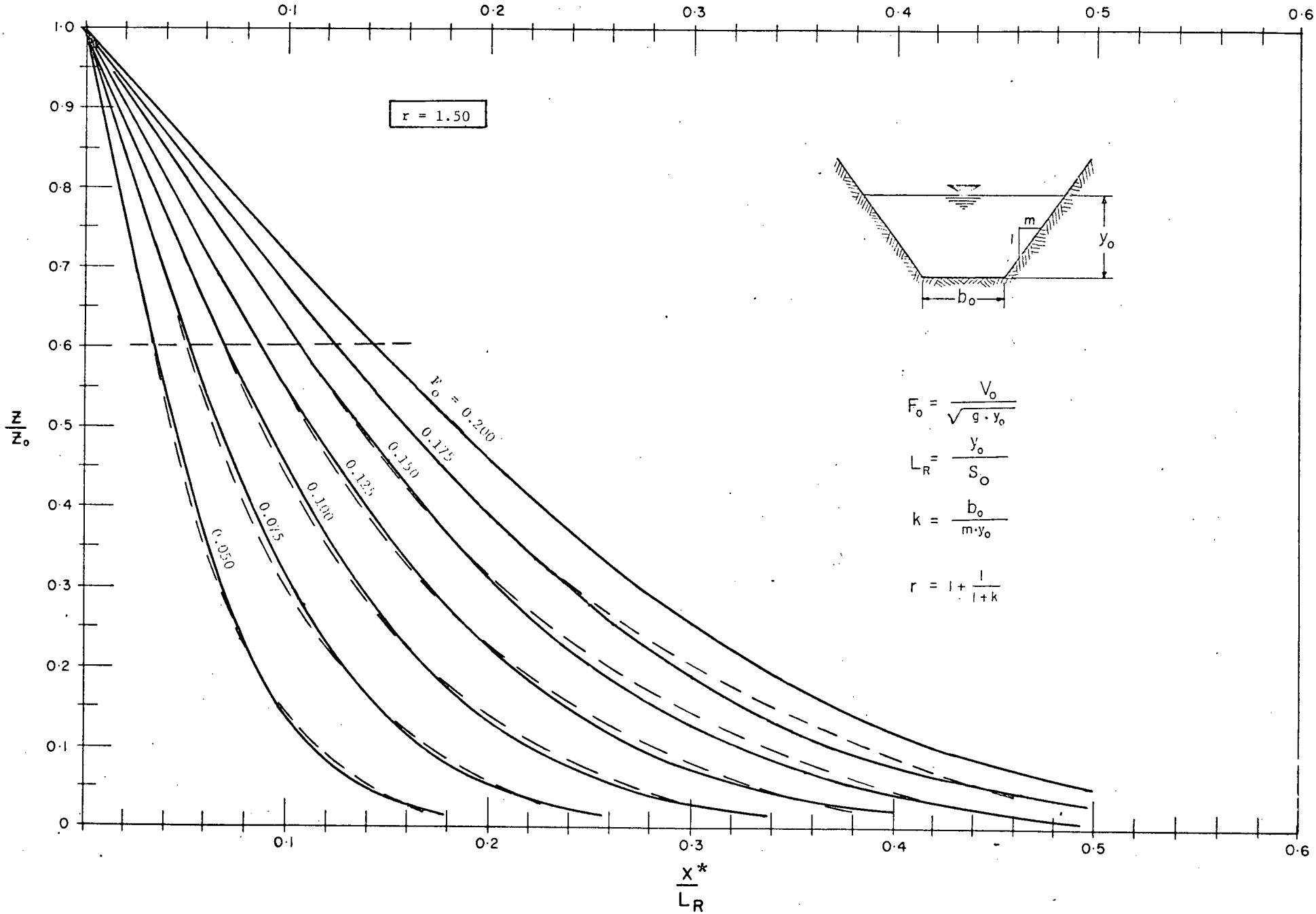

FIG. 4-5 VARIATION OF WAVE HEIGHT OF A POSITIVE SURGE PROPAGATING ALONG A TRAPEZOIDAL POWER CANAL FOR r = 1.50

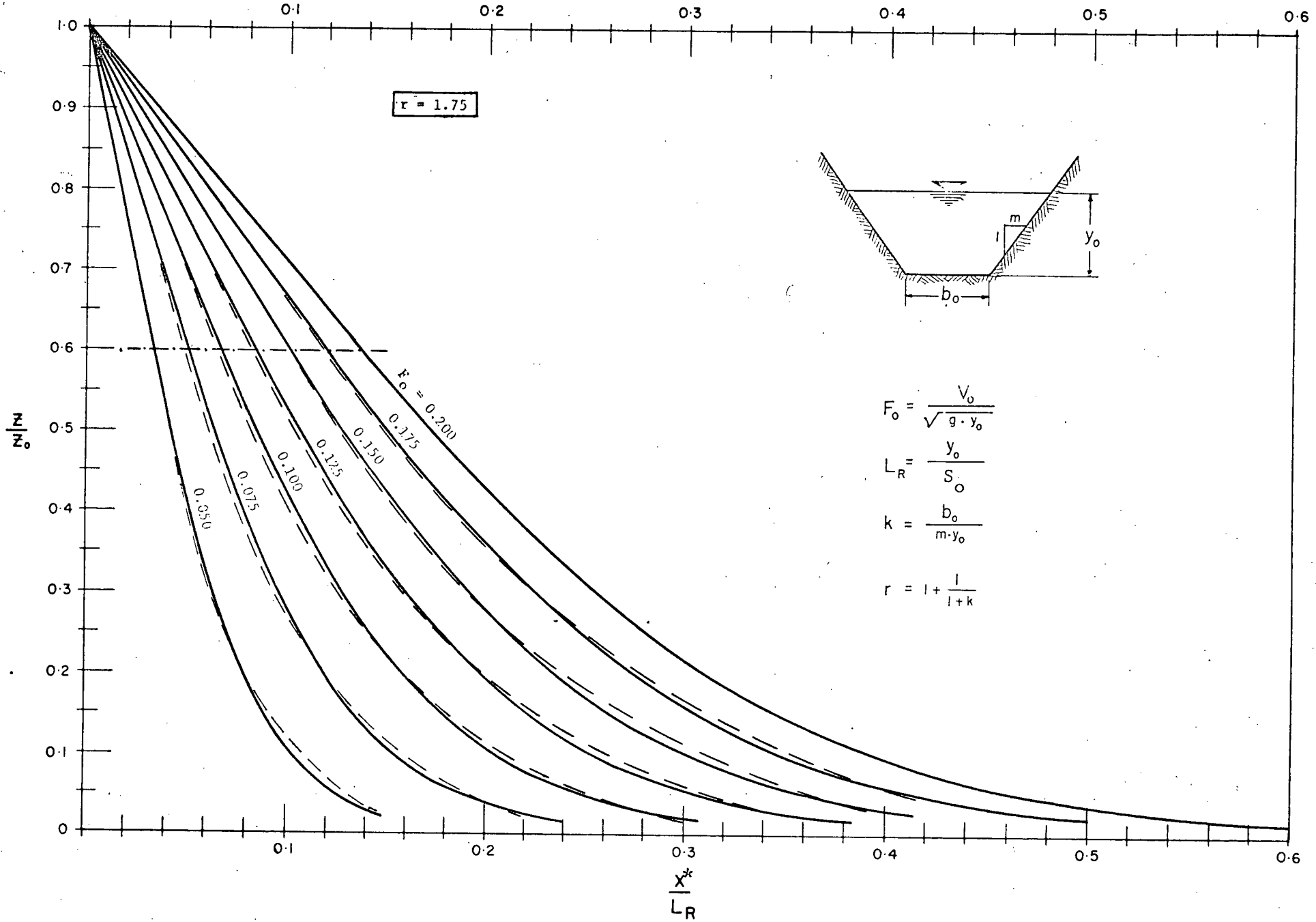

FIG. 4-6 VARIATION OF WAVE HEIGHT OF A POSITIVE SURGE PROPAGATING ALONG A TRAPEZOIDAL POWER CANAL FOR r = 1.75

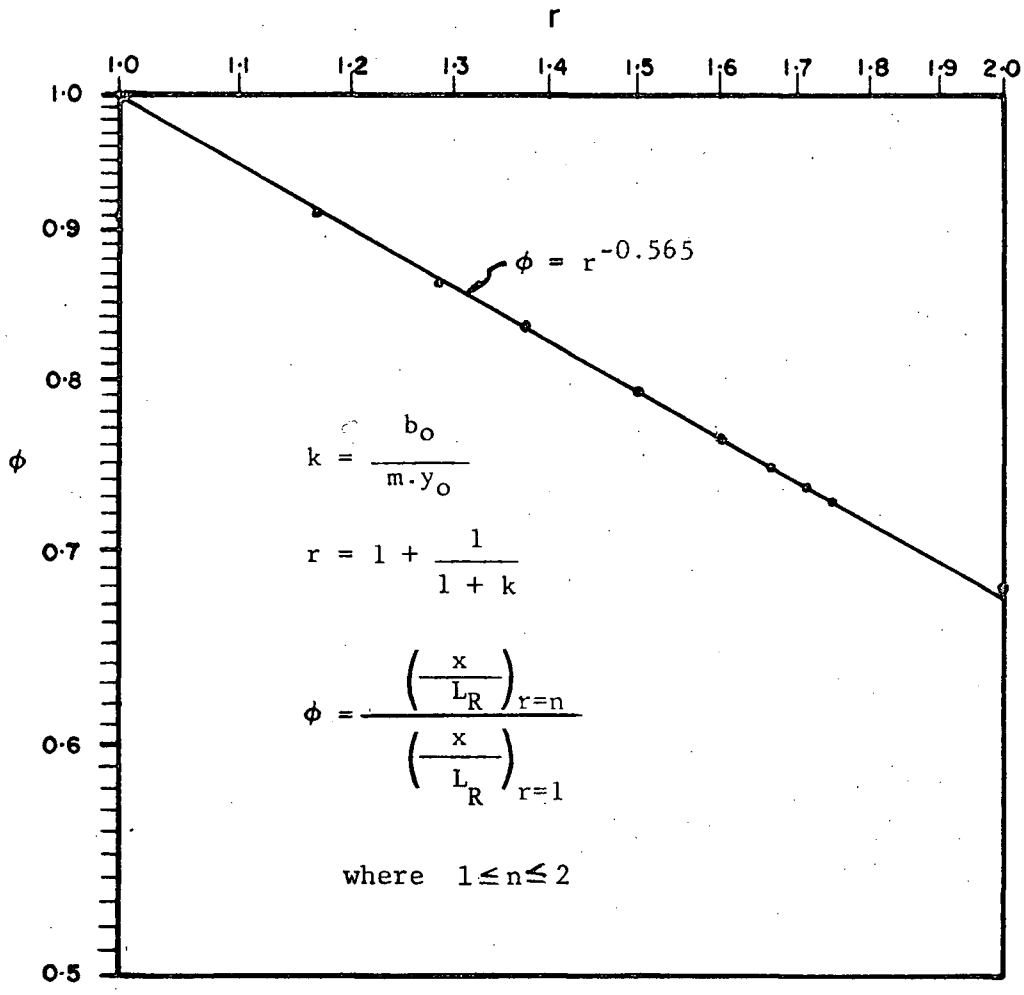

FIG. 4-7 EFFECT OF SHAPE FACTOR OF A CANAL ON THE VARIATION OF WAVE HEIGHT OF A POSITIVE SURGE WAVE PROPAGATING ALONG THE CANAL

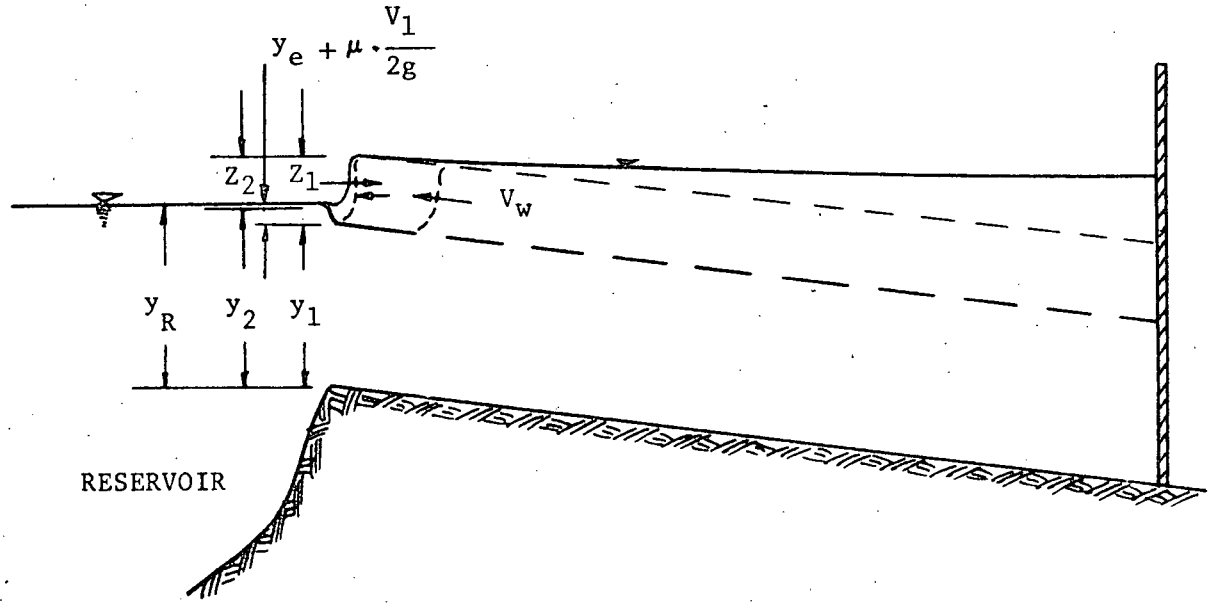

FIG. 4-8 SCHEMATIC DIAGRAM FOR A POSITIVE WAVE REACHING THE UPPER END OF THE CANAL

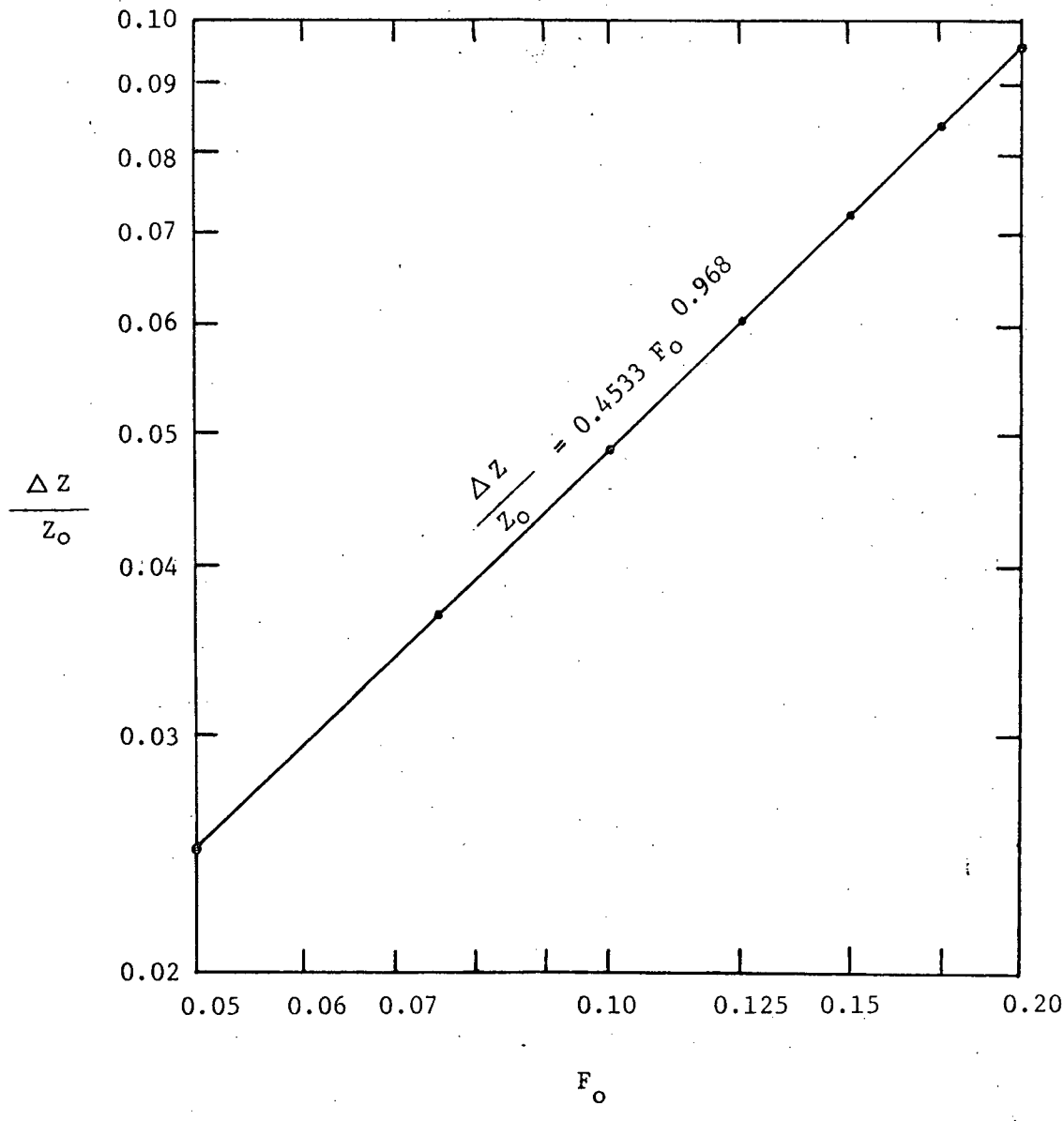

FIG. 4-9 REDUCTION OF THE NEGATIVE WAVE HEIGHT REFLECTED AT THE RESERVOIR AT THE UPPER END OF THE RECTANGULAR CANAL

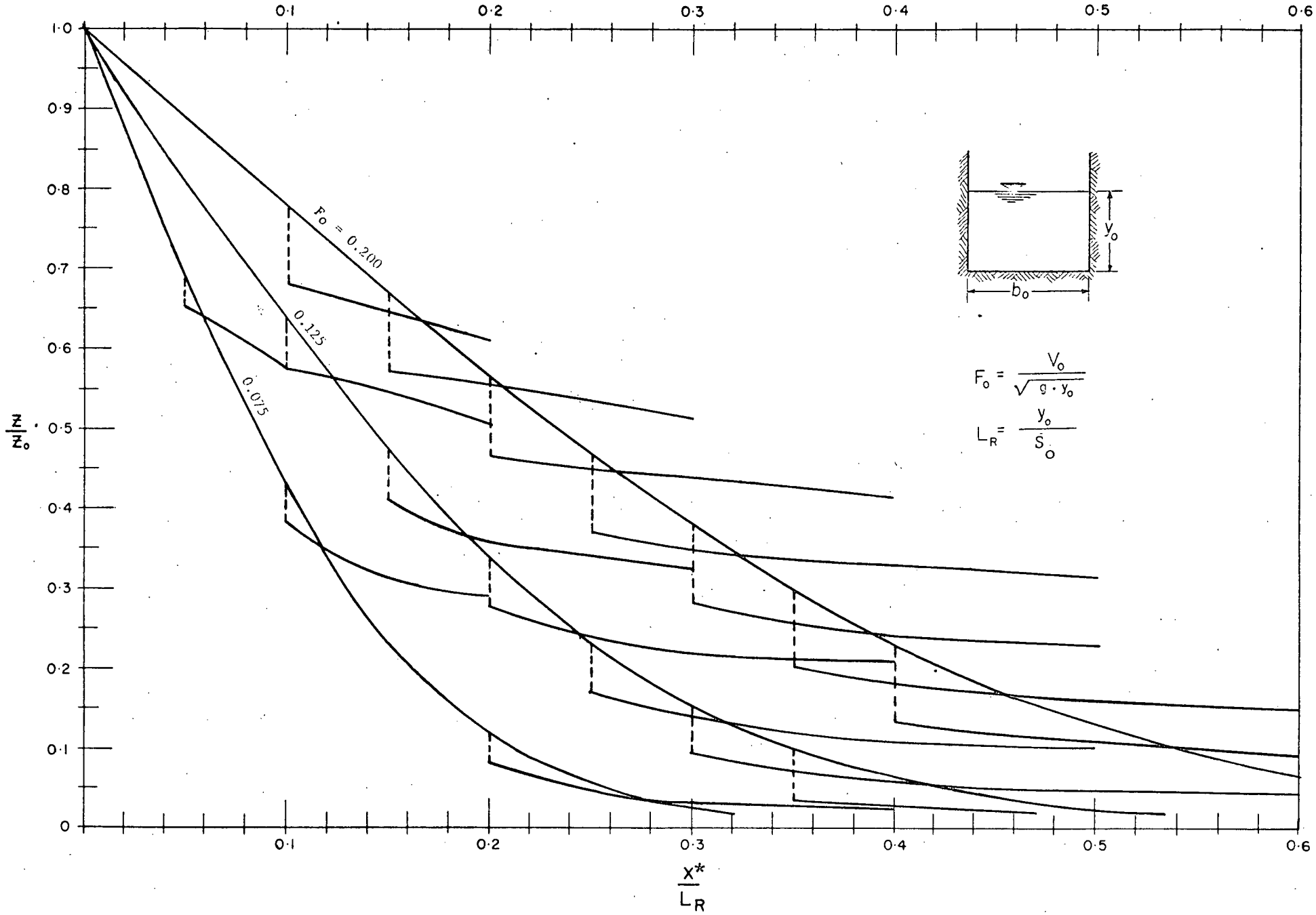

FIG. 4-10 (a) VARIATION OF WAVE HEIGHT OF A NEGATIVE SURGE PROPAGATING ALONG A RECTANGULAR POWER CANAL

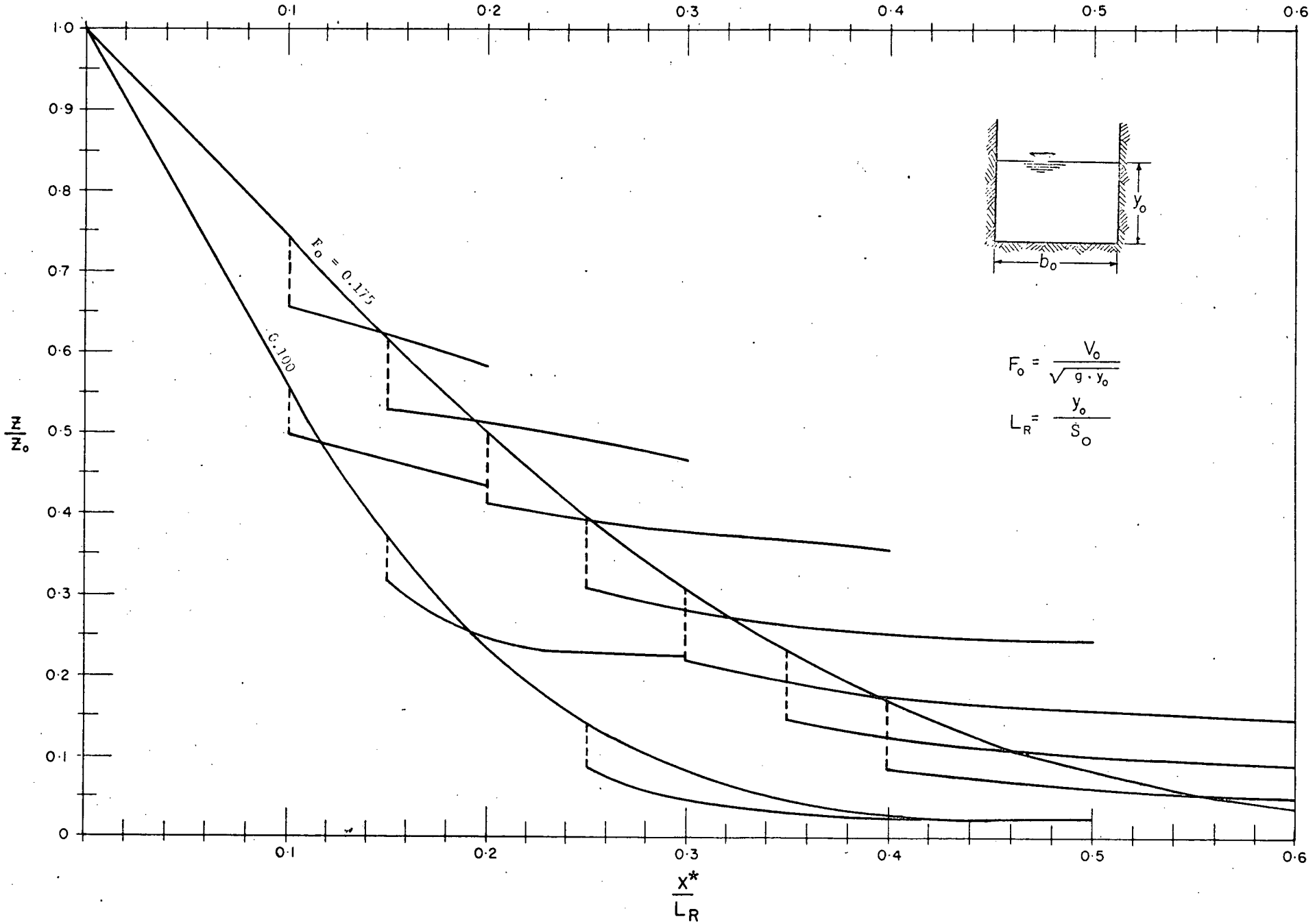

FIG. 4-10 (b) VARIATION OF WAVE HEIGHT OF A NEGATIVE SURGE PROPAGATING ALONG A RECTANGULAR POWER CANAL

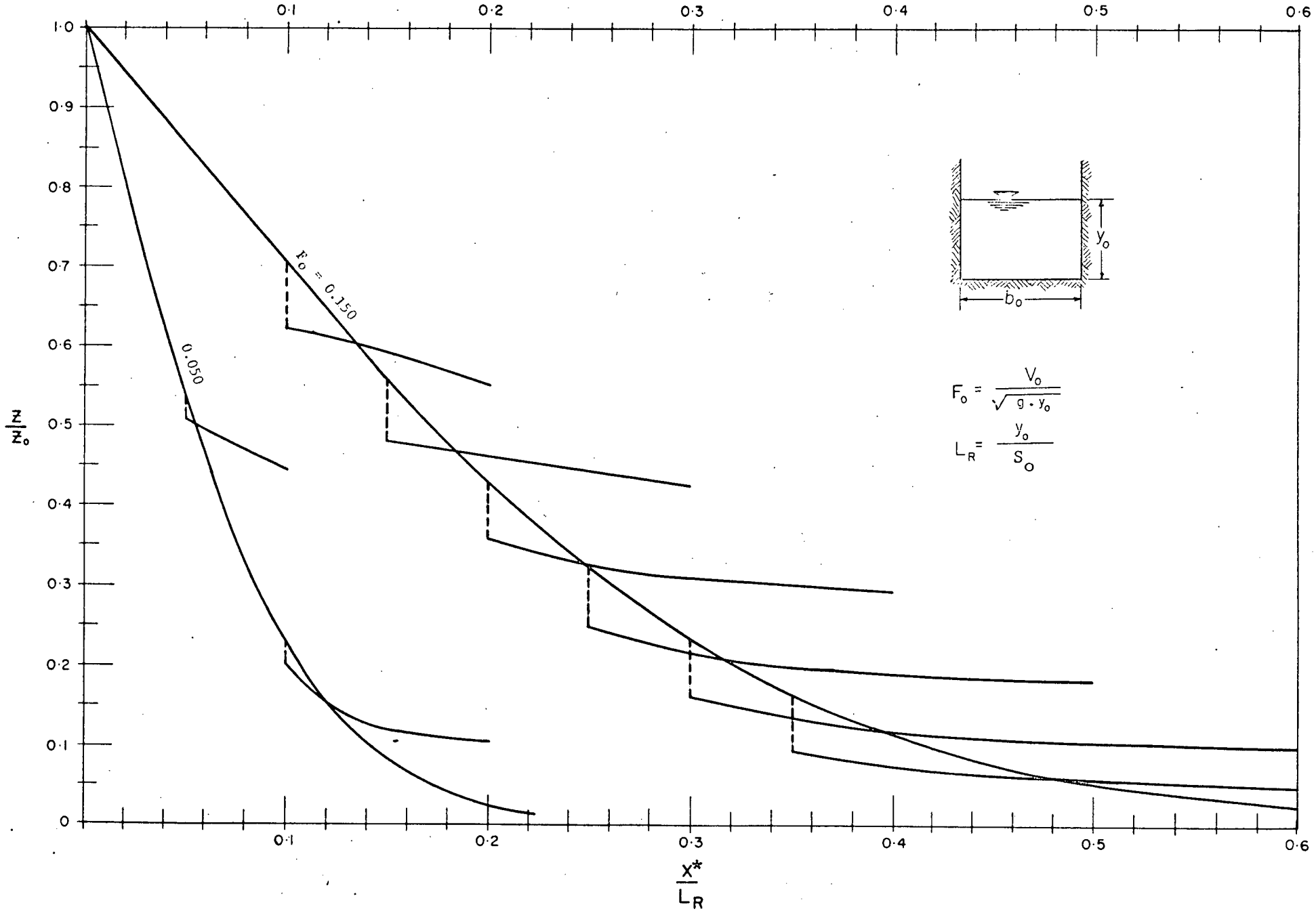

FIG. 4-10 (c) VARIATION OF WAVE HEIGHT OF A NEGATIVE SURGE PROPAGATING ALONG A RECTANGULAR POWER CANAL

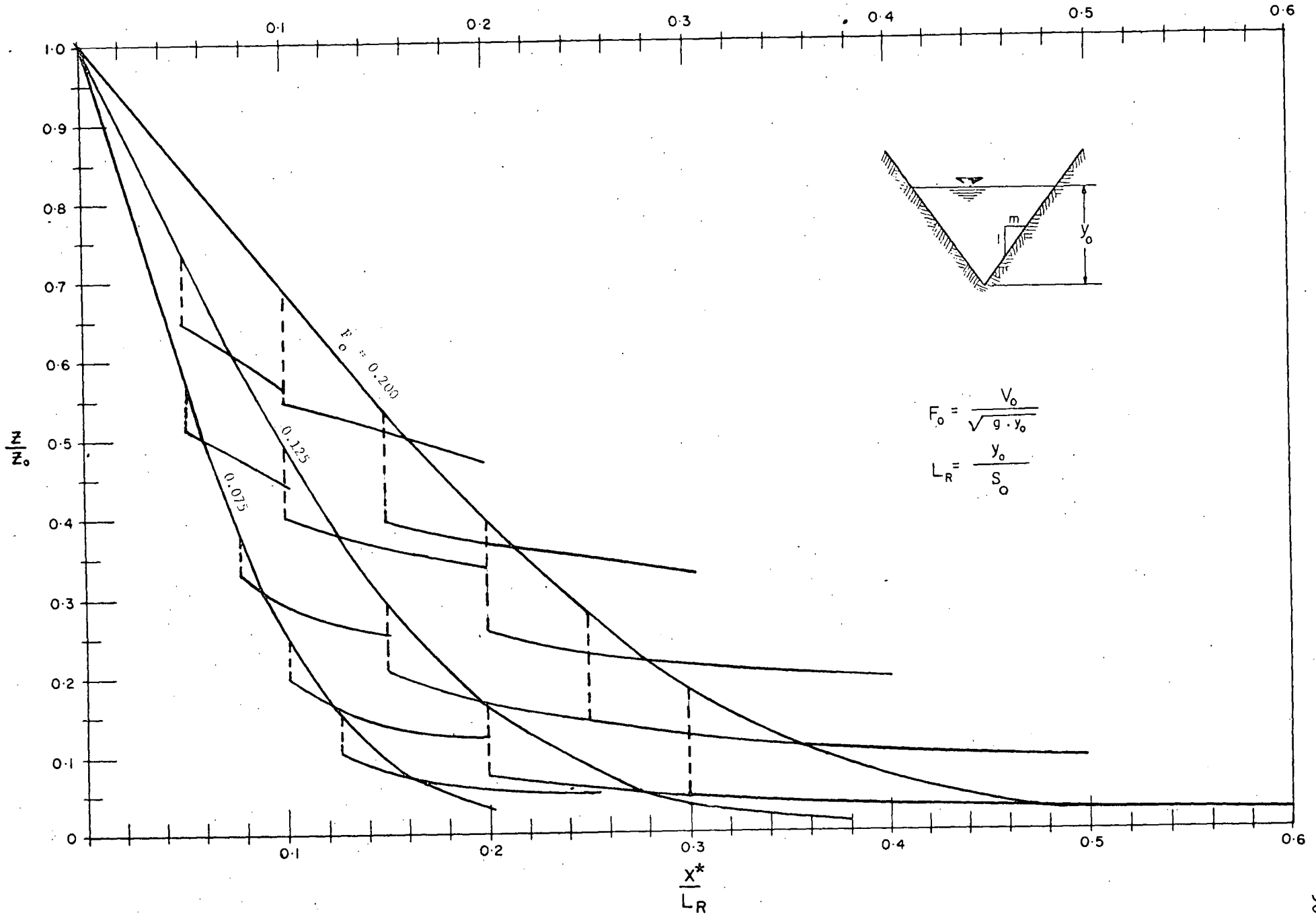

FIG. 4-11 (a) VARIATION OF WAVE HEIGHT OF A NEGATIVE SURGE PROPAGATING ALONG A TRIANGULAR POWER CANAL

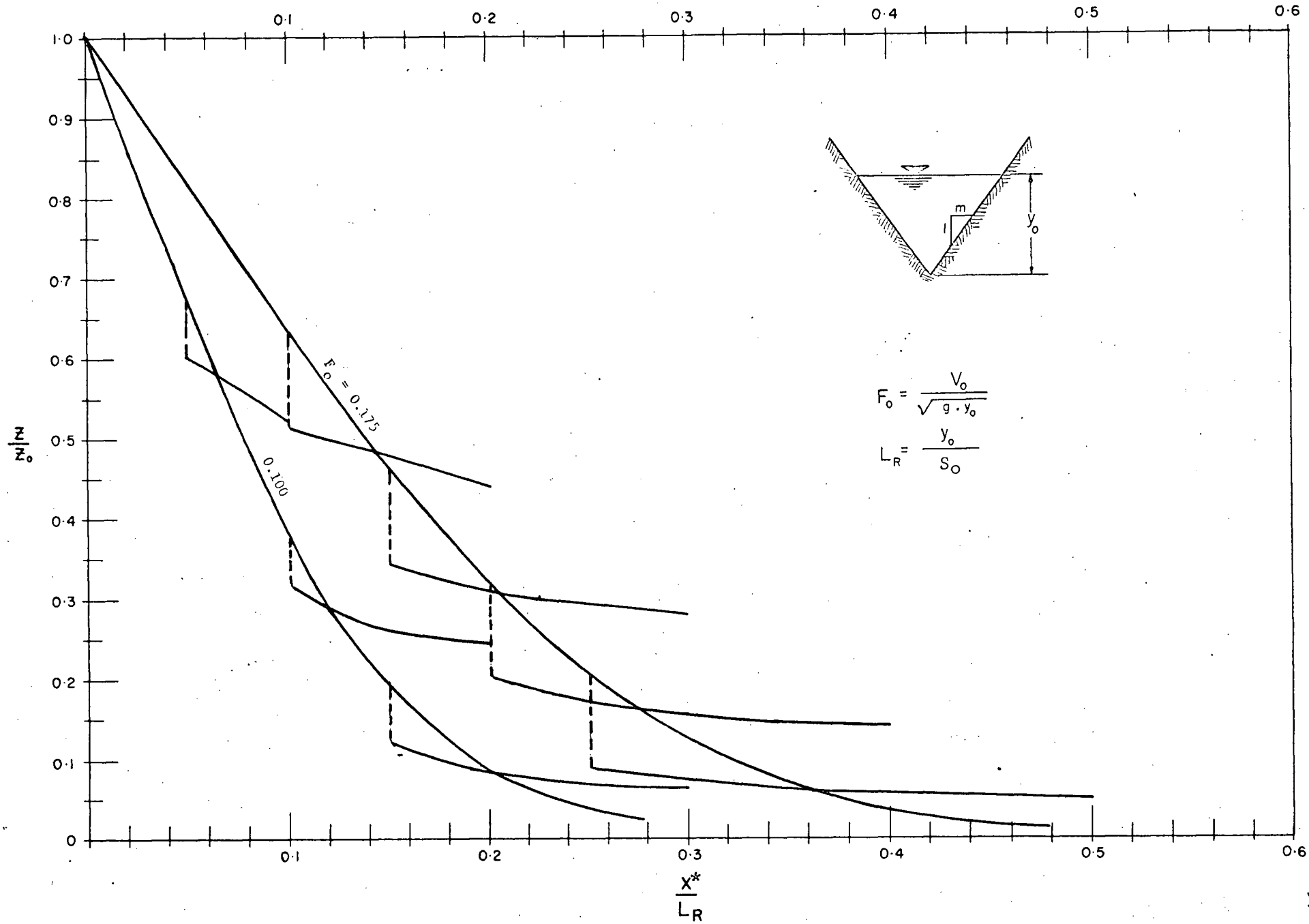

FIG. 4-11 (b) VARIATION OF WAVE HEIGHT OF A NEGATIVE SURGE PROPAGATING ALONG A TRIANGULAR POWER CANAL

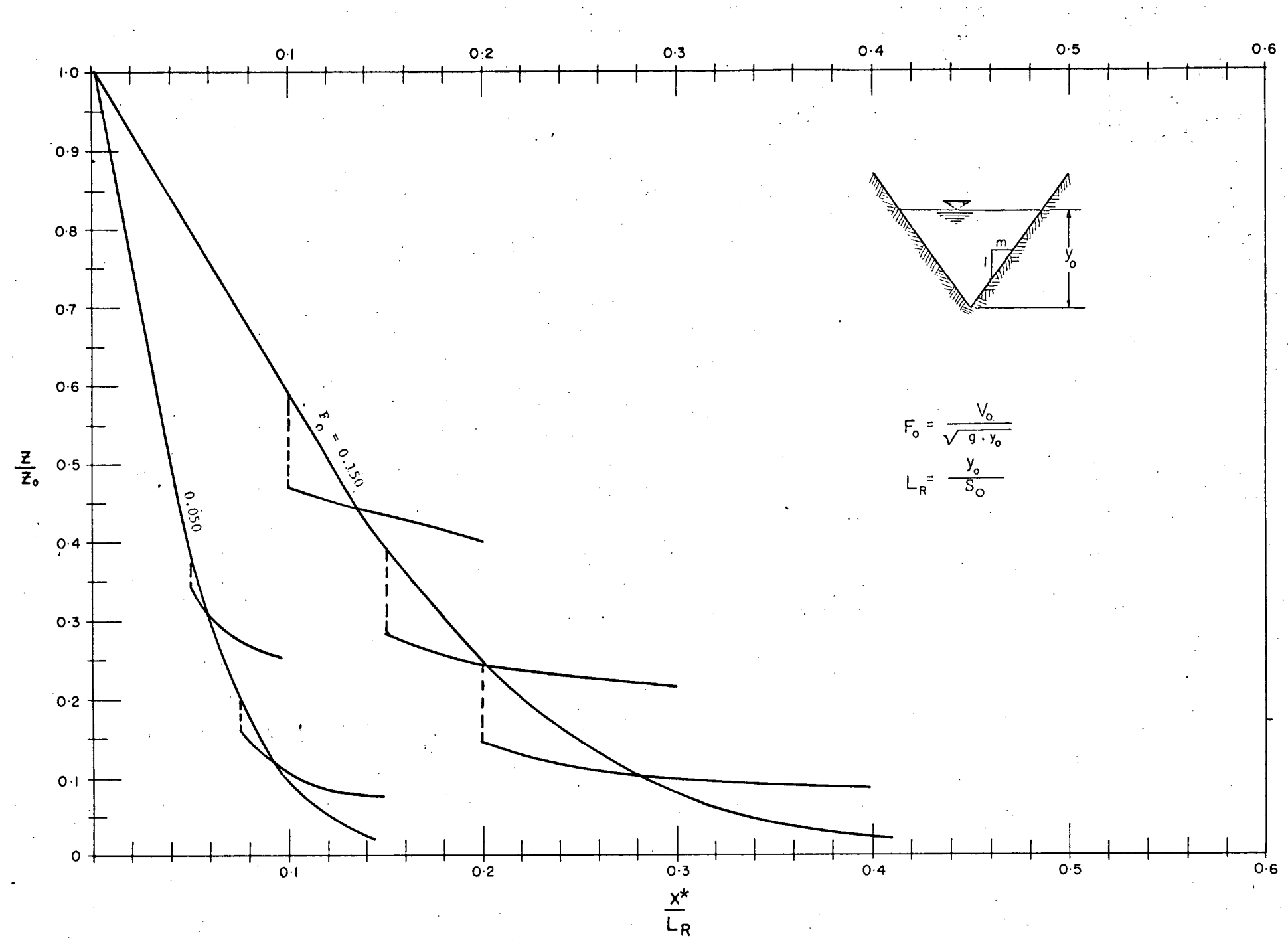

FIG. 4-11 (c) VARIATION OF WAVE HEIGHT OF A NEGATIVE SURGE PROPAGATING ALONG A TRIANGULAR POWER CANAL

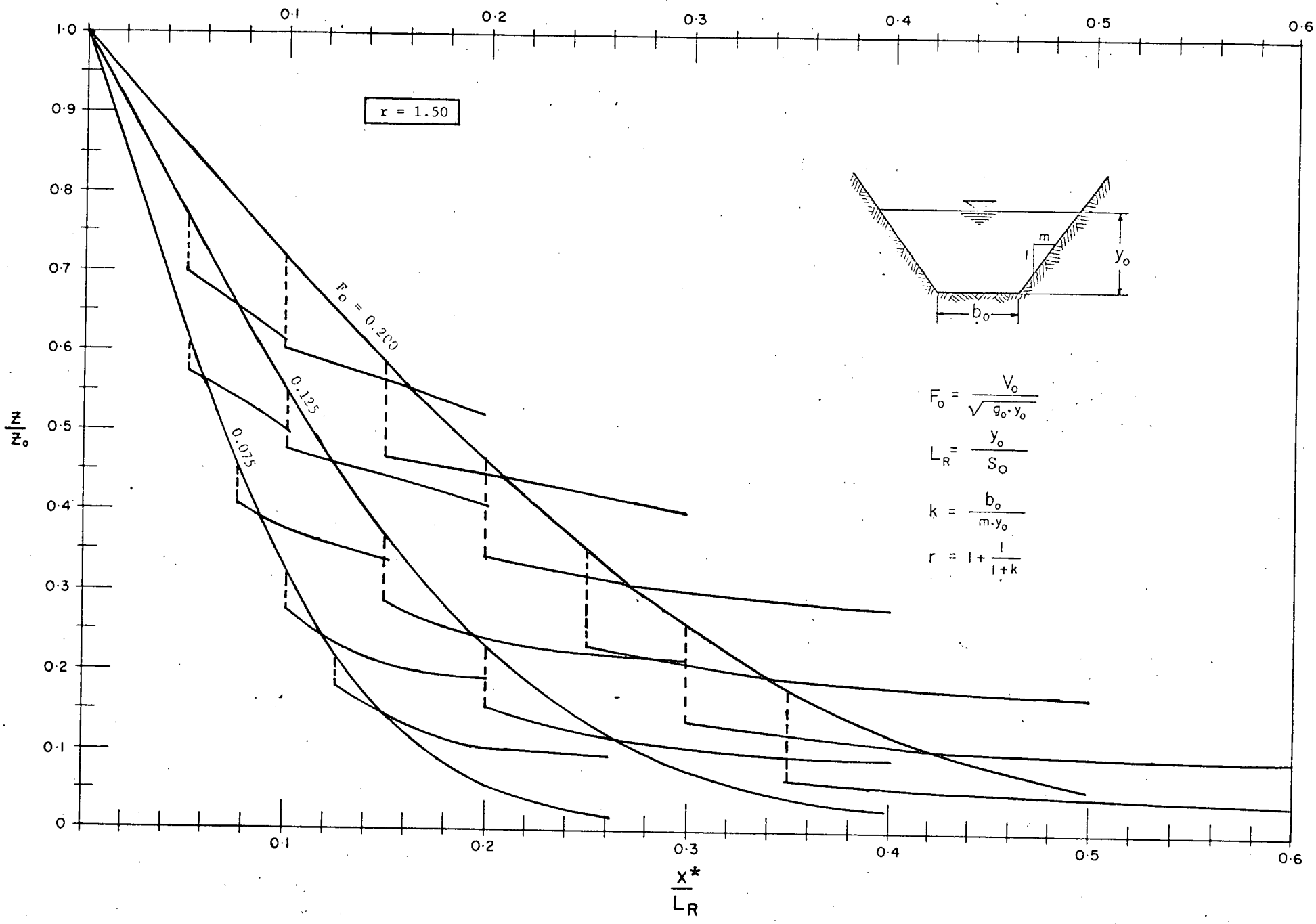

FIG. 4-12 (a) VARIATION OF WAVE HEIGHT OF A NEGATIVE SURGE PROPAGATING ALONG A TRAPEZOIDAL POWER CANAL FOR r = 1.50

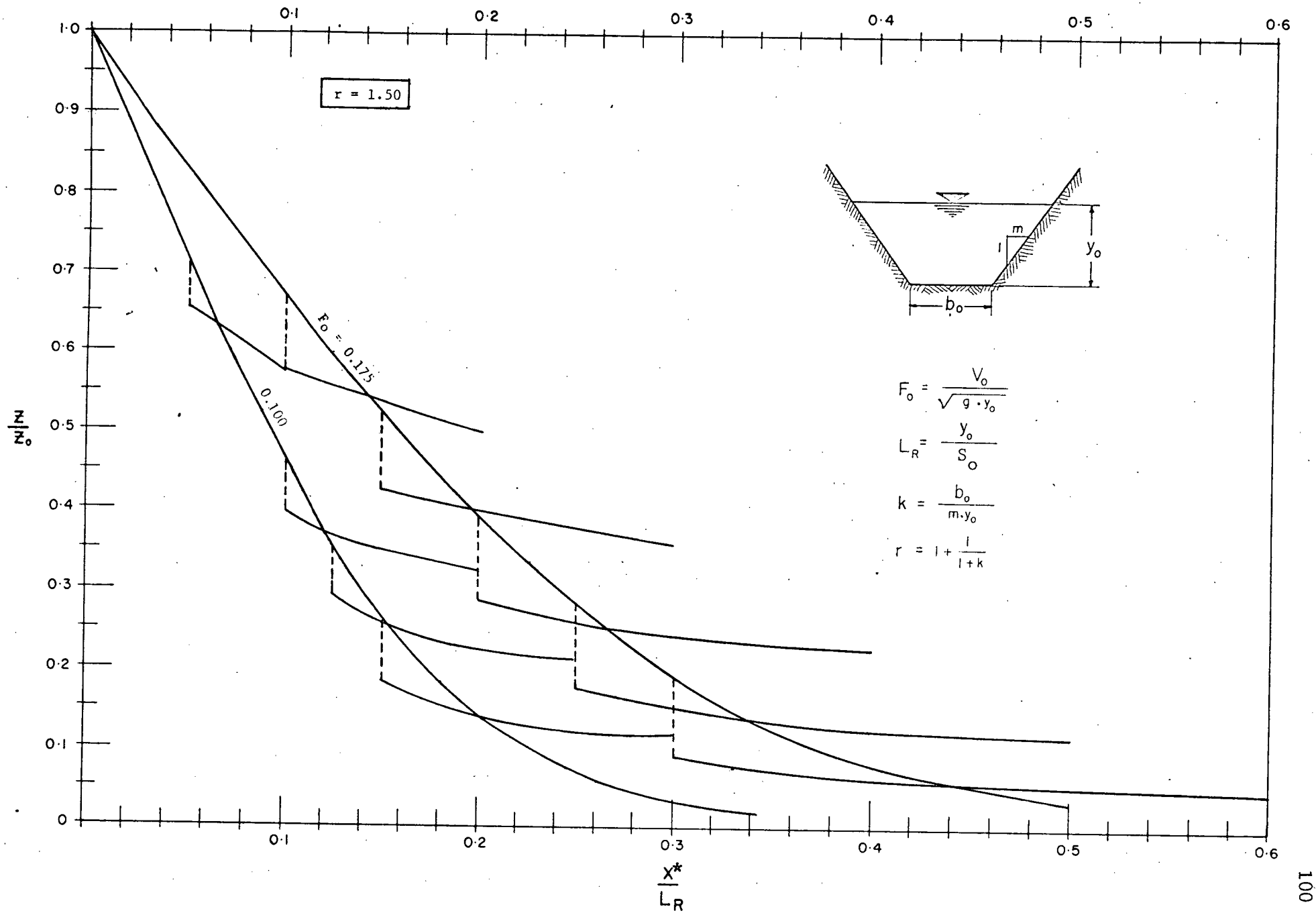

FIG. 4-12 (b) VARIATION OF WAVE HEIGHT OF A NEGATIVE SURGE PROPAGATING ALONG A TRAPEZOIDAL POWER CANAL FOR r = 1.50

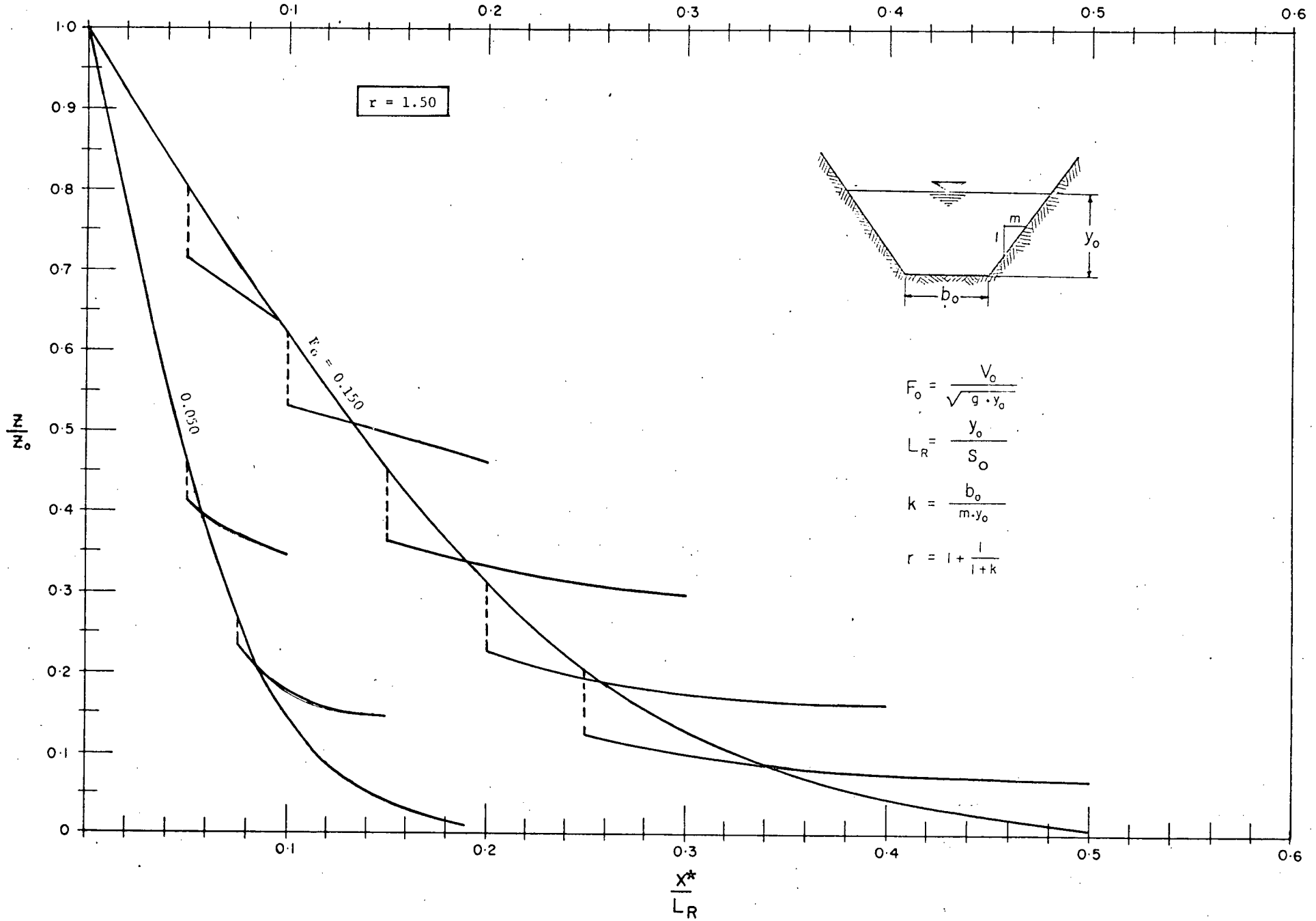

FIG. 4-12 (c) VARIATION OF WAVE HEIGHT OF A NEGATIVE SURGE PROPAGATING ALONG A TRAPEZOIDAL POWER CANAL FOR r = 1.50

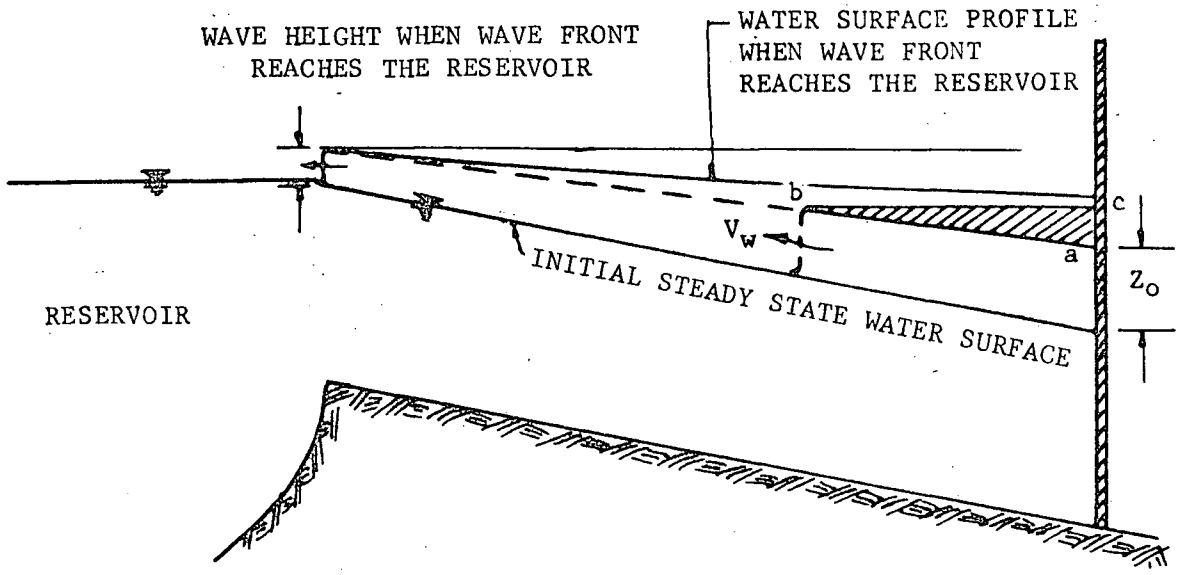

FIG. 4-13 SCHEMATIC DIAGRAM OF THE VARIATION OF WATER SURFACE FOR A POSITIVE WAVE PROPAGATING UPSTREAM ALONG THE CANAL

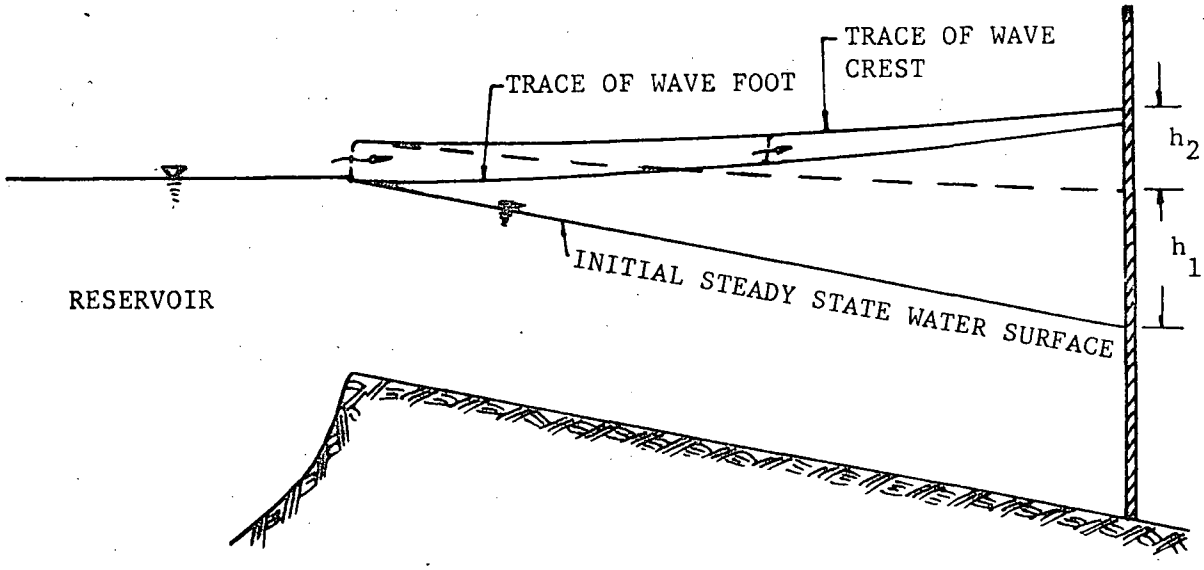

FIG. 4-14 SCHEMATIC DIAGRAM OF THE VARIATION OF WATER SURFACE FOR A NEGATIVE WAVE PROPAGATING DOWNSTREAM ALONG THE CANAL

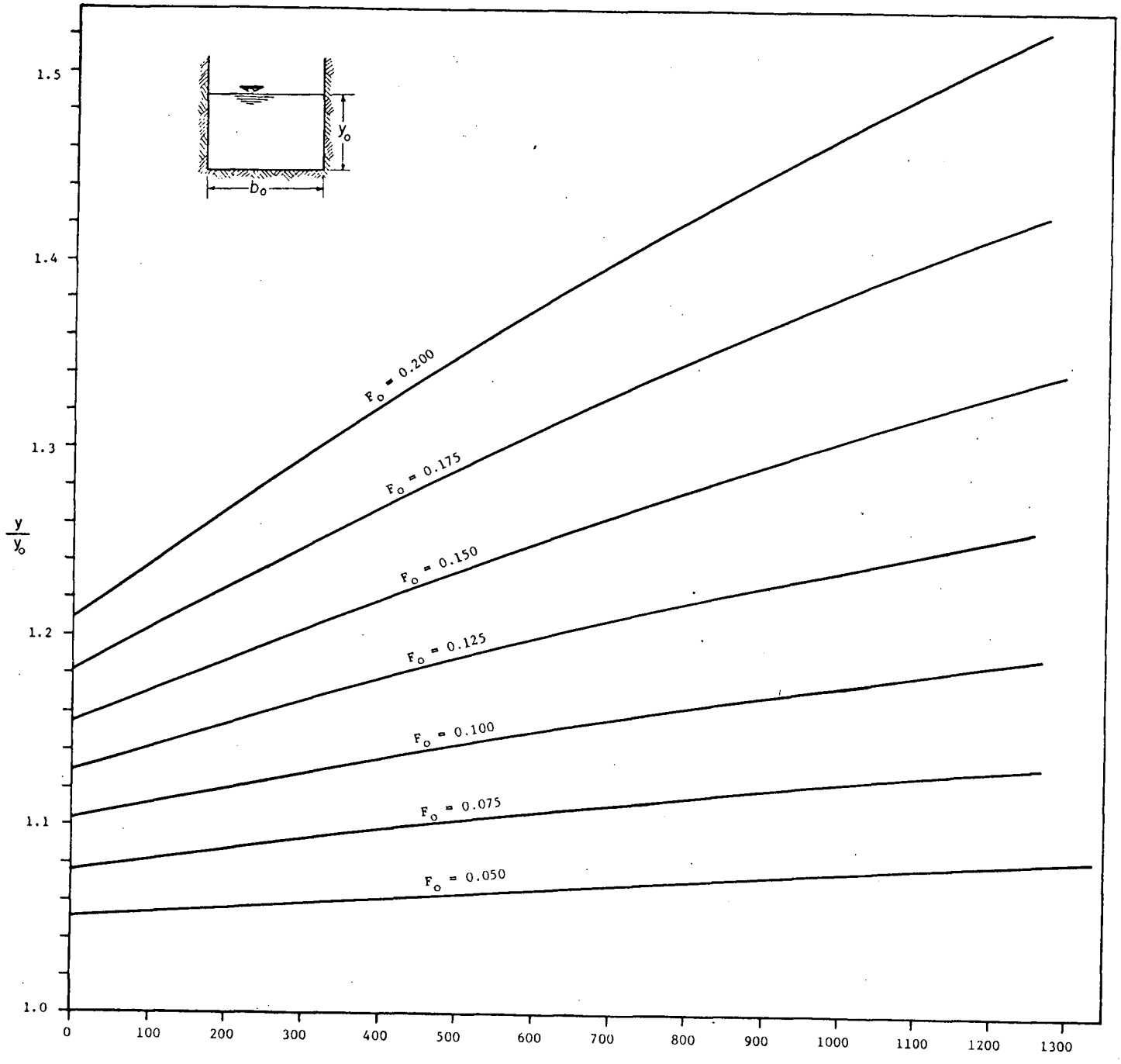

FIG. 4-15 VARIATION OF WATER SURFACE AT THE DOWNSTREAM END WITH RESPECT TO TIME FOR THE RECTANGULAR CANAL OF y_o = 30 ft., b_o = 30 ft. AND n = 0.03095

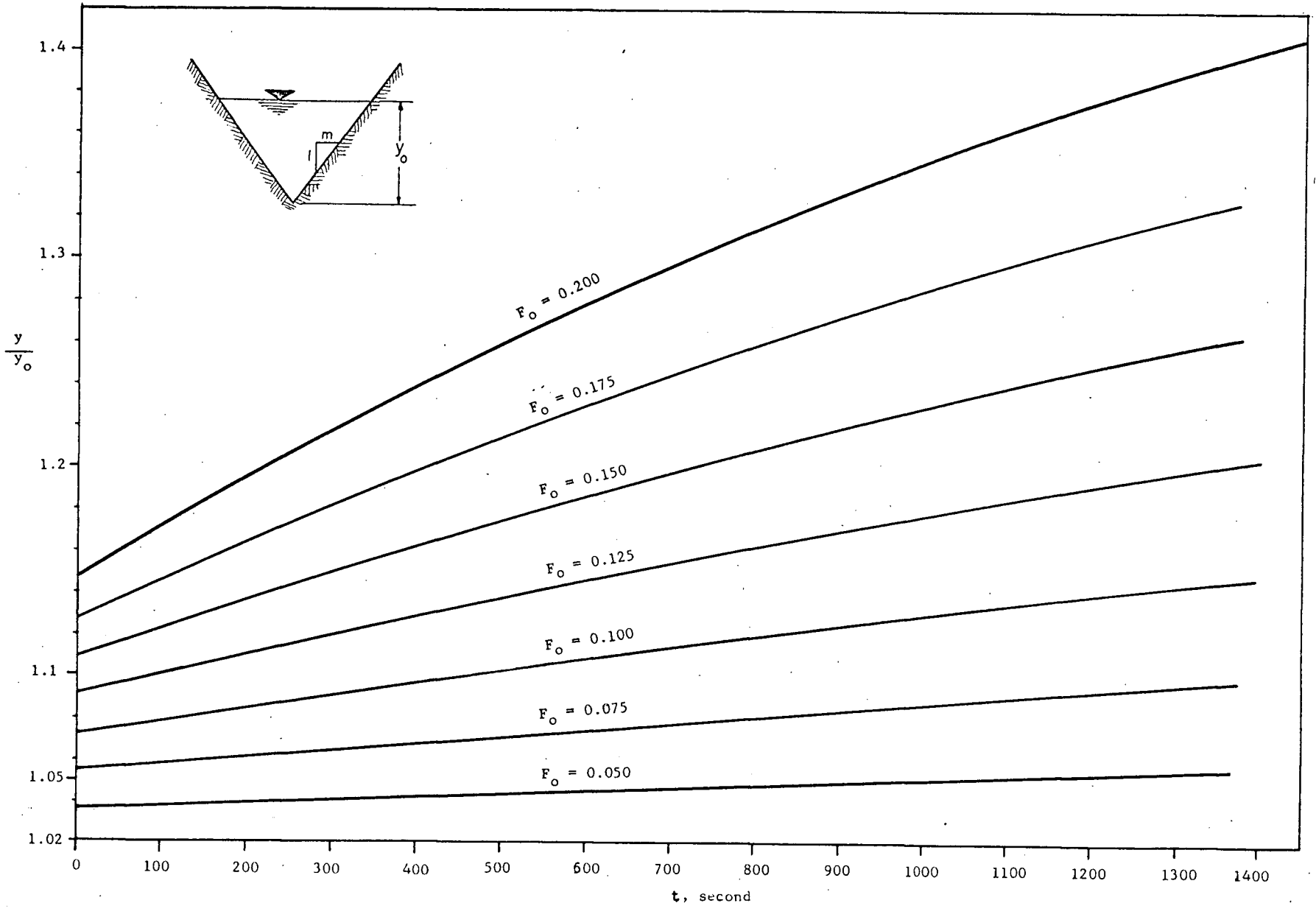

FIG. 4-16 VARIATION OF WATER SURFACE AT THE DOWNSTREAM END WITH RESPECT TO TIME FOR THE TRIANGULAR CANAL OF y_o = 22.36 ft. , m = 2.0 AND n = 0.03095

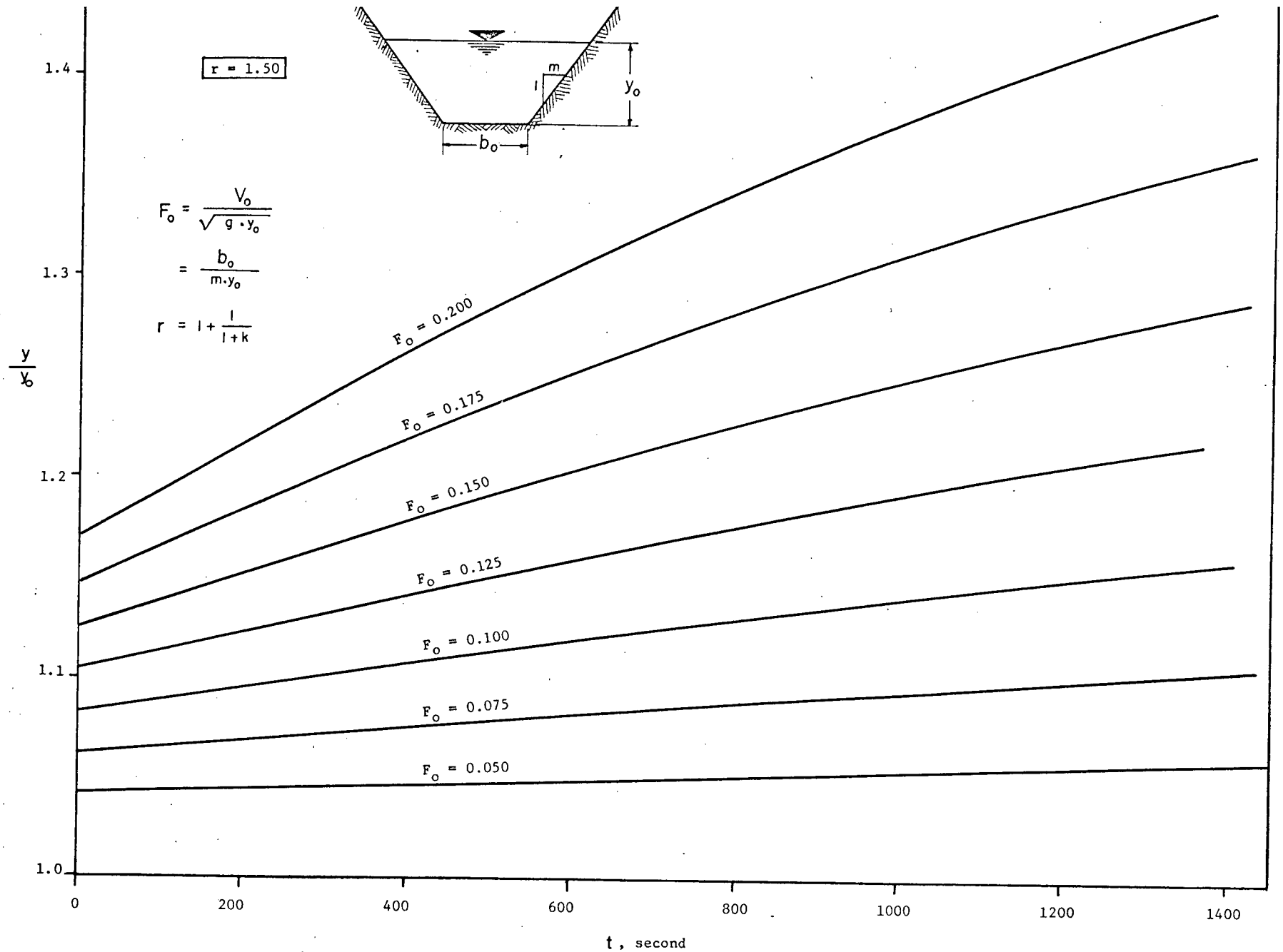

FIG. 4-17 VARIATION OF WATER SURFACE AT THE DOWNSTREAN END WITH RESPECT TO TIME FOR THE TRAPEZOIDAL CANAL OF m = 1.5 , b_o = 25.5 ft. , n = 0.03095 AND r = 1.50

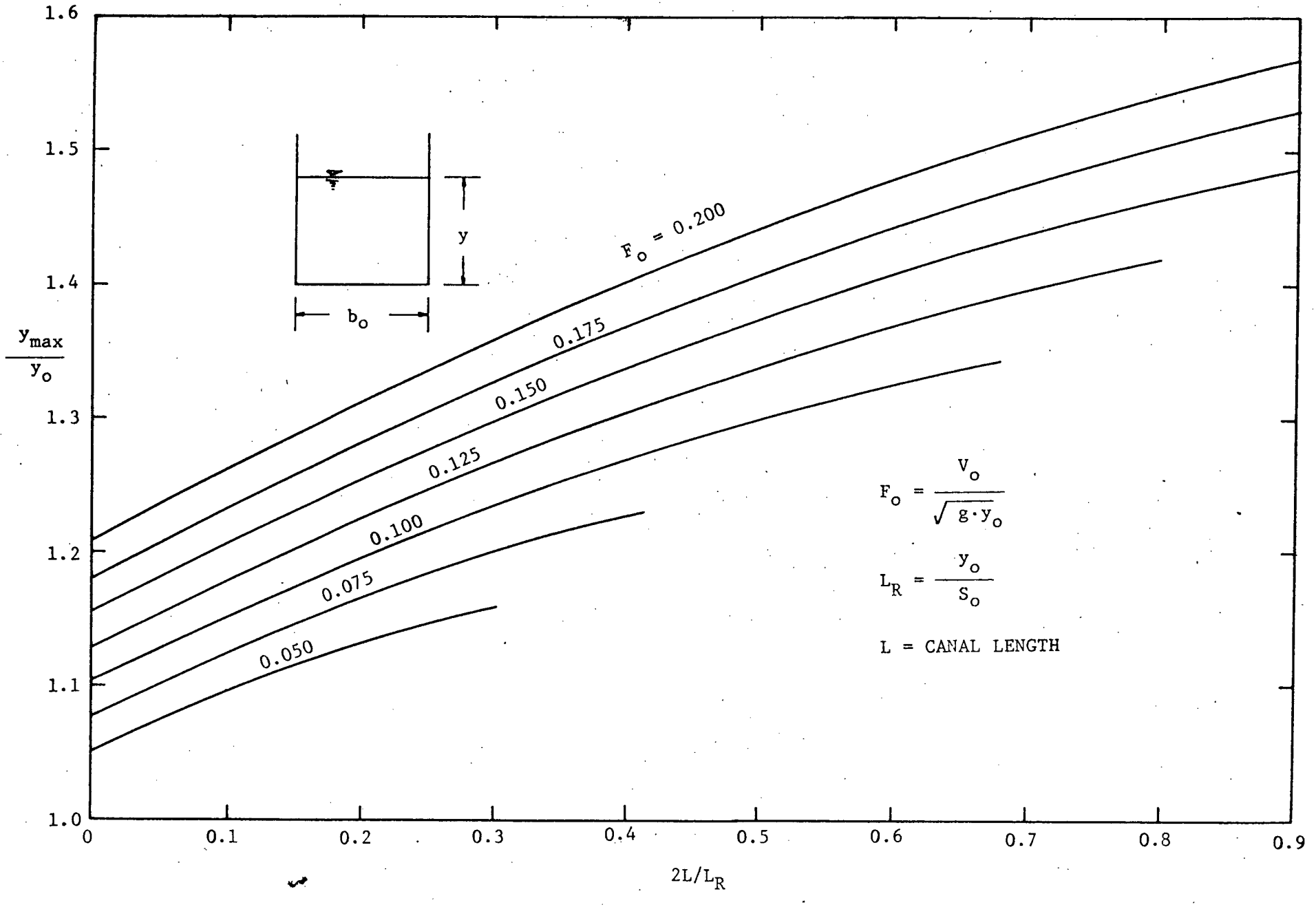

FIG. 4-18 MAXIMUM WATER DEPTH AT THE DOWNSTREAM END OF A RECTANGULAR CANAL

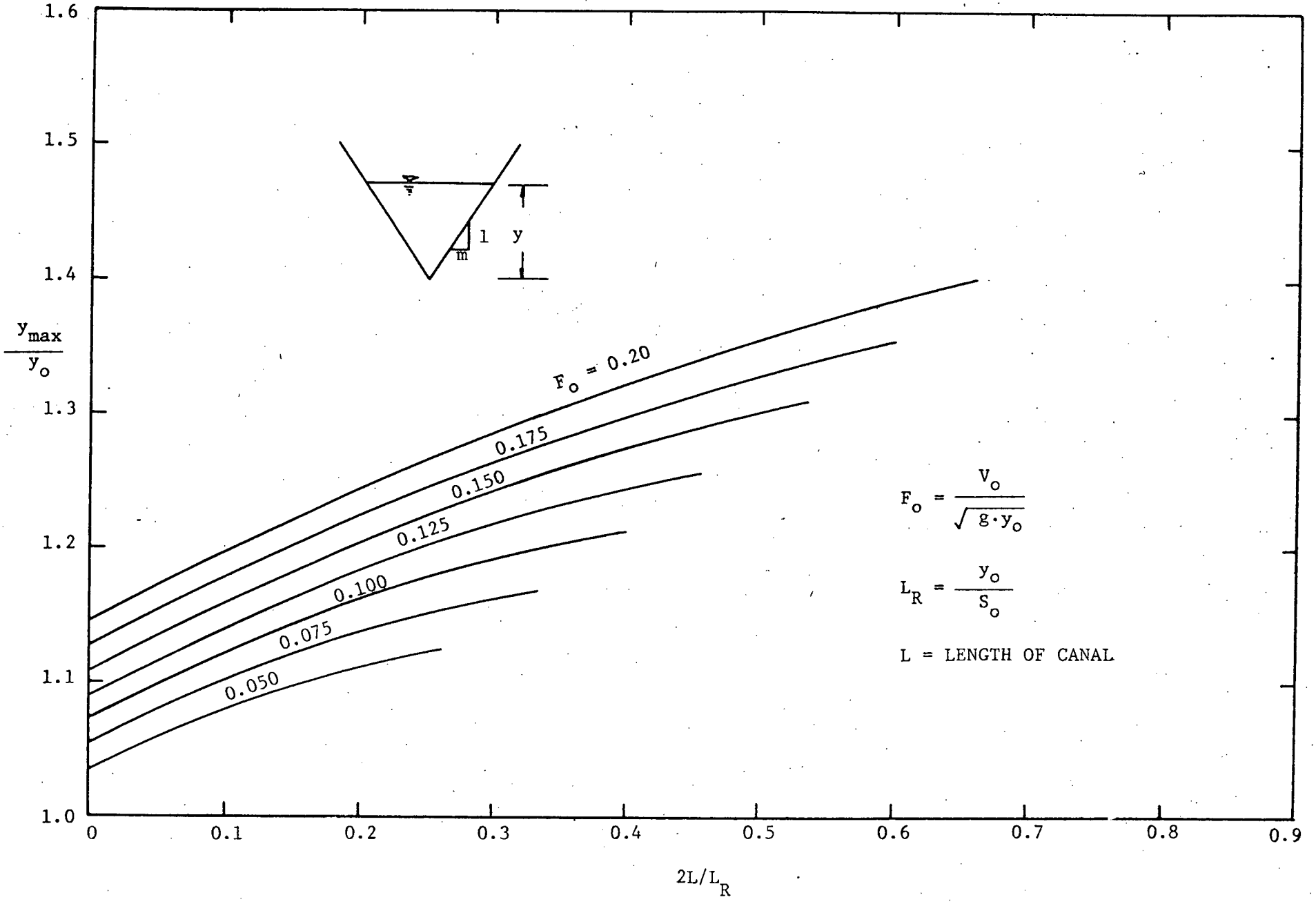

FIG. 4-19 MAXIMUM WATER DEPTH AT THE DOWNSTREAM END OF A TRIANGULAR CANAL

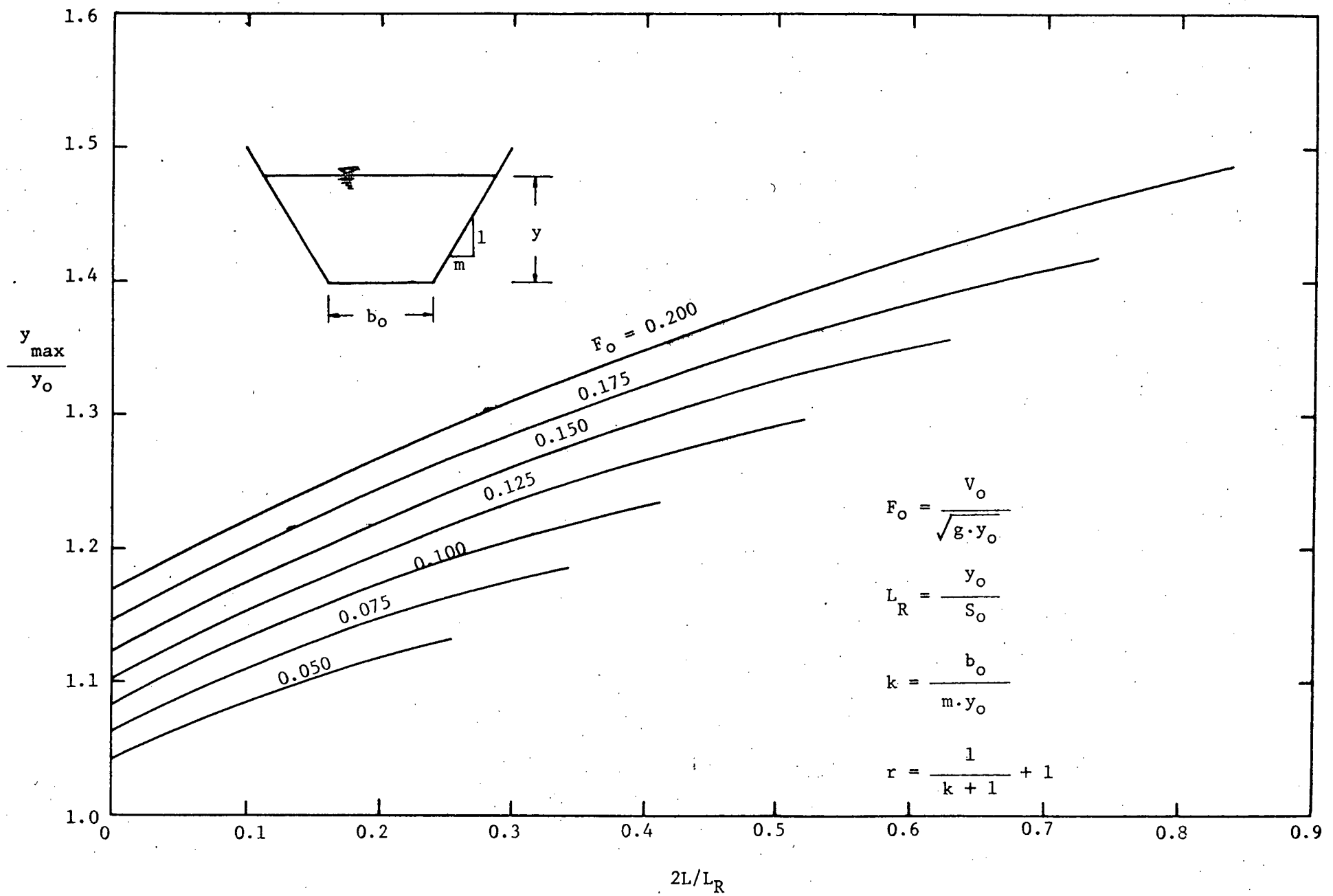

FIG. 4-20 MAXIMUM WATER DEPTH AT THE DOWNSTREAM END OF A TRAPEZOIDAL CANAL FOR r = 1.5

References

1. Johnson R.D.: The correlation of momentum and energy changes in steady flow with varying velocity and the application of the former to problems of unsteady flow or surges, in open channels, engineers and engineering (The engineers club of Philadelphia), July, 1922.

2. Favre, H.: Ondes de Translation, Dunod, Paris, 1935.

3. Streeter V.L. and Wylie E.B.: "Hydraulic Transients", McGraw-Hill Book Company, New York, 1967.

4. Rich G.R.: "Hydraulic Transients", Dover Publications, Inc., New York, 1961.

5. Jaeger C.: "Engineering Fluid Mechanics", Blackie and Son Limited, London, 1956.

6. Chow V.T.: "Open-channel Hydraulics", McGraw-Hill Book Company, New York, 1959.

7. Sandover J.A. and Zienkiewiez O.C.: Experiments on surge waves, water power, London, Vol. 9, No. 11, November, 1957.

8. Haws E.T.: Surges and Waves in Open Channels, Water Power, Vol. 6, No. 11 November, 1954.

9. U.S. Army Corps of Engineers: Hydraulic Design: surges in canals, Civil Works Construction, Engineering Manual, March 1949.

10. Henderson F.M.: "Open Channel Flow", MacMillan Book Company, 1966.

APPENDIX A(1)

Program Listing

```
C       EXAMPLE 15.6
C       OPEN CHANNEL SOLUTION BY CHAR GRID METHOD IN RECTANGULAR CHANNEL
        DIMENSION V(22,100), Y(22,100), X(22,100), T(22,100)
        WRITE(6,100)
        WRITE(6,101)
        READ(5,300) QO, B, G, HL, DX, HN,SO
        YO=8.
2       RO=YO*B/(B+2.*YO)
        VO=1.486*RO**0.667*SQRT(SO)/HN
        YONEW=QO/(B*VO)
        IF((YONEW-YO) .LT. 1.0E-3) GO TO 3
        YO=YONEW
        GO TO 2
3       YO=YONEW
        VO=QO/(B*YO)
        DO 10 I=1, 21,2
        V(I,1)=VO
        Y(I,1)=YO
        T(I,1)=0.
10      CONTINUE
        X(1,1)=0.
        DO 11 I=3, 21, 2
        J=1
        IM=I-2
        X(I,1)=X(IM,1)+DX
11      CONTINUE
        WRITE(6,102) J, (V(K,1), K=1, 21, 2 )
        WRITE(6,103) (Y(K,1), K=1,21,2)
        WRITE(6,104) (X(K,1), K=1,21,2)
        WRITE(6,105) (T(K,1), K=1,21,2)
C       FIND THE SOLUTION IN THE MIDDLE SECTION OF CHANNEL
        J=2
80      DO 40 I=2, 20, 2
        IM=I-1
        JM=J-1
        IN=I+1
        GR=SQRT(G/Y(IM,JM))
        GS=SQRT(G/Y(IN,JM))
        RG=SQRT(G*Y(IM,JM))
        SG=SQRT(G*Y(IN,JM))
        SSNUM=HN*HN*V(IN,JM)*ABS(V(IN,JM))
        RS=B*Y(IN,JM)/(B+2.*Y(IN,JM))
        SSDENO=2.21*RS**1.333
        GNS=G*(SSNUM/SSDENO-SO)
        RR=B*Y(IM,JM)/(B+2.*Y(IM,JM))
        RRDENO=2.21*RR**1.333
```

```
      RRNUM=HN*HN*V(IM,JM)*ABS(V(IM,JM))
      GNR=G*(RRNUM/RRDENO-SO)
      TPNUM=X(IN,JM)-X(IM,JM)+T(IM,JM)*(V(IM,JM)+RG)-T(IN,JM)*(V(IN,JM)-
     1SG)
      TPDENO=V(IM,JM)+RG-V(IN,JM)+SG
      T(I,J)=TPNUM/TPDENO
      TPR=T(I,J)-T(IM,JM)
      X(I,J)=X(IM,JM)+(V(IM,JM)+RG)*TPR
      TPS=T(I,J)-T(IN,JM)
      VRS=V(IM,JM)-V(IN,JM)
      Y(I,J)=(VRS+GR*Y(IM,JM)+GS*Y(IN,JM)-GNR*TPR+GNS*TPS)/(GR+GS)
      YPR=Y(I,J)-Y(IM,JM)
      V(I,J)=V(IM,JM)-GR*YPR-GNR*TPR
40    CONTINUE
      WRITE(6,106) J, (V(K,J), K=2,20,2)
      WRITE(6,107) (Y(K,J), K=2,20,2)
      WRITE(6,108) (X(K,J), K=2,20,2)
      WRITE(6,109) (T(K,J), K=2,20,2)
C     FIND THE SOLUTION AT THE UPSTREAM END OF CHANNEL
      JJ=J+1
      X(1,JJ)=0.
      I=1
      IN=I+1
      SG=SQRT(G*Y(IN,J))
      T(1,JJ)=T(2,J)-X(2,J)/(V(2,J)-SG)
      Q=720.+180.*SIN(0.03*T(1,JJ))
      GS=SQRT(G/Y(2,J))
      TPS=T(1,JJ)-T(2,J)
      RS=B*Y(2,J)/(B+2.*Y(2,J))
      SSDENO=2.21*RS**1.333
      SSNUM=HN*HN*V(2,J)*ABS(V(2,J))
      GNS=G*(SSNUM/SSDENO-SO)
      YP=Y(2,J)
18    VP=Q/(B*YP)
      VPS=VP-V(2,J)
      YPNEW=Y(2,J)+(VPS+GNS*TPS)/GS
      IF(ABS(YPNEW-YP) .LT. 1.0E-3) GO TO 19
      YP=YPNEW
      GO TO 18
19    Y(1,JJ)=YPNEW
      V(1,JJ)=Q/(B*Y(1,JJ))
C     FIND THE SOLUTION IN THE MIDDLE SECTION OF CHANNEL
      DO 50 I=3,19,2
      IM=I-1
      JM=JJ-1
      IN=I+1
      GR=SQRT(G/Y(IM,JM))
      GS=SQRT(G/Y(IN,JM))
      RG=SQRT(G*Y(IM,JM))
      SG=SQRT(G*Y(IN,JM))
      SSNUM=HN*HN*V(IN,JM)*ABS(V(IN,JM))
      RS=B*Y(IN,JM)/(B+2.*Y(IN,JM))
      SSDENO=2.21*RS**1.333
      GNS=G*(SSNUM/SSDENO-SO)
      RR=B*Y(IM,JM)/(B+2.*Y(IM,JM))
      RRDENO=2.21*RR**1.333
      RRNUM=HN*HN*V(IM,JM)*ABS(V(IM,JM))
      GNR=G*(RRNUM/RRDENO-SO)
      TPNUM=X(IN,JM)-X(IM,JM)+T(IM,JM)*(V(IM,JM)+RG)-T(IN,JM)*(V(IN,JM)-
```

```
     1SG)
      TPDENO=V(IM,JM)+RG-V(IN,JM)+SG
      T(I,JJ)=TPNUM/TPDENO
      TPR=T(I,JJ)-T(IM,JM)
      X(I,JJ)=X(IM,JM)+(V(IM,JM)+RG)*TPR
      TPS=T(I,JJ)-T(IN,JM)
      VRS=V(IM,JM)-V(IN,JM)
      Y(I,JJ)=(VRS+GR*Y(IM,JM)+GS*Y(IN,JM)-GNR*TPR+GNS*TPS)/(GR+GS)
      YPR=Y(I,JJ)-Y(IM,JM)
      V(I,JJ)=V(IM,JM)-GR*YPR-GNR*TPR
50    CONTINUE
C     FIND THE SOLUTION AT THE DOWNSTREAM END OF CHANNEL
      X(21,JJ)=HL
      I=21
      IM=I-1
      RG=SQRT(G*Y(IM,J))
      T(21,JJ)=T(IM,J)+(HL-X(IM,J))/(V(IM,J)+RG)
      GR=SQRT(G/Y(IM,J))
      TPR=T(21,JJ)-T(IM,J)
      RR=B*Y(IM,J)/(B+2.*Y(IM,J))
      RRDENO=2.21*RR**1.333
      RRNUM=HN*HN*V(IM,J)*ABS(V(IM,J))
      GNR=G*(RRNUM/RRDENO-SO)
      Y(21,JJ)=YO
      YPR=Y(21,JJ)-Y(IM,J)
      V(21,JJ)=V(IM,J)-GR*YPR-GNR*TPR
      WRITE(6,102) JJ, (V(K,JJ), K=1,21,2)
      WRITE(6, 103) (Y(K,JJ),K=1,21,2)
      WRITE(6, 104) (X(K,JJ),K=1,21,2)
      WRITE(6, 105) (T(K,JJ),K=1,21,2)
      IF( J .GT. 32 ) GO TO 70
      J=J+2
      GO TO 80
300   FORMAT(7F8.0)
100   FORMAT(4X,1HI,9X,1H1,9X,1H2,9X,1H3,9X,1H4,9X,1H5,9X,1H6,9X,1H7,9X,
     11H8,9X,1H9,8X,2H10,8X,2H11 )
101   FORMAT(1X,1HJ //)
102   FORMAT(I3,4X,1HV,11F10.3)
103   FORMAT(7X,1HY,11F10.3)
104   FORMAT(7X,1HX,11F10.3)
105   FORMAT(7X,1HT,11F10.3 //)
106   FORMAT(I3,4X,1HV,6X,10F10.3)
107   FORMAT(7X,1HY,6X,10F10.3)
108   FORMAT(7X,1HX,6X,10F10.3)
109   FORMAT(7X,1HT,6X,10F10.3 //)
70    STOP
      END
$ENTRY
```

APPENDIX A(2)

Program Listing

```
C       EXAMPLE 15.5
C       OPEN CHANNEL SOLUTION BY CHAR GRID METHOD IN RECTANGULAR CHANNEL
        DIMENSION V(22,100), Y(22,100), X(22,100), T(22,100)
        WRITE(6,100)
        WRITE(6,101)
        READ(5, 300) YO, B, G, HL, DX, AO, PO, HN, SO
        QO=132.*(YO-2.32)**1.5
        VO=QO/AO
        DO 10 I=1, 21,2
        V(I,1)=VO
        Y(I,1)=YO
        T(I,1)=0.
10      CONTINUE
        X(1,1)=0.
        DO 11 I=3, 21, 2
        J=1
        IM=I-2
        X(I,1)=X(IM,1)+DX
11      CONTINUE
        WRITE(6,102) J, (V(K,1), K=1, 21, 2 )
        WRITE(6,103) (Y(K,1), K=1,21,2)
        WRITE(6,104) (X(K,1), K=1,21,2)
        WRITE(6,105) (T(K,1), K=1,21,2)
C       FIND THE SOLUTION IN THE MIDDLE SECTION OF CHANNEL
        J=2
80      DO 40 I=2, 20, 2
        IM=I-1
        JM=J-1
        IN=I+1
        GR=SQRT(G/Y(IM,JM))
        GS=SQRT(G/Y(IN,JM))
        RG=SQRT(G*Y(IM,JM))
        SG=SQRT(G*Y(IN,JM))
        SSNUM=HN*HN*V(IN,JM)*ABS(V(IN,JM))
        RS=B*Y(IN,JM)/(B+2.*Y(IN,JM))
        SSDENO=2.21*RS**1.333
        GNS=G*(SSNUM/SSDENO-SO)
        RR=B*Y(IM,JM)/(B+2.*Y(IM,JM))
        RRDENO=2.21*RR**1.333
        RRNUM=HN*HN*V(IM,JM)*ABS(V(IM,JM))
        GNR=G*(RRNUM/RRDENO-SO)
        TPNUM=X(IN,JM)-X(IM,JM)+T(IM,JM)*(V(IM,JM)+RG)-T(IN,JM)*(V(IN,JM)-
       1SG)
        TPDENO=V(IM,JM)+RG-V(IN,JM)+SG
        T(I,J)=TPNUM/TPDENO
        TPR=T(I,J)-T(IM,JM)
        X(I,J)=X(IM,JM)+(V(IM,JM)+RG)*TPR
        TPS=T(I,J)-T(IN,JM)
        VRS=V(IM,JM)-V(IN,JM)
```

```
      X(I,JJ)=X(IM,JM)+(V(IM,JM)+RG)*TPR
      TPS=T(I,JJ)-T(IN,JM)
      VRS=V(IM,JM)-V(IN,JM)
      Y(I,JJ)=(VRS+GR*Y(IM,JM)+GS*Y(IN,JM)-GNR*TPR+GNS*TPS)/(GR+GS)
      YPR=Y(I,JJ)-Y(IM,JM)
      V(I,JJ)=V(IM,JM)-GR*YPR-GNR*TPR
50    CONTINUE
C     FIND THE SOLUTION AT THE DOWNSTREAM END OF CHANNEL
      X(21,JJ)=HL
      I=21
      IM=I-1
      RG=SQRT(G*Y(IM,J))
      T(21,JJ)=T(IM,J)+(HL-X(IM,J))/(V(IM,J)+RG)
      GR=SQRT(G/Y(IM,J))
      TPR=T(21,JJ)-T(IM,J)
      RR=B*Y(IM,J)/(B+2.*Y(IM,J))
      RRDENO=2.21*RR**1.333
      RRNUM=HN*HN*V(IM,J)*ABS(V(IM,J))
      GNR=G*(RRNUM/RRDENO-SO)
      YP=Y(IM,J)
27    YP3=(YP-2.32)**3
      VP=132.*SQRT(YP3)/(B*YP)
      VRP=V(IM,J)-VP
      YPNEW=Y(IM,J)+(VRP-GNR*TPR)/GR
      IF( ABS(YPNEW-YP) .LT. 1.0E-3) GO TO 26
      YP=YPNEW
      GO TO 27
26    Y(21,JJ)=YPNEW
      YP3=(Y(21,JJ)-2.32)**3
      V(21,JJ)=132.*SQRT(YP3)/(B*Y(21,JJ))
      WRITE(6,102) JJ, (V(K,JJ), K=1,21,2)
      WRITE(6, 103) (Y(K,JJ),K=1,21,2)
      WRITE(6, 104) (X(K,JJ),K=1,21,2)
      WRITE(6, 105) (T(K,JJ),K=1,21,2)
      IF( T(1,JJ) .GT. 2400.) GO TO 70
      J=J+2
      GO TO 80
300   FORMAT(9F8.0)
100   FORMAT(4X,1HI,9X,1H1,9X,1H2,9X,1H3,9X,1H4,9X,1H5,9X,1H6,9X,1H7,9X,
     11H8,9X,1H9,8X,2H10,8X,2H11 )
101   FORMAT(1X,1HJ //)
102   FORMAT(I3,4X,1HV,11F10.3)
103   FORMAT(7X,1HY,11F10.3)
104   FORMAT(7X,1HX,11F10.3)
105   FORMAT(7X,1HT,11F10.3 //)
106   FORMAT(I3,4X,1HV,6X,10F10.3)
107   FORMAT(7X,1HY,6X,10F10.3)
108   FORMAT(7X,1HX,6X,10F10.3)
109   FORMAT(7X,1HT,6X,10F10.3 //)
70    STOP
      END
$ENTRY
```

```
      Y(I,J)=(VRS+GR*Y(IM,JM)+GS*Y(IN,JM)-GNR*TPR+GNS*TPS)/(GR+GS)
      YPR=Y(I,J)-Y(IM,JM)
      V(I,J)=V(IM,JM)-GR*YPR-GNR*TPR
40    CONTINUE
      WRITE(6,106) J, (V(K,J), K=2,20,2)
      WRITE(6,107) (Y(K,J), K=2,20,2)
      WRITE(6,108) (X(K,J), K=2,20,2)
      WRITE(6,109) (T(K,J), K=2,20,2)
C     FIND THE SOLUTION AT THE UPSTREAM END OF CHANNEL
      JJ=J+1
      X(1,JJ)=0.
      I=1
      IN=I+1
      SG=SQRT(G*Y(IN,J))
      T(1,JJ)=T(2,J)-X(2,J)/(V(2,J)-SG)
      IF( T(1,JJ) .GT. 1799.) GO TO 17
      DQ=QO*T(1,JJ)/1200.
      IF( T(1,JJ) .LT. 1199.) GO TO 16
      DQ=QO*(T(1,JJ)-1200.)/1200.
      Q=2.*QO-DQ
      GO TO 17
16    Q=QO+DQ
17    GS=SQRT(G/Y(2,J))
      TPS=T(1,JJ)-T(2,J)
      RS=B*Y(2,J)/(B+2.*Y(2,J))
      SSDENO=2.21*RS**1.333
      SSNUM=HN*HN*V(2,J)*ABS(V(2,J))
      GNS=G*(SSNUM/SSDENO-SO)
      YP=Y(2,J)
18    VP=Q/(B*YP)
      VPS=VP-V(2,J)
      YPNEW=Y(2,J)+(VPS+GNS*TPS)/GS
      IF(ABS(YPNEW-YP) .LT. 1.0E-3) GO TO 19
      YP=YPNEW
      GO TO 18
19    Y(1,JJ)=YPNEW
      V(1,JJ)=Q/(B*Y(1,JJ))
C     FIND THE SOLUTION IN THE MIDDLE SECTION OF CHANNEL
      DO 50 I=3,19,2
      IM=I-1
      JM=JJ-1
      IN=I+1
      GR=SQRT(G/Y(IM,JM))
      GS=SQRT(G/Y(IN,JM))
      RG=SQRT(G*Y(IM,JM))
      SG=SQRT(G*Y(IN,JM))
      SSNUM=HN*HN*V(IN,JM)*ABS(V(IN,JM))
      RS=B*Y(IN,JM)/(B+2.*Y(IN,JM))
      SSDENO=2.21*RS**1.333
      GNS=G*(SSNUM/SSDENO-SO)
      RR=B*Y(IM,JM)/(B+2.*Y(IM,JM))
      RRDENO=2.21*RR**1.333
      RRNUM=HN*HN*V(IM,JM)*ABS(V(IM,JM))
      GNR=G*(RRNUM/RRDENO-SO)
      TPNUM=X(IN,JM)-X(IM,JM)+T(IM,JM)*(V(IM,JM)+RG)-T(IN,JM)*(V(IN,JM)-
     1SG)
      TPDENO=V(IM,JM)+RG-V(IN,JM)+SG
      T(I,JJ)=TPNUM/TPDENO
      TPR=T(I,JJ)-T(IM,JM)
```

APPENDIX B

Program Listing

```
C   SURGE WAVES IN THE POWER CANALS
C   WFP IS THE CONTROL PARAMETER IE POSITIVE OR NEGATIVE WAVE
C     BO=WIDTH OF W. S. AT YO SECTION
C    B=WIDTH OF CHANNEL BOTTOM
      DIMENSION V(70,58),Y(70,58)X(70,58)T(70,58)
    1 READ(5,101) F,RO,HKEI,GAMA,HITN,REFPT,XM,B,WFP
  101 FORMAT(9F10.0)
      IF(RO .LT. 0.0) STOP
      JDIM=60
      Q=0.0
      HNEG=-1.0
      UPEND=-1.0
      G=32.2
      HN=RO**0.6667/HKEI
      IF(GAMA .LE. 0.0 ) GO TO 1151
      YONUM=RO*(XM/GAMA+2.0*SQRT(1.0+XM**2))
      YO=YONUM/(XM*(1.0+1.0/GAMA))
      B=XM*YO/GAMA
      GO TO 1152
 1151 IF(XM .LE. 0.0 ) GO TO 1153
      YO=2.0*RO*SQRT(1.0+XM*XM)/XM
      GO TO 1152
 1153 YO=RO*B/(B-2.0*RO)
 1152 VO=F*SQRT(G*YO)
      SO=(VO/(1.486*HKEI) )**2
      BO=B+2.0*YO*XM
      YOBAR=YO*(BO+2.0*B)/(3.0*(BO+B))
      AO=(B+YO*XM)*YO
      QO=VO*AO
      PO=B+2.0*YO*SQRT(1.0+XM*XM)
      XL=YO/SO
       HLF=0.
      WRITE(6,140) F, RO,HKEI,GAMA,HITN,REFPT,XM,B ,YO,VO
  140 FORMAT(5X,3H F=,F6.3,2X,4H RO=,F5.1,2X,3H K=,F6.1,2X,6H GAMA=,
     1 F4.1,2X,6H HITN=,F6.1,2X,7H REFPT=,F5.2,4H XM=,F4.1,5X,3H B=,
     2 F6.1,2X,4H YO=,F6.2,2X,4H VO=,F6.2 // )
C  NEGATIVE WAVE REFLECT AT RESERVOIR ( CONSTSTANT VALUES OF X/LO)
C   THE NUMBER OF HITN HAS TO BE CHANGED AS HL CHANGES
C   HITN=NO. OF REACHES OF CHANNEL DIVIDED
C   REFPT=PT. OF NEGATIVE WAVE REFLECTING EXPRESSED BY X/LO
      DX=XL/HITN
      HIO=2.0*HITN*REFPT
      HL=XL*REFPT
      IO=HIO+0.1
      ION=IO+1
      IOM=IO-1
      IOA=ION
      IF(ION .GT. 20) GO TO 4
      K1=1
      GO TO 5
4     K1=ION-20
5     KN=KI+1
      XO=0.0
      DO 10 I=1,ION, 2
```

```
      V(I,1)=VO
      Y(I,1)=YO
      T(I,1)=0.
10    CONTINUE
      X(1,1)=0.
      NST=0
      J=1
C   LOCATION OF WAVES  NWPT
      NWPT=ION+1
      CHECK=3.
      DO 11 I=3,ION, 2
      IM=I-2
      X(I,1)=X(IM,1)+DX
11    CONTINUE
      J=2
      NJ=0
80    TEST=-1.0
      DO 81 LL=2, IO, 2
      I=IO-LL+2
      IM=I-1
      IN=I+1
      JM=J-1
      CALL GNRS(I,J,G,V,Y,X,T,B,HN,SO,IM,JM,GR,RG,GNR,XM)
      CALL GNRS(I,J,G,V,Y,X,T,B,HN,SO,IN,JM,GS,SG,GNS,XM)
81    CALL MID(X,V,T,Y,RG,SG,GS,GR,GNR,GNS,I,J,IN,JM,IM,JM)
C  FIND THE WAVE AT DOWNST. END
      J=J+1
      I=ION
      IM=I-1
      IN=I+1
      JM=J-1
      X(I,J)=HL
      V(I,J)=0.0
      C=SQRT(G*YO)
      ZO=0.4*YO
      BP=BO+2.0*ZO*XM
      BM=0.5*(BO+BP)
71    VW=C-VO
      ZO=(QO-Q)/(BM*VW)
      BP=BO+2.0*ZO*XM
      YP=YO+ZO
      BM=0.5*(BO+BP)
      AP=AO+ZO*BM
      YPBAR=YP*(BP+2.0*B)/(3.0*(BP+B))
      CNUM=(AP*YPBAR-AO*YOBAR)*G
      CDENO=AO*(1.0-AO/AP)
      CNEW=SQRT(CNUM/CDENO)
      IF(ABS(CNEW-C) .LT. 0.001) GO TO 72
      C=0.5*(CNEW+C)
      GO TO 71
72    Y(I,J)=YP
      VW=C-VO
      VWO=VW
      ZO=Y(I,J)-YO
313   NWPT=I
      NWAV=I
      XPR=X(I,J)-X(IM ,JM)
      BR=B+2.0*Y(IM,JM)*XM
```

```
      AR=(B+Y(IM,JM)*XM)*Y(IM,JM)
      RG=SQRT(G*AR/BR)
      T(I,J)=T(IM ,JM)+XPR/(V(IM ,JM)+RG)
      XX=HL-X(I,J)
      D=ZO/ZO
      Z=ZO
      E=VWO/VWO
      TTO=T(ION,3)
      TEST=2.0
      BETA1=XX/XL
      TT=T(I,J)-TTO
      WRITE(6,131)
  131 FORMAT(1X,1H1, 7X,2H Z,8X,3H VW,8X,2H D,9X,2H E,10X,3H XX, 4X,
     1 8H BETA1 ,5X,3H TT,5X,3H YY ,3X,13H DEP AT D END ,4X,2H Y,8X,5H Y
     1/YO,5X,2H T / )
      WRITE(6,133) Z,VW,D,E,XX,BETA1,TT,Y(I,J)
  133 FORMAT(5X,4F10.4,F12.2,F10.4 ,F8.1,F8.3 )
C     PUNCH 137, F,D,BETA1,YO,Z,VW,B,GAMA,HKE1,XX
C    FIND THE FLOW IN THE MIDDLE CHNL
C  CHECK THE WAVE LOCATION
      I=I-2
28    BIP=B+2.0*Y(I+2,J)*XM
      YIBAR=Y(I+2,J)*(BIP+2.0*B)/(3.0*(BIP+B))
      AIP=(B+BIP)*Y(I+2,J)/2.0
      CNUM=(AIP*YIBAR-AO*YOBAR)*G
      CDENO=AO*(1.0-AO/AIP)
      C=SQRT(CNUM/CDENO)
      VW=C-VO
      IM=I-1
      JM=J-1
      CALL GNRS(I,J,G,V,Y,X,T,B,HN,SO,IM,JM,GR,RG,GNR,XM)
      TPNUM=X(I+2,J)-X(IM,JM)+T(IM,JM)*(V(IM,JM)+RG)+T(I+2,J)*VW
      TPDENO=V(IM,JM)+RG+VW
      TP=TPNUM/TPDENO
      IN=I+1
      CALL GNRS(I,J,G,V,Y,X,T,B,HN,SO,IN,JM,GS,SG,GNS,XM)
      TPNUM=X(IN,JM)-X(IM,JM)+T(IM,JM)*(V(IM,JM)+RG)-T(IN,JM)*(V(IN,JM)-
     1 SG)
      TPDENO=V(IM,JM)+RG-V(IN,JM)+SG
      T(I,J)=TPNUM/TPDENO
      IF( TP .GT. T(I,J)) GO TO 22
45    K=NWAV-1
      L=ION+3-(K-NST)+NST-NJ*2
62    IF ( NWPT .NE. ION ) GO TO 24
      CALL WAVDON(K,L,G,V,Y,X,T,B,HN,SO,VO,YO,VP,YP,XP,TP,K+1,L-1,I-1,
     1 J-1,VW, HL,XM,AO,YOBAR)
      GO TO 25
24    CALL WAVMID(K,L,G,V,Y,X,T,B,HN,SO,VO,YO,VP,YP,XP,TP,K+1,L-1,I-1,
     1 J-1,VW,NST,XM,AO,YOBAR)
25    NWAV=K
      Z=Y(K,L)-YO
      D=Z/ZO
      E=VW/VWO
      XX=HL-X(K,L)
      BETA1=XX/XL
      TT=T(K,L)-TTO
      WRITE(6,133) Z,VW,D,E,XX,BETA1,TT,Y(K,L)
C     PUNCH 137, F,D,BETA1,YO,Z,VW,B,GAMA,HKE1,XX
```

```
      IF(U .LT. 0.020) GO TO 1
      IF(NWPT .LE. 1) GO TO 35
      NWPT=I
35    IK=NWAV-NWPT
      IF(IK .LT. 1) GO TO 34
      DO 36 ID=1, IK
      M=K-ID
      N=L-ID
      V(M,N)=V(K,L)
      Y(M,N)=Y(K,L)
      X(M,N)=X(K,L)
      T(M,N)=T(K,L)
      IF ( M .EQ. 1 ) GO TO 34
36    CONTINUE
34    IF( NWAV .EQ. IO) GO TO 33
      K=NWAV
      L=ION+3-(K-NST)+NST-NO*2
      KK=NWAV+1
      DO 32 K=KK, IO
      L=L+1
      KM=K-1
      KN=K+1
      LM=L-1
      CALL GNRS(K,L,G,V,Y,X,T,B,HN,SO,KM,LM,GR,RG,GNR,XM)
      CALL GNRS(K,L,G,V,Y,X,T,B,HN,SO,KN,LM,GS,SG,GNS,XM)
      CALL MID(X,V,T,Y,RG,SG,GS,GR,GNR,GNS,K,L,KN,LM,KM,LM)
      IF (L .GE. JDIM) GO TO 61
32    CONTINUE
C   FOND THE UNSTEADY FLOW AT DOWNSTREAM END
33    K=ION
      L=L+1
      X(K,L)=HL
      V(K,L)=0.0
      CALL DOWN(X,Y,T,V,K,L,B,G,HN,SO,XM)
      TT=T(K,L)-TTO
      YY=Y(K,L)/YO
      WRITE(6,398) Y(K,L),YY,TT
  398 FORMAT(100X,3F10.3 )
C   FIND THE FLOW IN THE FRONT OF WAVE
61    IF( NWPT .EQ. 2) GO TO 51
      IF(UPEND .GT. 0.0) GO TO 200
      I=I-2
64    IF( I .LT. NWPT ) GO TO 63
      I=I-2
      GO TO 64
63    IF( Y(I+1,J-1) .GT. YO) GO TO 45
      GO TO 28
22    HJ=J
      HJ2=HJ/2.0
      J2=HJ2+0.01
      HJ21=(HJ+1.0)/2.0
      J21=HJ21+0.01
      IF(J2 .EQ. J21) GO TO 26
C   IF J2=J21 J IS A EVEN NUMBER
      LLP=IO+2-1
      IOM=IO-1
      DO 27 LL=LLP, IOM,2
      I=IO-LL+2
```

```
      IM=I-1
      IN=I+1
      JM=J-1
      CALL GNRS(I,J,G,V,Y,X,T,B,HN,SO,IM,JM,GR,RG,GNR,XM)
      CALL GNRS(I,J,G,V,Y,X,T,B,HN,SO,IN,JM,GS,SG,GNS,XM)
27    CALL MID(X,V,T,Y,RG,SG,GS,GR,GNR,GNS,I,J,IN,JM,IM,JM)
      JEVEN=-1
      JODD=2
C   FIND THE FLOW IN THE UPPER STREAM END
      I=1
      X(I,J)=0.0
      Y(I,J)=YO
      CALL UPST(G,X,Y,V,T,I,J,B,HN,SO,XM)
      GO TO 31
26    JEVEN=2
      JODD=-1
      LLP=IO+2-I
      DO 29 LL=LLP, IO, 2
      I=IO-LL+2
      IM=I-1
      IN=I+1
      JM=J-1
      CALL GNRS(I,J,G,V,Y,X,T,B,HN,SO,IM,JM,GR,RG,GNR,XM)
      CALL GNRS(I,J,G,V,Y,X,T,B,HN,SO,IN,JM,GS,SG,GNS,XM)
29    CALL MID(X,V,T,Y,RG,SG,GS,GR,GNR,GNS,I,J,IN,JM,IM,JM)
31    J=J+1
      I=ION+3-J -NJ*2
C   GO BACK TO THE WAVE FRONT
C  CHANGE THE VALUES OF J
      IF (J .LE. 6) GO TO 39
      NJ=NJ+1
      J=J-2
      IK=ION+3-(6+(NJ-1)*2)
      DO 42 K=2, IK, 2
42    CALL VYXT(K,6,V,Y,X,T)
      K=IK
      L=6
      KK=K+1
      DO 43 K=KK, ION
      L=L+1
      IF(L .GE. JDIM) GO TO 630
43    CALL VYXT(K,L,V,Y,X,T)
630   IK=ION+3-(5+(NJ-1)*2)
      DO 37 K=1,IK,2
37    CALL VYXT(K,5,V,Y,X,T)
      K=IK
      L=5
      KK=K+1
      DO 38 K=KK, ION
      L=L+1
      IF(L .GE. JDIM) GO TO 640
38    CALL VYXT(K,L,V,Y,X,T)
640   L=J+(NJ*2)
      K=ION+3-L
      KT=ION-K-NST
      KS=ION-NWAV
      IF (KS .LT. KT) GO TO 39
      DO 47 KX=KT,KS
```

```
      K=ION-KX
      L=ION+3-(K+(NJ-1)*2-NST)+NST
      M=K
      N=L
68    IF(ABS(Y(M-1 ,N-1)-YO) .LT. 0.1) GO TO 69
      CALL VYXT(M-1, N-1, V,Y,X,T)
      M1=M-1
      N1=N-1
      M=M-1
      N=N-1
      GO TO 68
69    LL=0
      DO 47 K=K, ION
      L=L+LL
      IF(L .GE. JDIM) GO TO 39
      LL=1
47    CALL VYXT(K,L,V,Y,X,T)
39    I=ION+3-(J+NJ*2)
      IF ( (NWAV-NST) .LE. I) GO TO 61
      K=I
      L=J
      GO TO 62
51    I=1
      UPEND=1.0
      J=J+1
      GO TO 45
C  NEGATIVE WAVES
C    RESET THE VALUES AT PT. S
200   K=NWAV
      L=ION+3-(K-NST)+NST-NJ*2
      HNEG=-1.0
      IPR=1
      IE=3
      IS=5
      IPL=2
      ID=4
      IQ=6
      V(IS,2 )=V(K+2,L)
      Y(IS,2 )=Y(K+2,L)
      X(IS,2 )=X(K+2,L)
      T(IS,2 )=T(K+2,L)
C    RESET THE VALUES ALONG C+ PASSING REFLECT PT.
      KK=ION-NWAV
      IJKL=0
      DO 201 I=3,5,2
      IJKL=IJKL+1
      KN=KK+1
      DO 201 LK=1,KN
      M=K+LK-1+IJKL-1
      N=L+LK-1-IJKL+1
      IF(N .GT. JDIM) GO TO 202
      J=LK
      V(I,J)=V(M,N)
      Y(I,J)=Y(M,N)
      X(I,J)=X(M,N)
201   T(I,J)=T(M,N)
C    FIND THE INITIAL NEGATIVE WAVES
      GO TO 203
```

```
202   KK=LK-1
203   J=1
      IF(WFP .GE. 0.0) GO TO 1
      V(1,1)=V(3,1)
      Y(1,1)=Y(3,1)
      X(1,1)=X(3,1)
      T(1,1)=T(3,1)
      X(IPL,J)=X(IPR,J)
      T(IPL,J)=T(IPR,J)
      Y(IPL,J)=Y0+V0*V0/(2.0*G)
      BPR=B+2.0*Y(IPR,J)*XM
      APR=(B+BPR)*Y(IPR,J)/2.0
      YPRBAR=Y(IPR,J)*(BPR+2.0*B)/(3.0*(BPR+B))
      BPL=B+2.0*Y(IPL,J)*XM
      APL=(B+BPL)*Y(IPL,J)/2.0
      YPLBAR=Y(IPL,J)*(BPL+2.0*B)/(3.0*(BPL+B))
      VW=V(IPR,J)+SQRT(G*(APL*YPLBAR-APR*YPRBAR)*APL/(APR*(APL-APR)))
      V(IPL,J)=(V(IPR,J)-VW)*APR/APL+VW
      Z=Y(IPL,J)-Y(IPR,J)
      D=ABS(Z/Z0)
      E=VW/VW0
      XX=HL+X(IPR,J)
      BETA1=XX/XL
      TT=T(IPR,J)-TT0
      WRITE(6,133) Z,VW,D,E,XX,BETA1,TT,Y(IPR,J)
C     PUNCH 137, F,D,BETA1,Y0,Z,VW,B,GAMA,HKEI,XX
      V(4,1)=V(2,1)
      Y(4,1)=Y(2,1)
      X(4,1)=X(2,1)
      T(4,1)=T(2,1)
210   J=J+1
      CALL GNRS(I,J,G,V,Y,X,T,B,HN,SO,IS,J ,GS,SG,GNS,XM)
      JR=J-1
      CALL GNRS(I,J,G,V,Y,X,T,B,HN,SO,IE,JR,GR,RG,GNR,XM)
      CALL MID(X,V,T,Y,RG,SG,GS,GR,GNR,GNS,IE,J,IS,J,IE,JR)
C   FIND X,T,AT,PT. P
      BPR=B+2.0*Y(IPR,JR)*XM
      APR=(B+BPR)*Y(IPR,JR)/2.0
      YPRBAR=Y(IPR,JR)*(BPR+2.0*B)/(3.0*(BPR+B))
      BPL=B+2.0*Y(IPL,JR)*XM
      APL=(B+BPL)*Y(IPL,JR)/2.0
      YPLBAR=Y(IPL,JR)*(BPL+2.0*B)/(3.0*(BPL+B))
      VW=V(IPR,JR)+SQRT(G*(APL*YPLBAR-APR*YPRBAR)*APL/(APR*(APL-APR)))
      T(IPR,J)=(X(IS,J)-X(IPR,JR)+T(IPR,JR)*VW-T(IS,J)*(V(IS,J)-SG))/(VW
     1 -V(IS,J)+SG)
      X(IPR,J)=X(IS,J)+(V(IS,J)-SG)*(T(IPR,J)-T(IS,J))
C   FIND THE V Y AT PT. P BY MEANS OF INTERPOLATION
      Y(IPR,J)=Y(IS,J)+(Y(IE,J)-Y(IS,J))*(T(IPR,J)-T(IS,J))/(T(IE,J)-
     1 T(IS,J))
      V(IPR,J)=V(IS,J)+(V(IE,J)-V(IS,J))*(T(IPR,J)-T(IS,J))/(T(IE,J)-T(I
     1S,J))
C   ASSUME THE VALUE OF V(IPL,J)=V(IPL,J-1)
270   V(IPL,J)=V(IPL,J-1)
      X(IPL,J)=X(IPR,J)
      T(IPL,J)=T(IPR,J)
      BPR=B+2.0*Y(IPR,J )*XM
      APR=(B+BPR)*Y(IPR,J )/2.0
220   APL=(V(IPR,J)-VW)*APR/(V(IPL,J)-VW)
```

```
      IF(GAMA .LE. 0.0) GO TO 1181
      Y(IPL,J)=(-B+SQRT(B*B+4.0*XM*APL))/(2.0*XM)
      GO TO 1182
 1181 IF(XM .LE. 0.0) GO TO 1183
      Y(IPL,J)=SQRT(APL/XM)
      GO TO 1182
 1183 Y(IPL,J)=APL/B
C    DETERMINE THE PT. OF Q
 1182 IF(J .GT. 2) GO TO 221
      H=Y0+V0*V0/(2.0*G)
      X(IQ,J)=X(2,1)
      Y(IQ,J)=H
      CALL GNRS(IPL,J,G,V,Y,X,T,B,HN,S0,IPL,J,GP,PG,GNP,XM)
      T(IQ,J)=T(IPL,J)+(X(IQ,J)-X(IPL,J))/(V(IPL,J)-PG)
      V(IQ,J)=V(IPL,J)+GP*(Y(IQ,J)-Y(IPL,J))-GNP*(T(IQ,J)-T(IPL,J))
      GO TO 222
  221 CALL GNRS(IQ,J,G,V,Y,X,T,B,HN,S0,IQ,JR,GH,HG,GNH,XM)
      CALL GNRS(IPL,J,G,V,Y,X,T,B,HN,S0,IPL,J,GP,PG,GNP,XM)
      CALL MID(X,V,T,Y,HG,PG,GP,GH,GNH,GNP,IQ,J,IPL,J,IQ,JR)
C    DETERMINE THE PT. OF D
  222 CALL GNRS(ID,J,G,V,Y,X,T,B,HN,S0,ID,JR,GR,RG,GNR,XM)
      CALL GNRS(IQ,J,G,V,Y,X,T,B,HN,S0,IQ,J,GQ,QG,GNQ,XM)
      T(ID,J)=(X(IQ,J)-X(ID,JR)+T(ID,JR)*(V(ID,JR)+RG)-T(IQ,J)*(V(IQ,J)
     1 -QG))/(V(ID,JR)+RG-V(IQ,J)+QG)
      X(ID,J)=X(ID,JR)+(V(ID,JR)+RG)*(T(ID,J)-T(ID,JR))
      Y(ID,J)=(V(ID,JR)-V(IQ,J)+GR*Y(ID,JR)+GQ*Y(IQ,J)-GNR*(T(ID,J)-T(ID
     1 ,JR))+GNQ*(T(ID,J)-T(IQ,J)))/(GR+GQ)
      V(ID,J)=V(ID,JR)-GR*(Y(ID,J)-Y(ID,JR))-GNR*(T(ID,J)-T(ID,JR))
C    FIND THE NEW VALUE OF VPL BY MEANS OF INTERPOLATION OF POINTS Q,D,
C    AND P
      VPL=V(IQ,J)+(V(ID,J)-V(IQ,J))*(T(IPL,J)-T(IQ,J))/(T(ID,J)-T(IQ,J))
      IF(ABS(VPL-V(IPL,J)) .LT. 0.001) GO TO 250
      V(IPL,J)=0.5*(VPL+V(IPL,J))
      GO TO 220
  250 Z=Y(IPL,J)-Y(IPR,J)
      D=ABS(Z/20)
      E=VW/VW0
      XX=HL+X(IPR,J)
      BETA1=XX/XL
      TT=T(IPR,J)-TT0
      WRITE(6,133) Z,VW,D,E,XX,BETA1,TT,Y(IPR,J)
C     PUNCH 137, F,D,BETA1,Y0,Z,VW,B,GAMA,HKEI,XX
      IF(J .LT. KK) GO TO 280
      YYR=Y(IPR,J)/Y0
      YYL=Y(IPL,J)/Y0
      TTT=T(IPR,J)-TT0
      TTTT=T(IPL,J)-TT0
      WRITE(6,299) Y(IPR,J),YYR,TTT,Y(IPL,J),YYL,TTTT
  299 FORMAT(2X,25H MAX DEPTH AT DOWNST. END ,3F10.3,5X,3F10.3 /// )
  280 IF(HNEG .GT. 0.0) GO TO 1
      IF(D .LT. 0.02) GO TO 1
      IF(J .LT. KK) GO TO 210
C    NEGATIVE WAVE REACHES DOWNSTREAM END
      J=J+1
      JR=J-1
      X(IPR,J)=HL
      V(IPR,J)=0.0
      BPR=B+2.0*Y(IPR,JR)*XM
```

```
      APR=(B+BPR)*Y(IPR,JR)/2.0
      YPRBAR=Y(IPR,JR)*(BPR+2.0*B)/(3.0*(BPR+B))
      BPL=B+2.0*Y(IPL,JR)*XM
      APL=(B+BPL)*Y(IPL,JR)/2.0
      YPLBAR=Y(IPL,JR)*(BPL+2.0*B)/(3.0*(BPL+B))
      VW=V(IPR,JR)+SQRT(G*(APL*YPLBAR-APR*YPRBAR)*APL/(APR*(APL-APR)))
      T(IPR,J)=(X(IPR,J)-X(IPR,JR))/VW+T(IPR,JR)
      Y(IPR,J)=Y(IS,J-1)+(T(IPR,J)-T(IS,J-1))*(Y(IE,J )-Y(IS,J-1))/(T(IE
     1 ,J )-T(IS,J-1))
      HNEG=1.0
      GO TO 270
  137 FORMAT(F6.3,5F8.4,3F8.2,F10.2)
      END
```